Contents lists available at ScienceDirect

Earth-Science Reviews

journal homepage: www.elsevier.com/locate/earscirev

Invited review article

What we talk about when we talk about seasonality – A transdisciplinary review

Ola Kwiecien [*,a], Tobias Braun [b], Camilla Francesca Brunello [c,d], Patrick Faulkner [e], Niklas Hausmann [f], Gerd Helle [c], Julie A. Hoggarth [g], Monica Ionita [d,h], Christopher S. Jazwa [i], Saige Kelmelis [j], Norbert Marwan [b], Cinthya Nava-Fernandez [k], Carole Nehme [l], Thomas Opel [m], Jessica L. Oster [n], Aurel Perşoiu [h,o], Cameron Petrie [p], Keith Prufer [q], Saija M. Saarni [r,1], Annabel Wolf [a], Sebastian F.M. Breitenbach [a]

[a] Northumbria University, Department of Geography and Environmental Sciences, Newcastle upon Tyne NE1 8ST, United Kingdom
[b] Potsdam Institute for Climate Impact Research, Member of the Leibniz Association, 14473 Potsdam, Germany
[c] GFZ-Potsdam, Section Climate Dynamics and Landscape Evolution, 14473 Potsdam, Germany
[d] Alfred Wegener Institute Helmholtz Centre for Polar and Marine Research, Climate Sciences - Paleoclimate Dynamics Division, 27570 Bremerhaven, Germany
[e] Department of Archaeology, The University of Sydney, Sydney, Australia
[f] Römisch Germanisches Zentralmuseum (RGZM), Mainz, Germany
[g] Department of Anthropology and Institute of Archaeology at Baylor University, Waco, TX 76798, USA
[h] Emil Racovita Institute of Speleology, Romanian Academy, Cluj-Napoca, 400006, Romania
[i] Department of Anthropology, University of Nevada, Reno, USA
[j] Department of Anthropology and Sociology, University of South Dakota, Vermillion, SD, USA
[k] Sediment- and Isotope Geology, Institute for Geology, Mineralogy and Geophysics, Ruhr University Bochum, Universitätsstr. 150, 44801 Bochum, Germany
[l] University of Rouen Normandy, IDEES UMR 6266 CNRS, Mont Saint-Aignan, France
[m] Alfred Wegener Institute Helmholtz Centre for Polar and Marine Research, Helmholtz Young Investigator Group PALICE and Polar Terrestrial Environmental Systems, 14473 Potsdam, Germany
[n] Vanderbilt University, Department of Earth and Environmental Sciences, Nashville, TN 37212, USA
[o] Stable Isotope Laboratory, Stefan cel Mare University, Suceava, Romania
[p] Department of Archaeology, Cambridge University, Downing Street, Cambridge CB2 3DZ, UK
[q] Department of Anthropology, University of New Mexico, Albuquerque, NM 87106, USA
[r] Faculty of Biological and Environmental Sciences, Helsinki University, Finland

ARTICLE INFO

Keywords:
Seasonality
Speleothems
Varves
Invertebrates
Tree rings
Statistics
Archaeology
Historical climatology
Cave ice
Permafrost

ABSTRACT

The role of seasonality is indisputable in climate and ecosystem dynamics. Seasonal temperature and precipitation variability are of vital importance for the availability of food, water, shelter, migration routes, and raw materials. Thus, understanding past climatic and environmental changes at seasonal scale is equally important for unearthing the history and for predicting the future of human societies under global warming scenarios. Alas, in palaeoenvironmental research, the term '*seasonality change*' is often used liberally without scrutiny or explanation as to which seasonal parameter has changed and how.

Here we provide fundamentals of climate seasonality and break it down into external (insolation changes) and internal (atmospheric CO_2 concentration) forcing, and regional and local and modulating factors (continentality, altitude, large-scale atmospheric circulation patterns). Further, we present a brief overview of the archives with potentially annual/seasonal resolution (historical and instrumental records, marine invertebrate growth increments, stalagmites, tree rings, lake sediments, permafrost, cave ice, and ice cores) and discuss archive-specific challenges and opportunities, and how these limit or foster the use of specific archives in archaeological research.

Next, we address the need for adequate data-quality checks, involving both archive-specific nature (e.g., limited sampling resolution or seasonal sampling bias) and analytical uncertainties. To this end, we present a broad spectrum of carefully selected statistical methods which can be applied to analyze annually- and

* Corresponding author.
E-mail address: ola.kwiecien@northumbria.ac.uk (O. Kwiecien).
[1] Present address: Geology Section, Department of Geography and Geology, University of Turku, Finland.

https://doi.org/10.1016/j.earscirev.2021.103843
Received 15 June 2021; Received in revised form 20 October 2021; Accepted 22 October 2021

seasonally-resolved time series. We close the manuscript by proposing a framework for transparent communication of seasonality-related research across different communities.

1. Introduction

1.1. What we talk about when we talk about seasonality?

Seasonality is a common denominator for several academic disciplines and its accurate reconstruction is highly relevant across both the natural and human sciences. At a basic level, climate seasonality is expressed intuitively as the cyclical changes in temperature and/or rainfall over the course of the year, which in turn determines both the composition and the dynamics of ecosystems. Overall, climate seasonality plays a critical role in influencing the persistence of all living organisms. For example, the seasonal changes in precipitation and temperature affect different components of the climate system (e.g., soil moisture, snow cover, evaporation rates, river flows and lake levels). The changes in these variables lead further to changes in vegetation and ecologic requirements of plants and animals, which in turn influence the type and amount of food available for humans and other organisms. For the majority of multicellular organisms, the diurnal and seasonal cycles are the most important pacemakers of biological functions. For humans, the influence of seasonality affects the biological world they interact with and extends across the cultural domain, including construction of niches, subsistence, religious, and economic activities. Studying past changes in seasonality is of great interest and importance for palaeoclimatology, palaeoecology, anthropology and archaeology, and, last but not least, modern climate science, conservation and phenology, all of which face the uncertain future of global warming (Santer et al., 2018). Palaeoclimatology aims at documenting how seasonal changes affect the climate system through time (Crowley et al., 1986; Denton et al., 2005a), and *the amplitude of seasonal changes* (Luterbacher et al., 2004; Felis et al., 2004; Ferguson et al., 2011; Veski et al., 2015; Brocas et al., 2018). Palaeoecology deals with *the effect of seasonality changes on the ecosystem* (Rivals et al., 2018; Manzano et al., 2019), while anthropology and archaeology document *the effect of seasonality and changes in seasonality on human evolution, residency, subsistence strategies, and the adaptation of those strategies* (the latter two involving human-ecosystem interaction; (Prendergast et al., 2018), and references therein). Recent work by Degroot et al. (2021) emphasized pitfalls of integrating data and knowledge between academic disciplines with different practices and standards of evidence. Increasing scientific interest in what the authors termed 'history of climate and society' warrants proposing

Box 1
Definitions

'Seasonality' is widely used in many disciplines of palaeo-research, yet it is lacking a clear definition. In the scientific literature, references to changes in seasonality are as frequent as they are ambiguous. A survey of this literature raises many questions: what does *'increased'* or *'decreased seasonality'* actually mean? Can we quantify this change? And is the amplitude all that matters? What about temporal distribution? Does temperature and precipitation always respond symmetrically and harmonically? Pezzulli et al. (2005) highlighted that one should refer to the annual cycle rather than the seasonal cycle since the period is one year, not one season, and we endorse this approach. Here we define key concepts related to seasonality and how they will be used throughout this review.

Annual cycle of temperature – can be symmetric, sinusoidal, and is defined by maxima and minima. **Seasonality of temperature** refers to an amplitude between maxima and minima. In theory, the annual budget reaches zero, meaning that colder winters are counterbalanced by warmer summers.

Annual cycle of precipitation – is defined by magnitude (amount) and temporal distribution (timing – when: duration – for how long). **Seasonality of rainfall** should take all three of these components into consideration, which, in case of palaeoenvironmental archives and their limitations in resolution, is rarely feasible. In modern climatology the beginning of the hydrological year differs from the beginning of the calendar year.

Seasonality of temperature and seasonality of rainfall together make **climate seasonality**.

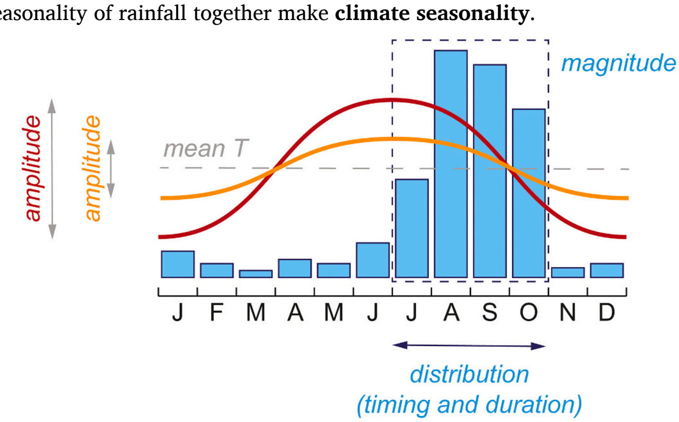

Annual cycle of human activities (e.g., foraging, farming, migration) – strongly related to natural temperature and precipitation cycles, which influence the growing season and availability of static resources and the movement patterns of mobile resources (see Box 5). The availability and sustainability of these resources influence human subsistence strategies, which in turn inform other types of cultural behavior. **Seasonality of an activity** refers to its timing and duration.

frameworks which facilitate interdisciplinary research. Thus, this review proposes a framework for addressing past climate seasonality changes.

An opinion piece by Carré and Cheddadi (2017) echoes the seminal work by Rutherford et al. (2005) and outlines the most important, but often overlooked, aspects of seasonality in palaeoenvironmental studies. Firstly, climate is defined not by annual means of temperature or precipitation, but by the annual cycles of these climate variables (see Box 1). Annual mean values, so often extracted from proxy records, while important, do not fully capture past climate variability. Secondly, relatively small changes in natural processes acting on a seasonal timescale are the drivers that foster large climate shifts. Not detailed by Carré and Cheddadi (2017) are the often simplified or overlooked aspects of spatial heterogeneity of environments and human actions, including the seasonality and timing of subsistence activities, which further influence the rhythms of other cultural behavior(s).

The two aspects of seasonality reiterated by Carré and Cheddadi (2017), namely: (1) the fact that it defines climate and (2) that the small changes accumulate in large-scale oscillations (e.g., glacial/interglacial cycles), constituting a challenge for scientists working with archives that often lack seasonal resolution and/or are biased towards one season only. Alternatively, archives record seasonal changes but are discrete in nature and represent only snapshots of time rather than a continuous interval. Consequently, regional palaeoclimate syntheses frequently suggest different responses to seasonality changes to account for discrepancies between different archives and proxies covering the same time span, or between data-based reconstructions and climate model output. The classical example comes from the Mediterranean region where Prentice et al. (1992) reconciled glacial lake levels, where high levels suggested increased humidity, with contemporary pollen records that indicate drier conditions, by proposing an increased seasonality in precipitation with wetter winters and drier summers. Yet, the term '*seasonality*', while so often used by the palaeo-community, lacks formal definition, and the phrase '*seasonality change*' is often used to refer to a bundle of processes encompassing changes in both the external forcing and internal conditions modulating the local response. The external forcing is prescribed by the orbital parameters (see Box 2).

The amount of insolation received at any point on the planet is a function of season and latitude. It can be theoretically calculated for the past and the future and broadly translated into relative temperature changes, with flat seasonal gradients in the tropics and steep gradients at the poles (see Box 3).

The internal forcing – atmospheric CO_2 concentration – is a global feature, and its changes are relatively well documented for the course of the Pleistocene and Holocene (Zhang et al., 2013; Augustin et al., 2004). The local conditions, however, are inherently heterogenic, and factors like continentality (landmass and ocean distribution), altitude, land cover, and atmospheric circulation patterns and volcanic activity play an important role in modulating insolation- and CO_2-prescribed local temperature (see Box 3). Thus, the resulting local expression of climate seasonality varies between sites along the same or similar latitude (see Box 4). Further, the natural archives exposed to seasonal changes might display a bias or an offset in recording the local signal (see Box 4). Last but not least, if the natural archives might be influenced by, or are the direct outcomes of human activity, considering anthropogenic aspects is essential. Depending on the nature of their adaptations, resilience and sustainability, humans developed different strategies to cope with and/or take advantage of seasonal changes (e.g., choosing migratory or stationary lifestyles, hunting and foraging or farming). Importantly, the degrees to which particular strategies are successful are likely to change through time, based on environmental circumstances, population size, and technology (see Box 6). Consequently, the archaeological archives related to human occupation sites constitute a special case, i.e., a confluence of natural changes and developing human adaptations (e.g., Petrie and Bates, 2017).

This review answers the call by Carré and Cheddadi (2017) for a reevaluation of the scientific focus and methodological habits of the scientific community. It is time to scrutinize '*seasonality changes*' and address individually different components which together produce the climate – and human history records we work with. Considering the breadth of the audience, first we take a step back and take up the issue of climate seasonality (see Box 1) at a fundamental level of external forcing (see Box 2) internal, regional and local changes (see Boxes 3 and 4). Further, we summarize how seasonality is reflected in different archives and explore advantages and potential limitations of each archive. The next chapter demonstrates statistical methods useful in extracting and analyzing seasonal information from high-resolution but often irregularly sampled archives. Finally, we suggest a framework for discussing scientific observations in order to avoid confusion and promote transparency in multi- and transdisciplinary research.

1.2. Brief justification of selected archives

The beauty of seasonally resolved archives, whether continuous or discrete, lays in their capacity of recording the baseline of seasonal variation. Deviation from this baseline can inform on frequency and magnitude of events (e.g., floods or droughts), while stepwise change suggests the reorganization of the large-scale atmospheric and/or oceanic circulation (e.g., glacial termination). Anchoring seasonal changes in a wider palaeoenvironmental narrative allows for insight into the complex dynamics of Earth's system's and human response to external climate forcing.

Not all palaeoenvironmental archives have the potential of recording seasonal variability. Of those which can, not all can be dated with annual resolution. Here, we first focus on instrumental and historical data as these have natural and direct connection to the Present. Next, we move to archaeological records as an overarching subject discussing relevance of seasonal changes for humanity's past, beyond instrumental and historical reach. This chapter alludes to natural archives which are often found either directly at sites of human occupation or in close vicinity and have the potential to record seasonal changes. The different archives (i.e., marine biogenic carbonates, stalagmites, tree rings, laminated lake sediments, glacier ice, cave ice, and permafrost ground ice) are highlighted in the following chapters.

The element conspicuous by its absence is pollen. When calibrated, pollen records indisputably provide information on temperature and precipitation ranges in physical units (°C and ml) and as such can be related to specific seasons (Chevalier et al., 2020). Applying transfer functions to pollen assemblages is a powerful tool for quantifying past environmental change. Alas, the temporal resolution of this proxy is inherently coupled with the sedimentation rate of the media it resides in and this review addresses seasonally resolved archives rather than proxies.

2. Seasonality in historical climatology

Historical climatology aims to extend temperature and precipitation data back to pre-industrial periods, bringing together direct and indirect sources on weather and climate (Fig. 1). Various types of records serve as unique functions in historical climate reconstruction by (i) providing precise climate and weather information, from annual to daily resolution, at defined locations for all seasons and (ii) defining their societal impacts, perceptions and reactions. Information derived from historical records can inform on past seasonality if the collected data are of sufficient resolution and cover time period of at least a few years.

Direct observations include quantitative measurements of temperature, rainfall, and other climatic information from various land stations and ships around the world (Fig. H1). Whereas instrumental records provide consistent measurements, indirect sources of information or references considered herein as proxies (e.g., personal documents, narrative and episcopal sources, archival and pictorial materials, flood markers) provide descriptions of the historical context of natural background climate variability (Fig. 1). Additionally, synthesized historical

Box 2
Orbital influences on annual and diurnal cycles

The diurnal (Earth rotation around its axis, 24 h) and annual (Earth rotation around the Sun, 1 year) cycles can be observed and experienced during a human lifetime. On longer, multi-millennial time scales, these cycles are influenced by changes in Earth's orbital parameters, obliquity, eccentricity, and precession. Changes in orbital parameters have been calculated theoretically (Milankovitch, 1930) and their persistence on Earth climate has been documented in geological record (Hays et al. (1976) and more). Fundamentally, seasonal variability is controlled by the amount of incoming solar radiation (**insolation**), arriving at different latitudes at different angles as Earth orbits the sun. Below we consider four different scenarios to illustrate how changes in orbital parameters influence the annual insolation distribution and the length of day.

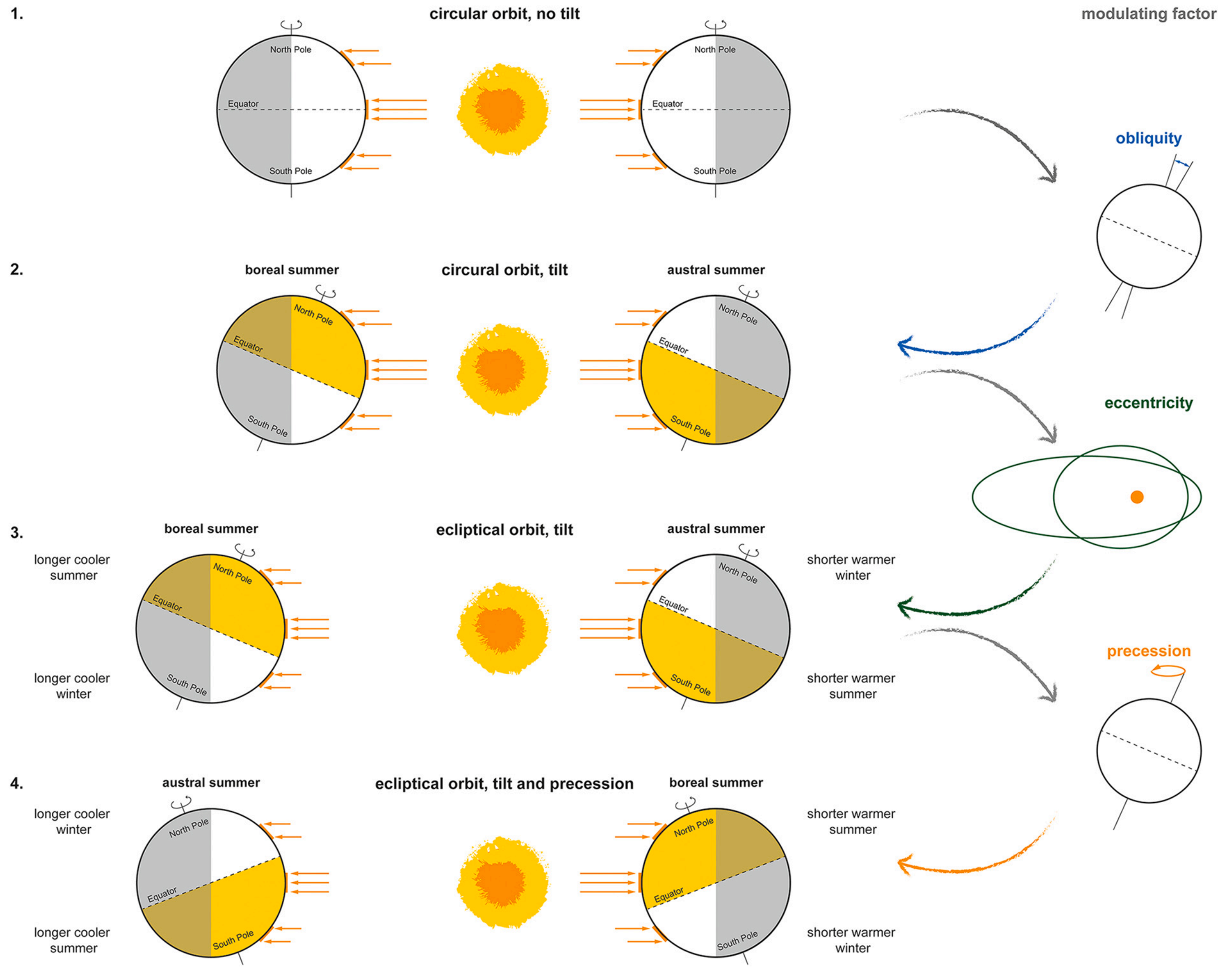

1. If the Earth's rotational axis was perpendicular to the orbital plane, the insolation angle for each latitude would be constant throughout the year. Insolation gradients would exist between the latitudes, but there would be no seasonal changes. Daytime would have the same length at each latitude.

2. Increasing the tilt (**obliquity**) changes the insolation angle during Earth's rotation around the sun. The hemisphere tilted towards the sun experiences warmer temperatures (summer), and longer days. The amplitude of seasonal differences increases with the tilt. The length of the obliquity cycle is ca 42 ka. At the equator, the length of the daytime is roughly constant throughout the year, it gets longer (24 h) towards the 'summer' pole and shorter (0 h) towards 'winter' pole. Summer and winter are of equal length in both hemispheres.

3. Changing the shape of the orbit (**eccentricity**) influences the distance of the Earth to the sun and the length of the seasons. **Eccentricity of the orbit modulates the effect of the obliquity.** The seasons at aphelion are colder (the Earth is further away from the sun) and longer (further away from the sun it's gravitational pull is weaker, so the Earth moves slower) than at perihelion. Eccentricity has two cycles, a short one, ca. 100 ka, and a long one, ca. 400 ka. In the presented scenario (corresponding to modern day conditions) the gradient between summer and winter insolation (here, translated into temperature) is steeper in the southern hemisphere (SH) compared to the northern hemisphere (NH).

4. The wobble of Earth's rotational axis (**precession**) changes the direction of the tilt and determines which hemisphere is tilted towards the sun at perihelion (summer). The same hemisphere will be tilted away from the sun at aphelion (winter). **Precession thus determines on which hemisphere the amplitude of annual change in insolation is larger.** The overall length of the precessional cycle is ca 23 ka.

While systematic changes in insolation are, next to atmospheric CO_2 concentration, the most important driver for seasonal temperature variations, other factors can modify temperature variations (see Box 3).

Box 3
External and internal forcing, and internal feedbacks

The energy received from the sun per unit area (insolation) is kept in check by Earth's atmospheric CO_2 concentration. Insolation changes (**external forcing**) are periodic and fixed for a given season and latitude (see Box 2) and as such are predictable. In pre-industrial times CO_2 concentration (internal forcing) varied little between the hemispheres, following the respective vegetation season, and large variations in CO_2 level were global (Royer et al., 2004; Augustin et al., 2004).

At the low latitudes the total amount of the insolation received is larger than that received at the high latitudes and the poles, but the amplitude of annual change is very small. Hence in low latitudes annual cycle is expressed in precipitation changes (wet and dry season). The amplitude of annual insolation change increases with distance from the equator and manifests itself in temperature and daylight duration changes.

Still, the Earth unit area receiving insolation is rarely homogeneous and the surface properties can modulate (dampen, amplify, or delay) the local response. **Internal feedbacks** are semi-stochastic.

A novel (in a geological sense) element of internal feedback, referred to as anthropogenic climate variability, combines greenhouse gas emission, deforestation and land use change. The sensitivity of a given archive can further influence the palaeoenvironmental record.

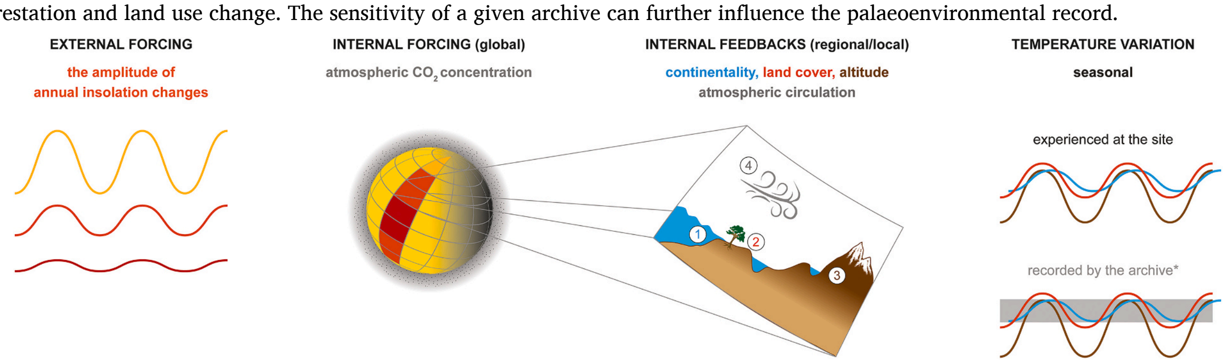

- **Continentality**: a measure of the difference in the annual temperature maxima and minima that occurs over land compared to water. The oceans capacity for storing heat (thermal inertia) is greater than that of the continents which means it warms slower but also cools slower than land masses. Further, the upper ocean layer can distribute heat both, vertically and horizontally. By storing heat in summer and releasing it in winter oceans considerably dampen the annual cycle of temperature. In contrast, the continental interiors experience much larger annual temperature differences. The large thermal inertia of the oceans shifts the annual temperature maxima and minima of surface water and coastal regions in relation to temperature over continental interiors. The land-ocean distribution is also important in moderating the insolation-prescribed hemispheric seasonality contrast: under modern day conditions the gradient between summer and winter insolation is steeper in the SH compared to the NH; however, the SH ocean/land ratio counteracts the large temperature gradients. Size and distribution of the continents have also impact on the seasonal precipitation patterns, with continental interior receiving less rainfall than coastal regions.
- **Land cover**: differences in surface properties represented by vegetation changes (e.g.: forest vs steppe vs bare rock), snow cover, or surface water distribution affect the albedo and the heat capacity of the surface. The effect of these differences on the overlying atmosphere is analogous to the ocean surface temperature anomalies, but on a much smaller spatial scale.
- **Altitude**: temperature in the troposphere (lowest layer of atmosphere) decreases with increasing altitude. The rate (lapse rate) is approximately 1 °C for every 100 m.
- **Atmospheric circulation patterns**: seasonal variability of precipitation and temperature is modulated by the large-scale atmospheric circulation patterns and by the ocean circulation, operating on interannual to multidecadal time scales (e.g., El Niño-Southern Oscillation (ENSO), the North Atlantic Oscillation (NAO), the Pacific North American pattern (PNA), the Pacific Decadal Oscillation (PDO) and the Atlantic Multidecadal Oscillation (AMO), among others). These atmospheric and ocean modes of variability can influence the precipitation and temperature in different ways. For example, NAO exerts a strong influence on the hydroclimate variability of Europe, while the PNA strongly influences the hydroclimate of the U.S.
- **Volcanic activity**: volcanic eruptions inject large quantities of aerosols into the atmosphere, and stratospheric circulation distributes them across the planet. In general, aerosols have a cooling effect. However, the scale of this effect depends on where (hemisphere and latitude), when (season), how much (the volume), and for how long (single or multiple eruption events) the material was injected.

climate data (indirect references) derived from a combination of instrumental, written and pictorial documents improve our understanding of the climatic impact on social behavior and the organization of social groups in the past, even on short time scales (daily or seasonally) (Brázdil et al., 2005; Chuine et al., 2004; de Kraker, 2006; Luterbacher et al., 2004). These types of studies have been pivotal for exploring seasonal changes, with documentary data being translated into numerical indices, e.g., to study seasonal rainfall variability in Iberia (Rodrigo and Barriendos, 2008) or seasonal temperature in the Mediterranean (Brasseur et al., 1996).

2.1. *State of the art*

Interest in documenting historical climate and weather patterns started in Europe since at least the 14th c. with systematic weather observations in England (Mortimer, 1981), Germany (Schwarz-Zanetti and Schwarz-Zanetti, 1992) and the Netherlands (Buisman and Van Engelen, 1995). One of the main motivations behind recording meteorological phenomena is their impact on agriculture and society. Understanding the mechanisms behind all aspects of daily weather (e.g., wind, temperature, rainfall) was imperative to develop mitigation strategies. With the development of new instruments (standardized rain gauge, thermoscope, thermometer, etc.) in the 17th c., recording of

Box 4
Combined influence of latitude, continentality, and altitude

Köppen (1936) classification of climate divides climate zones into 5 main groups (tropical - A, dry - B, temperate - C, continental - D and polar - E), based on seasonal temperature and precipitation patterns. This grouping takes into consideration not only latitude but also continentality and altitude. Köppen's climate zones are the best example of differences in amplitude of seasonal change along the same latitude (the theoretical line subjected to the same insolation forcing). We have chosen 7 examples of archaeologically relevant sites from around the globe to illustrate the possible range of local seasonal temperature and precipitation (modern data from https://en.climate-data.org). Tropical and temperate climates are characterized by larger amplitude of precipitation changes, dry and continental climate by larger amplitude of temperature. In case of tropical site in the Andes, the altitude is responsible for low temperature values. Note that the plot does not account for potential evapotranspiration.

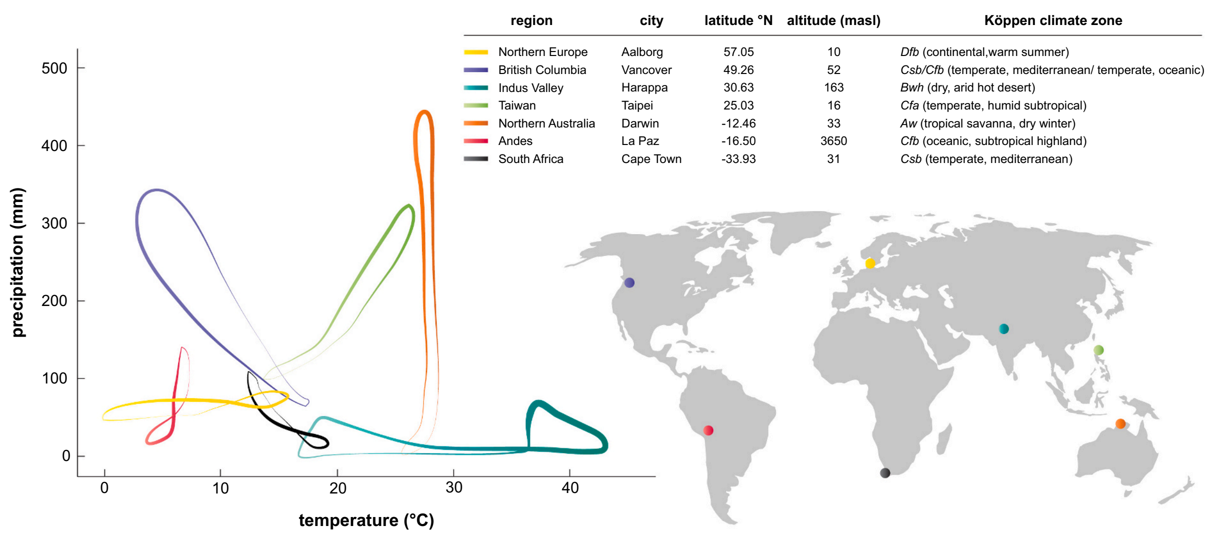

weather conditions evolved from a mainly descriptive method into accurate and regular measurements of atmospheric and hydrological conditions (Brázdil, 2002). In the 19th c., climate and weather became increasingly important for the military and were more institutionalized. In the 20th c., large compilations of instrumental data on centuries of past winters in England were collated (Britton, 1938) and compared with temperature. Other indirect compilations on weather include information on harvest timings, flood events and glacier retreats in Switzerland (Pfister, 1992), Germany (Glaser et al., 1999), Italy (Camuffo, 1987), Spain (Vallve and Martin-Vide, 1998) and France (Ladurie and Baulant, 1980). Europe, having long written traditions has also the largest account of historical climate data (Jones, 2008).

Instrumental series from individual stations or regions, some of them reaching back as far as the 17th c., allow for direct investigation of past temperature and/or rainfall. Prior to the establishment of national meteorological networks, information on past climates can be drawn from non-instrumental sources. A historical source on climate can be a printed document (e.g., manuscript, book, newspaper, parish or administrative registers, diaries), a picture or an artefact (e.g., flood mark, inscriptions, amulets) referring to weather patterns or impacts of climate on social behavior or agriculture (e.g., religious rituals or harvest density and timing, respectively). The term documentary evidence includes all kinds of anthropogenic historical sources, with several types of data (Fig. 1). Chronicles often combine descriptive data (e.g., descriptions of weather events) with documentary proxy data or observed features in the cryosphere (e.g., snowfall, snow cover), hydrosphere (e.g., floods, low water tables), biosphere (e.g., stages of vegetation cover), and atmosphere (e.g., features linked to volcanic eruptions). A well-documented example of this type are the Medieval Irish chronicles (Ludlow et al., 2013), which reveal a statistically significant link between cold events in Ireland and explosive volcanism in the northern hemisphere between 431 CE and 1649 CE. Brázdil (2002) used a similar approach and compared personal daily diaries regarding meteorological events with independent meteorological observations from weather stations in the Czech Republic and adjacent European countries for the 1780–1789 CE period. Both, the documentary evidence and instrumental data reveal extreme seasons at the end of the 18th c., like the hot summer of 1783, and the hard winters of 1783/84 and 1788/89, the latter being the coldest December ever recorded in Europe.

2.2. *Reconstructing seasonality signals from documentary sources*

Reconstructing temperature or rainfall changes from indirect documentary evidence requires looking at all kinds of, mainly economic, activities characteristic for a specific season. Importantly, the type of documented activity or events (e.g., harvest, sowing, etc.) influences the number, length, and pattern of the identified seasons and the data should be treated with care. Temperature records can be constructed from two major types of sources: (i) accounts on transportation and shipping and (ii) phenological data. Rainfall records can be constructed from (i) financial/economic, official administrative documents and (ii) religious chronicles and ceremonies.

2.2.1. *Reconstructed temperature data from documentary sources*

Accounts on transportation and shipping. During the pre-industrial period canals and rivers formed major transportation routes and any kind of interruption was deemed harmful to the economy. Thus, all profits and losses were administered very accurately, often on a daily basis through archives such as tolls, leasing out of barges, passing and repairs of locks/bridges. The most important cause for the interruption

Box 5
Relevance of seasonal bias recognition and adapting sampling strategy

Treating seasonally biased records as representing annual means might lead to flawed interpretations. The opposite is also true: records reflecting annual means should be treated with caution when interpreting seasonal changes in temperature or rainfall.

In our conceptual example here, some archives record the full range of annual temperatures, while others only a portion. The correct recognition of the recorded interval is crucial for further interpretation, regional or global synthesis, and comparison (Bova et al., 2021; de Winter et al., 2021b). Adequate sampling is an additional challenge, in particular when the sedimentation/growth rate of the archive is low. de Winter et al. (2021a) discuss in depth how sampling strategy might influence obtained results and propose a schematic guide for choosing the optimal approach. Depending on archive sensitivity and sampling strategy, the shift of the baseline without change in the amplitude might be inaccurately perceived as an increase or decrease in seasonality of respective parameter. Further, comparing the same proxies (e.g., $\delta^{18}O$) from different archives, or the same, but geographically distant, archive does not guarantee that they record the same season.

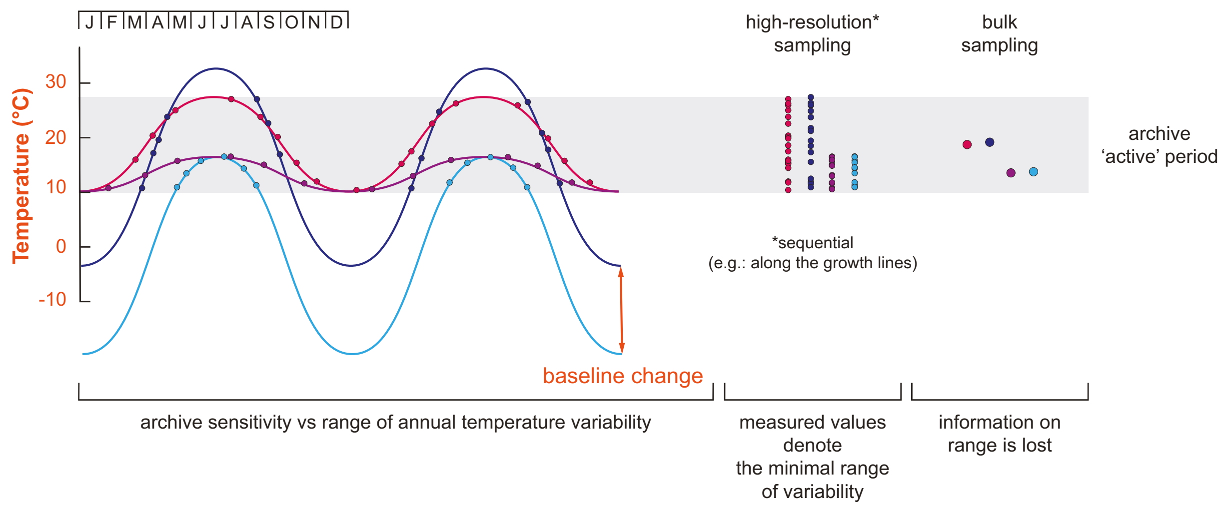

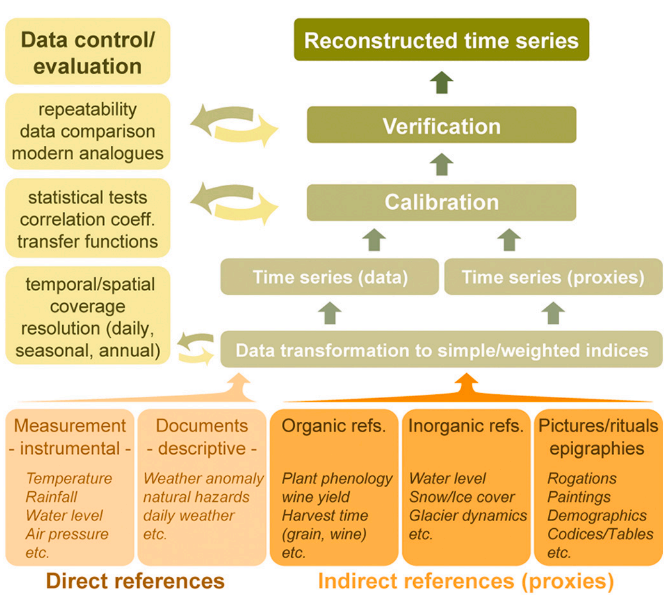

Fig. 1. Processing direct and indirect data from documentary references into quantitative (reconstructed) climate time series (after Brázdil, 2002; Brázdil et al., 2005; de Kraker, 2006).

of shipping or water mills was ice coverage of waterways. Most accounts record the beginning and ending of these frost periods and provide additional data on the severity of the winter cold, and thus seasonal information of winter temperatures. De Vries (1977) reconstructed winter sea ice expansion and long-term variability of winter severity in the Northern Sea from the 17th to the 19th c. by analyzing the number of days shipping was interrupted on the Haarlem canals. He then demonstrated complex dynamics of winter temperatures during the Little Ice Age (LIA). The methodology of translating the length of the frost period into temperatures was later improved (van Engelen et al., 2001) to derive a quantitative frost index. The latter was more robustly correlated to temperature via a classification for frost-temperature data in recent periods. Based on the reconstruction of the LIA winter ice index similar studies were conducted in the Baltic Sea (Koslowski and Glaser, 1999) and northern Europe (Tarand and Nordli, 2001).

Documentary sources related to agricultural activities considered "phenological data" are represented by various printed sources, including official registers, diaries, manuscripts and accounts, detail crop production quantities and time of harvest. The tithes' taxation that was collected at a fixed date prior to harvesting in medieval Christian Europe comprises another indirect climate proxy. These data are often related to the winter, spring, or summer temperatures and can thus give insights into past seasonal variability. Cold/dry and warm/wet weather conditions considerably impact crop production and harvest date. For example, cold winters can affect the production of certain crops such as *Brassica oleracea* (e.g., cabbage, Golicz et al., 2016). Reconstructing the production of such cultivars from documentary sources can inform on the variability of winter severity on longer timescales. Other crops are documented in detail because of the high economic value (e.g., wine production). Grapes serve as excellent summer/autumn climate proxies because they are highly sensitive to the insolation length and summer temperature. A long hot summer sets a harvest date for grapes in mid-September, whereas a colder summer generally delays the harvest into October. De Vries (1977) and Ladurie and Baulant (1980) were among the first to reconstruct temperature from harvest timing for winter and summer crops. Ladurie and Baulant (1980) compiled harvest dates in France of several grapes in a long time series which starts in 1484 and reflects changes in early summer mean temperature during the LIA (Burkhardt and Hense, 1985; Lauscher, 1985). Other phenological evidence comes from grain harvest dates (e.g., rye, wheat, oats) (Glaser et al., 1999) or the first date of cherry tree blossoming (Pfister and Brázdil, 1999). Recent studies on grape and grain harvesting in SE France (Daux et al., 2012; Chuine et al., 2004), Hungary (Kiss et al., 2011), Lithuania (Tarand and Nordli, 2001), and SE Asia (Wang and Wang, 1990; Garcia et al., 2001; Hao et al., 2020) provide more robust methodological and statistical strategies to disentangle the Medieval climate optimum (MCO) and LIA climatic dynamics by combining documentary evidence with independent proxy data.

Overall, time series of grape harvesting (Fig. 2) may provide a combined spring and summer temperature signal, while the index-based time series of the number of frost days may provide a winter temperature signal. As with other archives (e.g., tree rings), influence of precipitation or a signal noise cannot strictly be excluded. The expected temperature signals are renounced from datasets by smoothing or filtering. High correlation coefficients between document-based reconstructed index values and recent instrumental data increase confidence in the index as temperature indicator. Reconstructed temperatures might then represent average winter, spring, or summer temperatures.

Most written sources on water availability (rainfall, drought, floods) record extreme weather events because they are strongly perceived as being the cause of disasters, potentially even leading to the collapse of societies (Hassan, 2007; Weiss, 2017). Extreme events, such as severe storm surges causing large-scale flooding (Fig. 2B), or severe droughts or extended frost periods that led to food shortage and famine, and consequently higher mortality rates, were frequently noticed by chroniclers (Fig. 2). Such information is also available not only from Europe but also the Americas. Nineteenth century explorer logs from the Canadian Arctic have helped dispel the myth that navigation through the Northwest Passage was impeded during periods of intense cold, such as the LIA (Overland and Wood, 2003). Similarly, 19th c. meteorological diaries kept by the family of James Madison contain climatic data that allowed the reconstruction of precipitation in the northeastern United States (Druckenbrod et al., 2003). Even earlier correspondence between local officials and governing bodies, and other sources in the Yucatan peninsula, Mexico, detail periods of drought, and instances of food shortfalls resulting from a series of droughts during the Colonial period (Acosta et al., 2003; Hoggarth et al., 2017). Historical documents from Ecuador, Peru, Bolivia, Chile, and Argentina offer direct information on climatic variability since the European conquest. A large corpus of historical data from South America from 1550 to the mid-20th c., compiled by del Rosario Prieto and Herrera (2009), allows the identification of long-term regional climatic trends.

Earlier historical evidence comes from Pre-Columbian societies with written languages. Although surviving historical texts from the Pre-Columbian Americas focus particularly on religious or ceremonial knowledge and political histories, some give details about climatic events. For example, a hieroglyphic text from Comalcalco describes drought and famine in 783 CE (Zender, 2004: 257, 543). Both droughts and excessive rainfall are discussed in Maya codices, tables and almanacs, for example a severe drought in 818 CE that affected the crop yield (Bricker and Bricker, 2020). Another example comes from the Aztec Empire, who recorded a series of drought events, such as during the Famine of One Rabbit in 1454 CE (Therrell et al., 2004). Despite the wealth of information in these documentary sources, reconstructing a seasonal signal of water availability requires more systematic chronicles with daily to monthly resolved data on events directly linked to winter, spring or summer seasons, or social/religious ceremonies that reflect social behavior driven by seasonal events.

2.2.2. Rainfall records from major categories of documentary sources

Financial/economic records, books of city, and official administrative documents. Administrative sources consist of official documents which

Fig. 2. Historical archives and its relation to seasonality. **A**: drought marker ('Hungerstein') at Elbe river, Dresden, South-East Germany; **B**: flood marker at the Oder river, Frankfurt, East Germany; **C**: Illustration of monks harvesting wine in Bourgogne, France at the end of 19th c. **D**: September calendar showing Grape harvest and wine pressing. Photos A and B mark historical floods or droughts along rivers. The study of compiled historical markers as indirect proxies for seasonality give insights in changes in season's dynamics and trends. More frequent drought events during certain periods might reflect hot/longer summer seasons, whereas recurrent flood events can reflect severe/longer winter or spring season with higher amount of water/snow melt. Fig. C is an extract B.11.4 (f. v recto.) of 'Psalterium', a manuscript from the 13th c., in which M.R. James describes the scene thus: "*Cuts grapes from vine with sickle and holds the hand of a nude man in a vat.*" From the James Catalogue of Western Manuscripts, digital library of the Trinity College, Cambridge. All photos are under CC licence.

contain exact, and often numerical, information on socio-economic impacts, such as the low quantity or quality of harvests, level of food shortage, loss of domestic animals, or taxation due to harvest loss. The different economic aspects of drought may be listed more systematically compared to other types of sources, giving an opportunity to obtain additional information on droughts on annual basis, and to evaluate the intensity of spring or summer droughts. Camenisch and Salvisberg (2020) reconstructed drought events for the Swiss city of Bern between the 14th and 18th c. when the Republic of Bern was able to expand its political and territorial power and to establish the largest city state in the Northern Alps. Narrative sources and the proceedings of the city council - the "Ratsmanuale" - as well as other sources of the cities' administration from the nearby areas mainly document summer drought events allowing the reconstruction of summer drought variability in Switzerland during the LIA. Examples of seasonal floods were documented in the upper Rhine Basin in Southern Germany and Switzerland (Wetter et al., 2011). In the city of Basel, pre-instrumental data such as flood marks, and documentary sources describing flood events from the 13th c. were calibrated using comparisons with daily hydrological measurements for the overlapping period of the 19th c. Wetter et al. (2011) show that summer (JJA) floods were particularly frequent between the 17th and 18th c., when total precipitation was also above normal. However, despite a significant increase in winter precipitation, severe winter (DJF) floods have not occurred since the late 19th c., mainly due to the installed river regulation systems.

Religious chronicles and ceremonies Climatic information derived from private letter correspondence of the Jesuit order in Castille (Spain) during the mid-17th c. reveal a prevalence of intense rainfall and cold waves in the recorded period (Rodrigo et al., 1999). Retsö (2002) used similar documentary sources to characterize winter weather patterns from the early 16th c. in Sweden. Recently, new data sources from religious rituals (songs, prayers, etc.) showed climatological potential to derive water availability data (e.g., droughts, floods). For instance, the Catholic Church in Spain organized rogation services (rogativas) directed to end climatic stress situations connected with long dry or wet spells which jeopardized the harvests. Ecclesiastical authorities developed a system of activities in which five levels of rogation can be distinguished regarding the severity of dryness. Vallve and Martin-Vide (1998) used these rogation data to analyze spring/summer droughts in the Iberian Peninsula at the end of the 17th c. Rodrigo et al. (2001) used, among other sources, religious chronicles and books of city and church archives for the reconstruction of seasonal precipitation changes in Andalusia and its links to the winter North Atlantic Oscillation back to AD 1500. In the Americas, earlier documentary sources from religious leaders record climatic changes (De Landa and Garibay Kintana Garibay, 1978), e.g., in the Book of Chilam Balam of Chumayel (Roys, 1967), which describes a pilgrimage to the sacred cenote at Chichén Itzá to conduct a ritual to appeal for rain in 1535 CE.

2.3. Methodological advances

Direct observations from historical narratives on climate anomalies and weather patterns, as reported in documentary sources come with a variety of drawbacks. First, such accounts are often sporadic or event specific, and possibly contain gaps when considering long time periods (Pfister, 2010). Nash and Adamson (2014) note that the discontinuous nature of many records can cause major issues, but those are balanced by the excellent dating control and high temporal resolution that is available from these accounts. Since the 1990s, the methodologies were improved in order to evaluate archived documentary data in such a way to exclude anomalies (filtering), smooth the qualitative data with data assessment using fixed average times, evaluating the consistency and reproducibility of chronicles with sufficient overlapping time windows, or correlation with recent observations, and finally creating quantitative indices using a categorization process of the targeted proxy (temperature, rainfall, wind) and transfer functions (Brázdil et al., 2005; Brázdil et al., 2020; de Kraker, 2006; Wang and Wang, 1990; Gimmi et al., 2007; Dobrovolný et al., 2010; Ogilvie and Farmer, 1997; Noone et al., 2017). Additional work has focused on developing techniques for assessing the quality of documentary sources. To test authenticity and/or consistency, Pfister (2010) suggest that documentary sources should be critically evaluated in relation to broader historical contexts. Similarly, Jones et al. (2009) suggests rigorous inter-comparison of sources to construct basic reliability measures for each type of evidence. Despite such issues that may plague documentary sources, these are among the most relevant types of data for understanding climatic conditions, particularly for the pre-instrumental time intervals.

Overall, the field of historical climatology has contributed greatly to understanding the climate variability of the recent millennium and to extract the seasonal signals from documentary sources. First, this field unlocked a wide variety of documentary sources dating back to the pre-instrumental period and provided indirect references (e.g., proxy data) on climate conditions. Other direct references are dated back to the instrumental period. Both direct and indirect data provide a seasonal signal (temperature, precipitation, pressure) which has been used to compile long time series of climate related signals. Secondly, special methods were developed in order to transfer the indirect reference signal into data which would be directly comparable to the data provided by instrumental measurements. These methods contributed to extending the time series of instrumentally measured temperature back into the 16th century in different parts of the world, including Europe, Central America, and South-East Asia.

3. Seasonality in the human past: relevance, major research questions and methods

Human behaviour has been shaped deeply by seasonality, but understanding these effects requires transdisciplinary approaches drawing from different components of the earth system (e.g., atmosphere, biology) as well as social sciences. This is especially the case when considering past populations. All life histories involve responses to seasonality, including adaptations to cyclical changes in temperature, humidity, rainfall, ocean currents, cloud cover, and wind (Boyce, 1979). In general, seasonal variations in temperature and moisture influence biological diversity and form the templates for a wide range of life history patterns and evolutionary processes (Varpe, 2017), affecting wide ranges of plants and animals (Conover, 1992; Tonkin et al., 2017; Wolda, 1988), including humans and our primate ancestors (van Schaik and Brockman, 2005). In this chapter, we outline several major research questions representing important current directions in archaeology, history, and the human past broadly. We also summarize methods commonly adopted by archaeologists to reconstruct patterns of seasonality, both directly and through collaborations with Earth system scientists and others. The success of the approaches discussed here for resolving seasonality in the present and the past is closely related to the temporal resolution and the sensitivity of the proxies to environmental change as well as analytical capabilities (e.g., Shackleton, 1973; Comboul et al., 2014; West et al., 2018).

For the definition of specialised terms refer to provided glossary (see Box 6).

Box 6
Glossary for archaeological terms

- **Cultural transmission**: related to TEK (see below), the process by which technology, behaviors, and other aspects of culture pass intergenerationally between individuals within a group or between populations.
- **Demic diffusion**: cultural diffusion of ideas, languages, and technologies accompanied by migrations of human populations.
- **Foraging**: collection or hunting of naturally available resources. While it contrasts food production, foraging still might modify landscape.
- **Traditional Ecological Knowledge (TEK)**: knowledge of ecology and human-environmental relationships developed and/or acquired by native of local peoples over long periods of time through direct engagement with their local environments.
- **Pastoral community**: a population in which herd animals influence cultural systems and make up a large proportion of subsistence resources.
- **Qanat**: ancient underground tunnel systems found in the Middle East and North Africa and Central and West Asia that move infiltrated groundwater, surface water, or spring water to the earth's surface using gravity for irrigation and drinking water.
- **Seriation**: the pattern of stylistic and technological change in artifacts for a particular cultural group in a region. Seriation is often used to determine age of archaeological sites.
- **Subak**: a water and irrigation management system for intensification of terraced paddy fields on Bali island, Indonesia which was developed in the 9th century and is closely related to regional political, economic, and religious systems.
- **Subsistence resources**: resources necessary for individuals or a population to survive. Although this term is often synonymous with food resources, it can include clothing, tools, and shelter.
- **Subsistence strategies**: systems within which humans obtain the resources necessary to survive. They can include hunter-gatherer, agriculture, pastoral, etc.
- **Swidden farming**: also known as slash-and-burn farming, a cyclical farming technique of cutting and burning biomass to create a nutrient base for crop production with the longer part of the cycle is devoted to fallowing to allow biomass to regenerate. Practiced primarily in the tropics where farming is rainfall dependent.

3.1. *Relevance of seasonal changes and traditional ecological knowledge*

Generally, humans are well attuned to their environment and seasonality plays an important role in decision making (Spengler, 2014). Human responses to seasonality are a key aspect of Traditional Ecological Knowledge (TEK), which represent knowledge production systems frequently overlooked by scientists and policy makers (Whyte, 2013). Adapting to seasonally available resources is one of the earliest forms of hominid TEK, predating the emergence of *Homo sapiens* (Speth, 1987). Among our earliest ancestors, the evolution of increased human sensorimotor intelligence is linked to the ability to identify and exploit seasonally available fruiting plants (Melin et al., 2014).

Knowledge of seasonal patterns has always been a component of foraging, pastoral and agricultural strategies. Residential mobility among foragers relies on TEK to determine when particular plants are fruiting, track the seasonal reproductive cycles of marine resources, or predict the locations of animals based on seasonal migratory patterns. Among some pastoralist communities, human birth intervals are tied to seasonality, with conception occurring when both rainfall and food supplies are at their highest levels and when women are attaining their peak nutritional status (Leslie and Fry, 1989). Traditional swidden farmers engage in rainfall dependent agriculture primarily in tropical environmental zones and rely on TEK for cues as to when to clear, burn, and plant crops based on knowledge of seasonal cycles, some very specific and based on TEK knowledge of when monsoon rains begin (Falkowski et al., 2019).

As human populations grew following the advent of surplus agriculture, humans began to rely on engineering to modify their environments to intensify food production beyond the limits of more passive adaptations to seasonal cycles which often involved mobility. The most obvious of these are investments in water management systems to extend growing seasons beyond the range of seasonal rainfall distributions which can vary from the use of terracing to conserve moisture, to draining wetlands to create fertile growing beds (Wealker, 2000), to the massive investments in moving water over longer distances. This includes the Qanat, which originally spread from Persia to Iberia with the Romans, and the Moroccan Khettara (Beckers et al., 2013). Humans developed water management systems for seasonal and perennial arid lands that inevitably impacted the biodiversity and seasonal distributions of plant and animal communities (Barthel and Isendahl, 2013; Tavabe and Azarnivand, 2013). We know that some of these technologies developed concomitant with increasing human populations like the massive Amazonian floodplain fisheries based on an extensive network of earthen fish weirs and overbank ponds in the Llanos de Moxos in Bolivia (Blatrix et al., 2018). These functioned to capture seasonally abundant floodwaters and fish and create a food supply during the dry season. Perhaps the most elaborate example of technological innovation is the Balinese system of water temples and wetland rice irrigation systems which made large scale production possible where it otherwise was seasonally limited. The 1000-year-old Subak system permeates all levels of human economic, religious, and political organization on the island (Lansing, 1987). While most of these systems also emerge from TEK, they also tend to spread by demic diffusion or cultural transmission and to be modified along the way for different environmental conditions, population sizes, or changes in climate and seasonality.

3.2. *Research questions in archaeology*

Seasonally occurring patterns of environmental change have influences on human behaviour and are thus important to consider in the interpretation of archaeological sites and historical records (e.g., Monks, 1981). For this reason, many of the central research avenues within modern archaeology can benefit from the applications of the methods discussed in this review. While most research questions involving the seasonality of past human subsistence and settlement patterns usually fall under the purview of archaeologists, transdisciplinary studies have been at the forefront of understanding the role of seasonality in human-environmental relationships. Current applications are broad, ranging from research on hunter-gatherer populations to complex agricultural societies (e.g., Kennett, 2005; Kennett and Winterhalder, 2006; Lieberman et al., 1993; Monks, 1981).

Archaeologists are not only interested in what resources were available to past populations at different times, but also the decisions that people made in the context of seasonal resource access. Thus, seasonality not only describes environmental conditions, but also the activities that occurred during specific seasons, including how this is reflected in the archaeological record. Traditional chronometric methods including radiocarbon dating and seriation lack the resolution to associate cultural materials with individual seasons, so seasonality-based approaches are used to provide a better understanding of short-term activities that were either conducted every year during specific seasons or during a short period of time during a specific year. After Milner (2005), some of the major applications of seasonality in archaeology are to: (1) gain an understanding of the seasons of a particular activity (e.g., harvests, fishing); (2) identify the season of site occupation (e.g., winter shelter); (3) aid in an interpretation of the function of a special purpose site (e.g., hunting camp); (4) model mobility across a settlement system; and (5) recognise sedentism and perennial occupation sites. These methodological applications of seasonality studies can be applied to address some of the research questions of interest to large swaths of the archaeological community. Furthermore, reconstructing seasonal fluctuations and interannual and longer-term patterns of environmental change can help us to understand the timing and processes behind some of the major changes in human history.

In a general sense, adaptive strategies from throughout the evolutionary history of modern humans and earlier hominin species have been linked to seasonality (Lee-Thorp and Sponheimer, 2015; Potts, 1998). Hominin evolution largely occurred during the variable climates of the Pliocene and Pleistocene (deMenocal, 1995). In this perspective, seasonal fluctuations in temperature and rainfall, and especially interannual variability in these changes, may be one of the factors influencing evolution at different times (Potts, 1998). For example, in coastal environments in South Africa, shellfish availability varies throughout the tidal cycle, but return rates are also influenced by the season, with the most adverse weather which limits intertidal access occurring during the winter from June to September (De Vynck et al., 2016). Although the hypothesis has been challenged (Klein and Bird, 2016), Marean (2016) has argued that mastery of tidal cycles was one of the important factors influencing human evolution.

Environmental change has been associated with shifts in the patterns of seasonal movement across the landscape among a variety of human populations. This can be more broadly aligned with cultural change. In an example from the northern Channel Islands near the coast of Santa Barbara, California, relatively drier conditions during the middle Holocene (7550–3600 cal BP) appear to be associated with increased sedentism and predictable seasonal mobility (Kennett, 2005). During this time, short term low-density occupation sites appear to have been supplanted by a greater focus on the windward northwest coast of Santa Rosa Island. This manifested as high-density coastal sites at the mouths of the largest and wettest drainages on the island, with evidence from the $\delta^{18}O$ record of California mussel shells indicating summer movement to large interior residence bases, where people would have more reliable access to fog water and possibly plant resources (Jazwa et al., 2015). More predictable patterns of annual mobility and higher density within settlement sites allowed for increases in social complexity, which began locally around that time (Glasgow, 1997; Kennett, 2005).

Changes in subsistence and settlement mobility associated with increased social complexity can be representative of broader patterns of culture change related to resource scheduling in response to seasonal variability. In a prominent example, one of the major transitions that occurred in human history was the shift from hunting and gathering to food production, which was an important factor often associated with the development of social complexity (Gordon Childe, 1936). Most of the changes associated with food production and increased sedentism occurred during the Holocene, despite the fact that modern humans have existed for much longer (e.g., Kennett and Winterhalder, 2006). At the least, the climate of the Holocene has been conducive to the appearance of these patterns. Seasonal variability in food resources can be mitigated through storage of grains and other domesticated foods (e.g., Souvatzi, 2008; Testart et al., 1982; Winterhalder et al., 2015) or even wild foods like salmon in the Pacific Northwest (e.g., Cannon and Yang, 2006). Storage among both complex hunter-gatherers and agriculturalists allowed for seasonally available resources to be available during lean seasons and to account for less predictable interannual variability (e.g., Cannon and Yang, 2006; Souvatzi, 2008).

Another broad area of research is the role of seasonal environmental fluctuation in the ability of people to colonize new areas. For example, despite earlier arguments for initial migration into the Americas through an ice-free corridor between the Cordilleran and Laurentide Ice sheets between 13,000 and 14,000 years ago (Haynes, 1964; Martin, 1973; Fiedel, 2000), currently the most prevalent theory is that that the Americas were colonized earlier and the route was more likely along the Pacific coast (e.g., Erlandson et al., 2011; Braje et al., 2020). An important question related to this initial migration is the nature of how these migrants crossed the Cascade and Sierra Nevada mountain ranges into interior zones, including the Great Basin. These high elevation zones would have been snow-covered during much of the year. In the Cascades, sources of high-quality obsidian that were used by Paleoindian populations are above the snowline and would have only been accessible seasonally (e.g., Reaux et al., 2018). For these reasons, reconstructing seasonality in the Great Basin and adjacent mountain ranges is necessary for understanding the initial peopling of the continental interior.

During the late Holocene, there was an expansion in how these high elevation zones were used. In addition to accessing lithic raw materials, people also incorporated high-elevation zones of the Sierra Nevada into their patterns of seasonal mobility in part to hunt (Morgan, 2009). This includes the use of permanent food processing features like bedrock mortars above the snowline. These late Holocene patterns of settlement and mobility were obviously very different from those of the initial settlers of the region, but it is clear that high elevation zones could provide subsistence resources and at the least had to be traversed during entry into the continental interior. Therefore, it is necessary to understand seasonal variations in resource availability and access to migration routes at high elevations to reconstruct the timing and process of population expansion. Other similar migrations to new locations around the world, including out of Africa, into Australia, and to remote Polynesia could also benefit from an understanding of seasonal variability in weather, which could affect food availability, severe weather events, and ocean currents.

In the New World, the transition to agriculture occurred first in the Neotropics and then later in temperate North America. The earliest evidence of this transition related to seasonality comes from the late Pleistocene in the Amazon where humans engaged in seed dispersal of large fruiting trees and palms, a role previously dominated by megafauna (Doughty et al., 2016a,b). Across the Neotropics, the early Holocene heralded warmer temperatures, distinctive seasonal contrasts, and changes in forest and savannah composition as humans emerged as ecological dominants (Piperno and Pearsall, 1998). Domesticates first appear in South America between 10,000–8000 BP (Iriarte et al., 2020) and neotropical Mexico by 8,000 BP, with early cultivation of *Manihot* sp., *Cucurbita* sp., *Dioscorea* sp., *Capsicum* sp., and *Zea* mays, an annual grass and perhaps the most impactful seasonal crop developed in the New World, was first domesticated in Mexico by 8900 BP (Piperno, 2011) but underwent secondary improvements of key traits in South America (Kistler et al., 2018, 2020) before being adopted as a staple there by 5000 BP (Tung et al., 2020) and in Central America by 4000 BP (Kennett et al., 2020). Following the adoption of maize, most neotropical agriculture followed TEK related to the seasonal life-cycle of that crucial plant. Domesticated maize moved to North America after 4000 BP (Swarts et al., 2017), where is joined a host of other domesticates (Piperno, 2001).

3.3. Methodological approaches for applying seasonality in studies of human past

Seasonal changes in precipitation and temperature can dramatically influence the availability of subsistence resources. This includes variability in plant growth and animal migration patterns. For example, ecologists and animal biologists trace the seasonal movement and breeding schedules of migratory animal species (e.g., Overton and

Taylor, 2018). Zooarchaeological studies have focused on identifying the presence/absence of migratory species to estimate season of site occupation (Monks, 1981:180). For example, Monks, 1977: 298 identified the presence of "*birds, sea mammals, and fishes known to prey on herring… to indicate a late winter and early spring occupation of the last two prehistoric components at Deep Bay*". Other methods to identify seasonality in the zooarchaeological record include physiological events, including bone fusion, tooth eruption and wear, antler growth, incremental structures (see Section 4.2), and population structure to name a few (Monks, 1981:185–222). Studies of past populations frequently use botanical or faunal remains to explore how humans adapted their scheduling (patterns of population size, distribution, and mobility) to accommodate the seasonal availability of desirable resources, primarily water, plants, and animals within local or regional ecosystems (Kennett and Voorhies, 1996; Cross, 1988; Loftus et al., 2019). These can be compared with analogous studies conducted among modern hunter-gatherer populations (e.g., Jochim, 1998; Bliege Bird et al., 2008) to understand seasonal foraging strategies. This can include dendrochronology, which can be applied to wood from archaeological sites or logs from trees that grew contemporaneously to human occupation of the region. Tree rings can be used to infer year to year variability in rainfall patterns in environments with predictable seasonal variation (see Section 6).

Bony fish have been studied within archaeological and modern palaeoenvironmental studies to understand seasonality. Methods to identify seasonal variability include presence and absence of seasonally sensitive taxa (Reitz et al., 2012), growth increments and isotopic measurement of fish otoliths (Van Neer et al., 1993; Kennett and Voorhies, 1996), and body-size frequency distributions (Sanger et al., 2020:5–6). Stable isotopic measurements, most frequently $\delta^{18}O$, and elemental ratios, including Sr/Ca and Ba/Ca, in otoliths, the calcium carbonate inner-ear structures of bony fish, offer information on seasonality by indicating changes in water temperature, salinity, and element availability throughout the year (Campana, 1999). Fish otoliths often offer important information on seasonality since the formation of those structures exhibit daily and annual growth increments and therefore allow for the identification of the season of death for the fish, and hence the human fishing activity (Pannella, 1971). In one study in southern Norway, $\delta^{18}O$ from two Stone Age sites showed seasonal patterns for the fish during the formation of the otolith 1 to 2 years before its death. Water temperature estimates from the most recent growth bands correspond to the late winter or early spring (Hufthammer et al., 2010). In another example, red cod (*Pseudophycis bachus*) otoliths from the Shag River in New Zealand allow for the identification of winter and fall seasons of prehistoric occupation of cultural layers at human settlements (Higham and Horn, 2000).

Similarly, $\delta^{18}O$ values for mollusk shell carbonate have frequently been used to estimate seasonal patterns of archaeological site occupation in coastal environments (e.g., Shackleton, 1973; Kennett and Voorhies, 1996; Loftus et al., 2019; Branscombe et al., 2020). These measurements can be used to infer season of death of individual mollusks, which in aggregate provide a way to determine during which seasons individuals targeted those species (see Section 4.2). Based on the context of the site and the rest of the artifact assemblage, we can estimate whether this is reflective of seasonal variations in which food resources are targeted or seasonal mobility between sites. Conversely, consumption of that species during all seasons indicates year-round occupation of the site and consistency in diet.

Water availability can also be an important factor influencing seasonal human behaviour, particularly in arid or semi-arid locations. In Mediterranean environmental zones, for example, freshwater undergoes predictable seasonal fluctuations, with winters typically cool and wet and summers usually warm and dry (Lionello et al., 2012; Gabriela et al., 2021). While longer-term droughts are more readily visible in palaeobotanical and isotopic data from lake sediments (see Section 7), seasonal variability in freshwater can have tremendous effects on settlement patterns, including site distributions and mobility patterns. Fast growing tropical speleothem archives have the potential to produce intra-annual signals to assess seasonal variability through time (see Section 5).

Archaeological studies have used direct measures of seasonality through isotopic measurements of other biological proxies, including human hair from mummified remains (Knudson et al., 2007) or incremental sampling of tooth enamel from domesticated animals (Balasse et al., 2002) and humans (Buzon and Bowen, 2010) to look at seasonal mobility and investments in management of freshwater resources. Furthermore, bioarchaeological applications of tooth cementum annulations (TCA) or cementochronology have the capacity to inform on seasonality as well as other life history events in human and nonhuman species (Naji et al., 2016). Cementum, a growing dental tissue that is regularly deposited and does not remodel throughout the life course, has repeatedly been applied to zooarchaeology, palaeopathology, and bioarchaeology to reconstruct age-at-death and season of death because of its high accuracy (Burke and Castanet, 1995; Dias et al., 2010; Naji et al., 2016; Wall-Scheffler and Foley, 2008; Wittwer-Backofen et al., 2004). Cementochronology had its earliest applications in zooarchaeology and has been a successful tool for estimating season of death and age-at-death in over 72 species of mammals across 21 families and 9 orders (see Naji et al. (2016) for a review of this literature). From archaeologically recovered teeth, it is possible to estimate the age and season of death from seasonal bands in dental cementum that result from variations in microstructure, which reflect changes in the rate of tissue growth attributable to seasonality (Carrel, 1994; Lieberman et al., 1993; Medill et al., 2010; Wall-Scheffler and Foley, 2008). Zooarchaeological analysis of cementum in the context of human settlements have routinely proved useful for reconstructing past patterns of seasonal mobility and subsistence (Rendu, 2010). This method also has utility in historical archaeology as a way of distinguishing seasonality in historic faunal assemblages that include evidence for butchering (Landon, 1988).

In summary, our ability to reconstruct past human behaviours, understand how and why humans developed cultural niches, and untangle how we evolved and diverged from our evolutionary ancestors is contingent on contextualizing adaptations within a seasonality framework. This can be achieved in collaboration with palaeoclimatologists whose complementary expertise on responses of the archives of interest to external forcing and internal feedbacks foster insightful interpretations. New advances in molecular methods and a focus on transdisciplinary collaborations are expanding our ability to ask and address more complex questions, aided by technological advances in chronology building and linking cultural data to climate.

4. Seasonality in marine invertebrates

As is the case with other proxies, one of the major concerns influencing the ability to assess seasonal patterns of change in marine records, and in turn make inferences about human subsistence and mobility, is the resolution of proxy time series. This includes both sampling resolution (i.e., the amount of time integrated in a single sample and spacing between them) and temporal resolution of the tested profile (often the archaeological record). West et al. (2018) comprehensively summarize the current state of sclerochronology, with emphasis on archaeological applications, de Winter et al. (2021) focuses on optimising sampling strategies. Here, we take a focused approach to the role of marine records in reconstructing past climatological patterns and seasonality.

This review focuses in part on the effects of seasonal environmental changes on humans, with implications for present-day climate change and necessary human responses. Archaeologists interact with these patterns in two important ways: (1) applying palaeoclimate datasets to targeted periods of interest (Jones et al., 1999; Kennett and Kennett, 2000; Jerardino, 2017); and (2) using environmental proxies archived in

Fig. 3. Examples of shell midden sites. **A**: Shell mound at Lake Siranda, Pakistan, occupied between 6,900 and 6,700 years ago. Photo taken January 2014 by P. Biagi; **B**: Dense oyster and mussel shell deposits at the dune top site D37, Baja California Sur, Mexico. Photo by C. Jazwa; **C**: Large mounded shell deposit (c. 3 m high) overlooking modern freshwater wetlands that formed following infilling of an embayment via progradation, Blue Mud Bay, Northeast Arnhem Land, Australia. Photo by P. Faulkner; **D**: *Tegillarca granosa* dominated mound BMB/029, Blue Mud Bay, formed between 2287 and 1985 cal BP, showing the dense shell deposit characteristic of these north Australian sites. Photo by P. Faulkner; **E**: Klerk-5, one of hundreds of shell middens along the coast of Peter the Great Bay, Russia, formed between 4,800 and 2,200 years ago. Photo by Y. Vostrezof; **F**: CA-SRI-338, a characteristic red abalone site on western Santa Rosa Island, California, occupied between 5,700 and 5,900 years ago during fall, winter, and spring. Photo by C. Jazwa.

materials recovered from archaeological sites (Shackleton, 1973; Stephens et al., 2008; Gutiérrez-Zugasti et al., 2015; Prendergast et al., 2018; Thomas, 2015; Leng and Lewis, 2016; Colonese et al., 2018). In (2), archaeologists may either do the palaeoenvironmental work themselves or collaborate with climate scientists (e.g., Sandweiss, 2012; Moss et al., 2019). Both approaches focus on one central goal, namely, to understand the environmental context for diachronic trends in human behaviour. This often includes patterns of settlement, mobility, and subsistence. In (1), datasets are often more chronologically detailed, but can be difficult to reconcile with the archaeological record because of differences in scale, resolution, and spatial distance to archaeological sites. In (2), there is a direct chronological (and often stratigraphic) relationship between human activity and the environment because the proxies are human-derived materials, but this leaves us at the whim of the archaeological record, which often includes hiatuses and can be subject to a range of post-depositional alterations (Fig. 3). Here, we focus on both approaches, but acknowledge that each has important limitations.

4.1. Marine proxies for seasonality

Marine carbonates are especially useful for reconstructing past environmental conditions because the ratio of the oxygen 16 and 18 isotopes ($\delta^{18}O$) varies with the isotopic composition of seawater (including salinity) and water temperature (Urey, 1947; Wefer and Berger, 1981). Both variables can fluctuate seasonally in predictable ways, with the geographic context influencing their relative importance. For example, in estuaries like San Francisco Bay, the seasonal variability in salinity results from seasonal snow melt and governs changes in $\delta^{18}O$ in mollusc shells (Schweikhardt et al., 2011). In open-ocean contexts, further from sources of freshwater, fluctuations in salinity are much smaller than seasonal sea surface temperature (SST) change, making $\delta^{18}O$ an effective paleothermometer (Shackleton, 1973; Kennett and Voorhies, 1996; Jazwa et al., 2012; Schöne, 2008; Butler et al., 2013; Hausmann et al., 2017; Prendergast and Schöne, 2017; Parker et al., 2017). In either case, seasonal changes can be tracked. Stable carbon isotope ratios ($\delta^{13}C$) can also provide information about environmental shifts, including differential patterns in upwelling (Sadler et al., 2012), but it is less frequently used as a seasonal marker and rarely applied without $\delta^{18}O$.

While geological archives allow high-resolution paleoenvironmental reconstructions, it is often difficult to obtain seasonal resolution. One of the highest resolved marine records of environmental change is the ODP 893A core that was taken off the coast of Santa Barbara, CA (Kennett and Kennett, 2000). Its top 17 meters (of a total of 200 m) represent the Holocene. The $\delta^{18}O$ signal of planktonic foraminifera reflects SST variability. For the most recent 3000-year period (the first 5 meters of the core), chronological resolution is 25 years, while for the rest of the Holocene, it is 50 years. The unusual high resolution stems from a confluence of environmental and depositional factors (Kennett and Kennett, 2000). Although it is useful for many archaeological purposes, this record does not allow for the extraction of seasonal patterns.

On the other hand, corals often provide a seasonally resolved archive of marine environmental conditions. As colonies, these small invertebrates integrate oxygen and trace elements into their aragonitic skeletal structure and grow large structures with often annual bands of carbonate that can lay the foundation for long-term chronologies of climate change. Coral-based research is often limited to tropical regions because of their narrow temperature tolerance. Long composite records with improved reliability and representation can be constructed using overlapping coral chronologies (e.g., Hendy et al., 2002; Comboul et al., 2014). High-resolution sampling of corals has been used to determine long-term sub-annual SST variations that are clearly visible in modern samples (LaVigne et al., 2013; Sayani et al., 2019). Since $\delta^{18}O$ of ambient seawater varies with both temperature and salinity, other SST-proxies like Sr/Ca and P/Ca ratios (LaVigne et al., 2013; Chen et al., 2018) are used together to allow for more reliable reconstructions of seasonal SST changes.

The possibility of obtaining high resolution data make coral records useful for tracing ENSO patterns (Comboul et al., 2014). For example, the unusually strong 1997–1998 El Niño appeared clearly in multiple coral records (LaVigne et al., 2013). Extending these records into the past, however, adds uncertainty to seasonal records, and thus, corals primarily remain useful for tracing only broad-scale climate changes (Chen et al., 2018). In addition, while some types of proxies rely on a single record from each context, corals can show considerable variability within the record of individual colonies from the same context. Therefore, it is necessary to include multiple corals from a site and develop age models to assess uncertainties (Comboul et al., 2014) to confidently attribute patterns to seasonal SST variation (Sayani et al., 2019).

Another frequently used marine proxy for paleoenvironmental reconstruction are mollusks, particularly those derived from the archaeological record (Fig. 4; e.g., West et al., 2018; Andrus, 2011; Thomas, 2015; Shackleton, 1973). This is a part of the rapidly growing field of sclerochronology, which incorporates growth and age studies of mollusk shells in combination with $\delta^{18}O$ records (West et al., 2018; Thomas, 2015; Butler et al., 2013; Prendergast et al., 2018). Mollusk shells used in sclerochronology are frequently derived from shell midden sites, which often provide stratified records that can bolster chronological resolution (see Koppel et al. (2016) for a more detailed analysis of shell stratigraphy and limitations). The rapid growth rate of certain mollusk species allows SST estimates at seasonal resolution and determination of the season that they were harvested. Shackleton (1973) recognized this characteristic feature and established a set of requirements that mollusk shells and their environments should fulfil to maximise their fidelity as seasonal markers.

Often, the most common components of an archaeological site are not necessarily the best mollusk species for sclerochronological and isotopic analysis. For example, California mussel (*Mytilus californianus*), a relatively fast-growing species that makes up the bulk of many middens along the west coast of North America, has been the target of numerous studies (Fig. 5; Coe and Fox, 1942; Jazwa et al., 2012; Jew et al., 2013; Thakar, 2014). While these analyses have been useful to

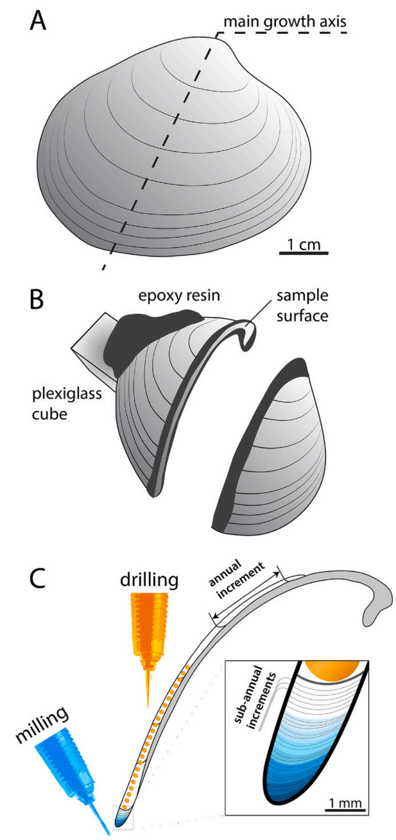

Fig. 4. Shell preparation and sample process of geochemical analyses, after Hallmann et al. (2009, Fig. 2). **A:** Shells are cut along the growth axis and ideally in the longest possible transect to provide a good sampling resolution. **B:** The use of epoxy resin along the cutting section helps to prevent broken and jagged sections. Cutting is often done using a diamond-blade saw. Rectangular objects glued onto the shell provide for a more practical fastening of the sample and a more controlled sectioning process. **C:** Sampling can take place using milling or drilling of the shell layers. Milling is usually done on a smaller scale (micrometers rather than millimeters) to access slow growing portions of the record. In comparison, drilling is more efficient when records need to be sampled extensively and on a millimeter scale. Note that sampling of shellfish records is usually carried out within one layer of the shell (exemplified by white and grey areas of the shell section).

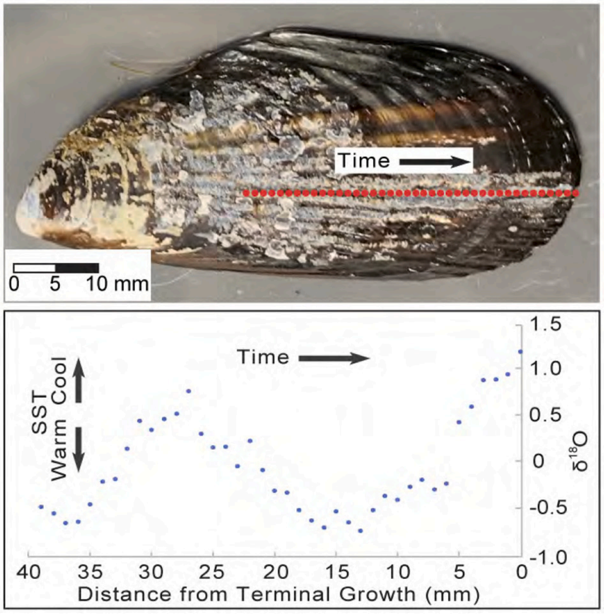

Fig. 5. A seasonal isotopic signature obtained from a *Mytilus californianus* δ^{18}O shell profile. This shell was collected from Santa Rosa Island, California in May 2018 and sampled at 1 mm increments (red dots) using a 0.5 mm drill bit on a Dremel tool at low speed. δ^{18}O has a negative relationship with ambient temperature, indicating decreasing temperature prior to harvest.

gain insights into past SST variability and inferences about seasonality, the considerable variability between individuals must be corrected for by increasing the number of samples collected per shell. Further, shell geometry can make controlled sampling more challenging than the shells from other mollusk taxa. In this regard limpets have proven very useful as they grow relatively evenly compared to other gastropods. In his seminal study on using shell isotopes for seasonal analysis, Shackleton (1973) focused primarily on *Scutellastra tabularis (syn. Patella tabularis)*, which he cross-sectioned in the centre before drilling, a method that is not easily applied to conical or helical shells. The curvature of these shells prevents them from easy sectioning in one straight line covering the entire record, requiring sampling along the outside or only in specific areas. In turn, species with curved shells often, but not always, produce shorter geochemical records of the latest growth period (Branscombe et al., 2020; García-Escárzaga et al., 2019; Hausmann et al., 2017; Prendergast et al., 2016). With the proper sampling strategy, archaeological material can offer climatic data over long periods and of high quality (Hallmann et al., 2009; Burchell et al., 2012; Gutiérrez-Zugasti et al., 2015; West et al., 2018), although many mollusk species (e.g., *Arctica islandica*) that would produce the best climatic datasets may not be abundant in archaeological sites (Butler et al., 2013; Román-González et al., 2017; Steinhardt et al., 2016).

As with corals, recent mollusk studies have also moved beyond isotope proxies to include minor or trace element data. Elemental ratios (e.g., Mg/Ca, Sr/Ca, Ba/Ca, and Li/Sr) in carbonate shells can reflect water temperature (Klein et al., 1996; Takesue and van Geen, 2004; Füllenbach et al., 2015; Ferguson et al., 2011; Bougeois et al., 2016), but are also influenced by internal processes (e.g. growth rates, Durham et al., 2017; Hausmann et al., 2017) or concentration of organics (Schöne et al., 2013). While element mapping has improved our understanding of elemental compositions (Shirai et al., 2014; Poulain et al., 2015) and in some species produced feasible solutions to disentangle different influences (Hausmann et al., 2017), many issues remain unsolved. This is often a product of species and individual specimen variability of elemental proxies within mollusk shells. Advances in rapid elemental analysis through Laser Induced Breakdown Spectroscopy (LIBS, Cáceres et al., 2017; Cobo et al., 2017; Hausmann et al., 2017) point towards elemental data becoming more accessible in the future, improving the datasets necessary to further untangle elemental patterns within marine carbonates.

4.2. Applications of marine shells in archaeological seasonality studies

Archaeological sites are often among the best sources for abundant mollusk shells from well-stratified and dated contexts. Because these shells can be directly associated with human actions, it is relatively straightforward to derive implications for past human activities. While archaeology uses a similar range of environmental archives as the geosciences, their geographic and chronological contexts must be rectified if they are not directly from archaeological sites to determine the environmental conditions encountered by humans. The archaeological relevance of an environmental archive is thus inversely related to its distance to human habitation. The two most frequent applications are (1) inferring seasonal SST fluctuations to evaluate long-term variability in seasonal climate patterns (Jazwa et al., 2012; Surge and Barrett, 2012; Wang et al., 2012) and (2) estimating harvest season from individual shells to interpret whether sites were occupied year-round or during specific seasons (Shackleton, 1973; Kennett and Voorhies, 1996; Gutiérrez-Zugasti et al., 2017; Loftus et al., 2019; Branscombe et al., 2020). Seasonal patterns of environmental change can influence human behaviour and are thus vital for the interpretation of archaeological sites (Monks, 1981).

Since at least the 1970s (Shackleton 1973), mollusk shells have been intensively studied to determine their 'season-of-death', the point in time when the mollusk was collected and consumed by humans. Environmental conditions at the time of death are determined from the last growth increment. Interpretations about the season during which this occurred typically require several measurements along the growth band (Jew et al., 2013; Thakar, 2014), conducted using either microscopic (Hallmann et al., 2009; Milano et al., 2017), and/or geochemical (Mannino et al., 2003; Leng and Lewis, 2016; West et al., 2018) methods. Exactly how many isotopic samples are required per shell is still a matter of debate, but it is clear that single measurements from each shell are inadequate. A single sample provides information about water temperature at the time of harvest (Kennett and Voorhies, 1996; Finstad et al., 2013), but alone has limited utility for determining harvest season because of (1) similar water temperatures recurring multiple times per year (e.g., spring and fall); (2) short-term SST fluctuations associated with weather; and (3) noise associated with imprecise sampling and incomplete mixing of drilled carbonate powder. Several studies resolve this issue (1) by using a sequence of samples which produce SST estimates prior to the terminal SST value and indicate the direction of change over the last month(s) of the individual's life (Mannino et al., 2003; Jew et al., 2013; Thakar, 2014). While this approach circumnavigates issue (1), it is still susceptible to issues (2) and (3). Further experiments have indicated that more samples will help to reduce errors associated with (2) and (3) (Burchell et al., 2012; Jew et al., 2013; Thakar, 2014). Increasing sample numbers per shell seems like a solution to this problem, but it remains to be seen at what point adding more samples does not appreciably increase predictive power. Testing more shells per context may prove more useful for estimating season of occupation of archaeological sites, particularly when considering limited time and funding for geochemical analysis. The ultimate goal of these tests is to maximize the confidence of archaeological interpretations regarding the representativity of the data across a site or time period (Thomas, 2015).

4.3. Reference studies and practical limitations

Modern reference studies are vital tools for building the foundation for any interpretation of archaeological mollusk remains. Ideally, the species found in archaeological contexts are still available today and can be sampled in a similar environment. Oysters and mussels are often still common and can have a long history of exploitation (Jerardino, 2016; Jazwa and Jantz, 2019). Conversely, the limpet *Patella ferruginea*, commonly found in prehistoric sites of the western Mediterranean (Colonese et al., 2011), is now a protected species (Templado and Moreno, 1997) and thus not readily available for reference studies. In other places, species availability has changed dramatically because shorelines have moved, changing the coastal environment (Bailey and Craighead, 2003; Bicho and Haws, 2008; Bourke and Willan, 2009) and complicating the testing of parallels between modern and fossil molluskan records. For example, coastal erosion and/or accretionary processes of progradation and sedimentary infilling may alter the structure of the coastline, modify shorelines and the associated habitats conducive to the growth of some species (Faulkner, 2013; Jazwa and Johnson, 2018). This disconnect of past archives and modern parallels feeds into the main challenges of projecting modern seasonal activities or the seasonal availability of plants or animals into the past.

Furthermore, these tests are often conducted on a single or only a few species for practical or cost-based reasons, limiting our understanding of interspecies variation (Monks, 1981). Understanding the biology and ecology of the tested species is important because they can influence our ability to interpret isotopic or elemental proxy data. Species undergo variations in growth rate through their lives, with rapid early growth and slowing with age, often associated with thinning of layers (Coe and Fox, 1942; Andrus, 2011; Schöne, 2008). Growth pauses (hiatuses) might also occur. Proxy variation may result from seasonal variability associated with SST changes (Coe and Fox, 1942; de Winter et al., 2021) or because of other, less predictable stresses (Andrus, 2011; Lutz and Rhoads, 1980). An example of these complexities relates to isotopic analyses of the infaunal mangrove bivalve *Geloina expansa*, a common component of archaeological assemblages across the Indo-West Pacific. Following preliminary analyses of two modern specimens and a small sample of this taxon (three specimens) from archaeological deposits at Niah Cave (Borneo) (Stephens et al., 2008; Twaddle et al., 2017) carefully analysed *G. expansa*, considering their physiology and ecology. Their results highlight numerous intrinsic (aerial respiration, shifts between deposit and filter feeding, cessation in shell growth with conditions moving outside of this taxon's tolerated environmental ranges) and extrinsic (salinity, temperature, aerial exposure and mixed meteoric, estuarine and marine influence on highly variable landward mangrove habitats) factors creating ambiguities in geochemical data at local scales.

Modern experiments can provide important data for the interpretation of isotopic data. For example, subjecting shells to high temperatures can influence δ^{18}O values (Milano et al., 2016; Jazwa and Jantz, 2019). This tends to be more pronounced in aragonitic carbonate than calcite, but in both cases, substantial changes can occur, which in turn would lead to erroneous estimates of SST and season of harvest. While these changes are limited to high temperatures (in contrast to boiling/steaming), it is possible that they may be encountered when people cooked their meals (Aldeias et al., 2016). Thus, these studies suggested that burned shells should be avoided. Furthermore, recent studies suggest that δ^{18}O and δ^{13}C values can be influenced by the depth in the water column where an intertidal mollusk lived, spending relatively more or less time submerged throughout a tidal cycle. While small in some species (*Mytilus californianus*), these differences can be statistically significant (Jazwa et al., 2020). Lastly, shell-based seasonal indicators can only give positive determinations in which season people occupied a site but cannot inform whether occupation continued during other seasons. Using multiple proxies often provides a more comprehensive overview, but the stratigraphic context and the palimpsest nature of many archaeological deposits must be considered (Bailey, 2007).

5. Seasonality and seasonal bias in speleothems

The manifestation of seasonality in speleothem records critically depends on processes in the atmosphere, the soil and cave environment and during speleothem formation. The seasonal cycle in rainfall distribution and temperature controls the timing and vigor of respiration within the plant community above a cave. This in turn determines the supply of CO_2 to the soil water, controlling the dissolution rate of limestone and precipitation of carbonate in the cave (Fairchild and Baker, 2012). Similarly, seasonal changes in effective rainfall lead to variations in infiltration, directing the flow rate of cave waters through the epikarst. Seasonal variations in temperature and surface winds drive seasonal ventilation within caves, regulating speleothem growth rates (Banner et al., 2007; Noronha et al., 2017; Breitenbach et al., 2015). This seasonal signal is inherently recorded in speleothems from caves located in seasonal climates or regions with a seasonal ventilation regime. Our current challenge is to determine how seasonality manifests in speleothem records, despite being a cave-specific signal, and how this climatic information can be retrieved from speleothems, even thought they grow at different rates. Further issues are the identification of speleothem proxies which are most sensitive to seasonality, such as lamina thickness, hiatuses, and chemical composition. A further challenge is to understand the mechanisms driving seasonal changes in speleothems proxies, e.g., ventilation, rainfall, vegetation and temperature. Additionally, we need to investigate the degree of bias in these mechanisms towards a particular season to provide a framework for interpreting seasonal signals embedded in speleothems.

5.1. *How is seasonality expressed in speleothems?*

Seasonality is generally expressed in speleothems via physical and chemical laminations, e.g. annual banding, similar to tree-rings or varves in lacustrine sediments (Vansteenberge et al., 2020). Due to their stratigraphic growth and layering, stalagmites are preferred as palaeoclimate archives over other forms of speleothems. Lamination in stalagmites is normally linked to seasonal changes of one or more environmental parameters that affect carbonate precipitation and composition. These parameters are manifold and include water supply, carbonate saturation state, dripwater composition, cave ventilation and resulting changes in temperature, humidity, or CO_2 degassing dynamics, which control stalagmite growth rates (Brook et al., 1999; Boch et al., 2011; Baldini, 2010; Noronha et al., 2017). Thus, stalagmite laminae can be related to (i) petrographic/crystallographic changes (such as matrix fabric, crystal density, density of inclusions, crystallization pattern (Frisia and Borsato, 2010; Mattey et al., 2010; Meyer et al., 2006)), (ii) variations of element content (Borsato et al., 2007; Ban et al., 2018; Mattey et al., 2010; Vansteenberge et al., 2020), (iii) changes in luminescence and fluorescence, due to presence or absence of organic acids (Baker et al., 1993, 1999; Shopov et al., 1994; van Beynen et al., 2001), (iv) alteration of the number, distribution density, or size of fluid inclusions (Scheidegger et al., 2010), or (v) changes in the isotopic composition of the carbonate (Mattey et al., 2010; Myers et al., 2015; Ridley et al., 2015), to name just a few.

Occasionally, stalagmites show more than one, or less than one growth layer per year (Shen et al., 2013), e.g. when a bimodal distribution of local effective rainfall and changing dripwater chemistry results in two separate growth periods per year. Alternatively, a growth layer can be obliterated if the dripwater is undersaturated with respect to carbonate during a certain season. This can lead to the dissolution of freshly deposited carbonate, forming a subannual micro-hiatus (Baldini, 2010). Finally, multi-annual, rather than seasonal banding, might be recorded if variation in local infiltration is driven by interannual cycles in meteoric precipitation (Brook et al., 1999; Genty and Quinif, 1996). Detailed monitoring is required to identify the relative importance of the highly variable and cave-specific underlying processes guiding carbonate deposition at each study site.

5.1.1. *Petrographic and mineralogical changes*

One of the most prominent types of layering in stalagmites results from changes in the crystallographic or mineralogical build-up (i.e.,

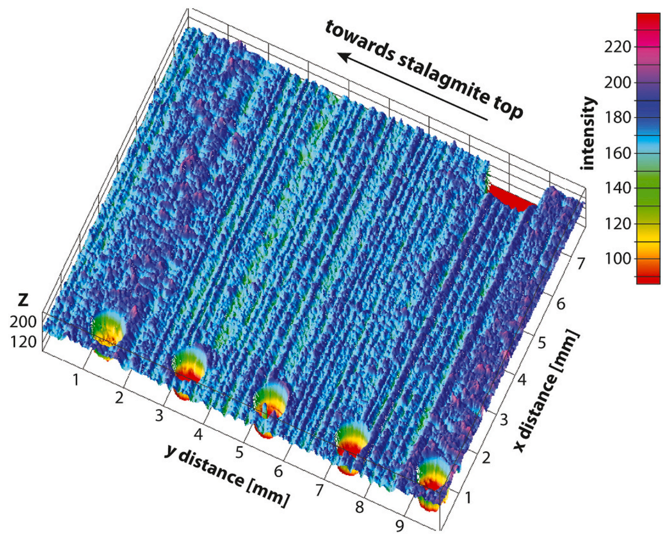

Fig. 6. Example of a false-color surface map of grey values from a stalagmite highlighting regular annual lamination in a stalagmite. Greyscale data were extracted from a high-resolution scan using ImageJ (Rasband, 1997-2018). Annual layers are between 130 and 450 μm thick. The holes represent low resolution drill holes for stable isotope analyses which each integrate 4–7 annual laminae.

crystal fabric, aragonite vs. calcite), which is easily recognizable. Often, growth layers vary seasonally between white, porous, columnar, and translucent, dense, compact laminae, with the latter being thinner compared to the former (Genty and Quinif, 1996; Boch et al., 2011; Mattey et al., 2010; Aharon et al., 2006; Vansteenberge et al., 2020). Occasionally, growth layers vary seasonally between fibrous aragonite and columnar calcite (Railsback et al., 1994). The observed sub-annual changes in growth dynamics and mineral composition are related to changes in dripwater chemistry and cave ventilation, both of which react to surface environmental conditions that include rainfall or temperature changes, effective infiltration, residence time in the the epikarst, temperature gradients between surface and cave air, or wind speed and direction, among others.

While petrographic changes can be revealed relatively easily using microscopy or scanning techniques (Fig. 6), it can be difficult to assign a certain season to a given fabric. The most promising way to solve this issue includes (i) detailed monitoring of the cave environment and hydrochemistry and (ii) high resolution, georeferenced analysis of the lamination pattern in question. The former will reveal modern links between surface, cave, and stalagmite and requires at least one, ideally more than 5 years, depending on the study site. The latter becomes more frequently used with improving instrumentation. Subsampling must be carefully planned to avoid sample cross-contamination, signal smoothing, or aliasing effects (Fairchild et al., 2006).

Regardless of the successful assignment of a proxy to a certain fabric, and fabric itself to a season, one important issue is that we can only work with the premise that modern conditions remained (relatively) similar in the past (modern analogue scenario). While we accept changes in relative strength of seasonal weather conditions, we normally do not expect a complete rearrangement, overturning the relationship between a given season and its assigned fabric. For example, while modern day monitoring might indicate that dark layers are related to wet *summer* season and bright layers to dry *winter* season this relationship might have reversed in the past if winters became wet and summers dry. While such drastic change can often be eliminated based on independent information, it can be of great importance in regions like southern Central Asia, where a Westerlies-derived winter moisture regime could potentially be replaced by a monsoonal regime characterized by summer rainfall (Cai et al., 2017; Fallah et al., 2017). In these settings, a multi-proxy approach with proxies for different aspects of seasonal conditions might be the only suitable strategy. The petrographic characterization of samples is of great importance for the correct interpretation of other proxies, including stable isotopes and trace elements, because of the 'crystallization filter' effect (Fairchild et al., 2006), e.g., crystal size, density or arrangement, can strongly affect the incorporation dynamics of elements, as well as stable isotopes (Gabitov et al., 2012).

5.1.2. Element variability in stalagmites

Speleothem element to calcium ratios (X/Ca), like Mg/Ca, Sr/Ca, or U/Ca are typical proxies for the amount of prior carbonate precipitation (PCP), which varies with water availability (Fairchild et al., 2006). Thus, the elemental composition of stalagmites can be a sensitive recorder for local environmental conditions in the cave system. PCP occurs as prior calcite precipitation (PCcP) or prior aragonite precipitation (PCaP), depending on the host rock composition (PCaP is more likely to occur in dolostone or dolomite) and aqueous solution chemistry (e.g., Mg availability) (Fairchild et al., 2000; Wassenburg et al., 2012, 2016, 2020; Jamieson et al., 2016). Seasonal precipitation patterns or ventilation regimes can drive seasonal variability in dripwater trace element ratios. Thus, trace elements can represent seasonal effective infiltration and/or ventilation-driven PCP.

Element-based PCP proxies are based on simple element-specific distribution coefficients (D_X), which describe the relation between the element/calcium ratio of the carbonate and the element/calcium ratio in the solution (Wassenburg et al., 2020). Crystallographic differences of the various carbonate mineral phases lead to mineral-specific D_X values, and therefore D_X values can be >1 or <1. While D_X values for a number of elements are available for calcite, much less thought has been given to D_X in aragonite (Fairchild et al., 2000; Wassenburg et al., 2016), and references therein). Elements with D_X <1 will show higher dripwater X/Ca ratios in response to a lack of effective precipitation, loss of CO_2 from solution in the epikarst and intensified PCP (e.g., Mg/Ca, Johnson et al., 2006; Wassenburg et al., 2020). Elements with D_X >1, however, will show lower dripwater X/Ca during enhanced PCP. For example, the D_X value for Mg (D_{Mg}) is <1 for both calcite and aragonite, so that dripwater Mg/Ca values will increase due to enhanced PCcP and PCaP in response to drier conditions, but D_U is <1 for calcite and >1 for aragonite, so that dripwater U/Ca ratios will increase in calcite in response to PCcP, but decrease thanks to PCaP in aragonite stalagmites (Jamieson et al., 2016). Since D_X for different elements depends also on other factors, like temperature, carbonate growth rate or initial solution chemistry (Day and Henderson, 2013; Jamieson et al., 2016; Wassenburg et al., 2016) multiple elements should be tested in tandem for robust environmental interpretations. In addition to hydrological changes, cave ventilation may also control PCP (Sherwin and Baldini, 2011; Wong et al., 2011). Cave ventilation can be driven via temperature contrasts between surface and cave air and resulting barometric gradients (Wong et al., 2011). Alternatively, seasonal changes in wind directions and intensity can also alter the exchange of cave air with the atmosphere (Noronha et al., 2017). Unfortunately, the different active processes that can influence X/Ca, e.g. residence time vs ventilation, are difficult to delineate without independent proxy data. Neither could these proxies inform on seasonal precipitation and ventilation changes in regions where ventilation is suppressed during the wet season (Wong et al., 2011). Recently, Ronay et al. (2019) found that the amplitude of seasonal variations in Mg/Ca in a modern speleothem from Mawmluh Cave near Cherrapunji, India, are more sensitive to dry season infiltration than summer monsoon rainfall. This observation can be explained by the influence of dry season ventilation, which enhances carbonate precipitation within the epikarst and the cave. These findings highlight the importance of dry season rainfall for the interpretation of palaeoclimate records. Lastly, seasonal changes in trace elements may be driven by water balance through non-PCP processes. Elements like Zn, Pb, Y, P and others are found in soil colloids, which can be washed into the cave in times of high infiltration (Borsato et al., 2007; Oster et al., 2017). Or they are incorporated into the carbonate depending on the dissociation rate of labile metal-organic complexes, and hence drip rate and water residence time on the stalagmite (Hartland and Zitoun, 2018). It should be noted that elements usually driven by PCcP and PCaP might be influenced by other local factors; e.g. Mg/Ca ratios can be affected by weathering of dolomite phases in soil and host rock (Tremaine and Froelich, 2013; Rutlidge et al., 2014; Belli et al., 2017; Oster et al., 2017). Thus, element dynamics must be evaluated carefully at each site to ensure correct palaeo-environmental inferences.

5.1.3. Oxygen isotope ratios in stalagmites

The isotopic composition of a stalagmite is the result of processes influencing (i) the isotopic composition of meteoric precipitation, (ii) the isotopic composition of dripwater and (iii) the isotopic fractions between dripwater and speleothem carbonate.

Seasonality in tropical and subtropical $\delta^{18}O$ in precipitation ($\delta^{18}O_{precip}$) is often expressed as lower $\delta^{18}O$ values in the rainy season versus higher $\delta^{18}O$ values during the dry season (Lachniet, 2009; Kennett et al., 2012; Partin et al., 2012), although exceptions have been reported (Partin et al., 2007). This empirical observation has been described as amount effect (Dansgaard, 1964; Partin et al., 2012) and is most pronounced in regions with significant seasonal aridity. However, this 'amount' effect can be the manifestation of various atmospheric processes (Galewsky et al., 2016; Bowen et al., 2019) that influence seasonal shifts in $\delta^{18}O_{precip}$, including moisture source changes from a continental to an oceanic source (Araguás-Araguás et al., 1998), or from one oceanic source to the other (Wolf et al., 2020). Seasonality in the stable water isotopes in precipitation is further influenced by climatic conditions at the primary moisture source, including relative humidity (Clark and Fritz, 2004), surface air pressure (Saranya et al., 2018), convection strength and cloud top height (Cai and Tian, 2016), microphysics during condensation (Konecky et al., 2019) and convective versus stratiform rainfall (Aggarwal et al., 2016; Lekshmy et al., 2018). The degree of rainout along the transport path of moisture, and thus the relative distance between moisture source and precipitation location, also plays a key role in controlling the seasonal cycle in low latitude $\delta^{18}O_{precip}$, especially in monsoonal settings (Yang et al., 2016). These processes are linked to large-scale shifts in the regional circulation pattern, mainly the seasonal migration of the ITCZ and SST anomalies in the oceans (Schneider et al., 2014). Thus, $\delta^{18}O$ in precipitation from (sub-)tropical regions is temporally and spatially highly dynamic and often not a simple function of rainfall amount.

In the mid-latitudes (ca. 23–66° N), outside the reach of the monsoon, seasonal variability in the speleothem $\delta^{18}O$ signal can be retained if $\delta^{18}O_{precip}$ either depends on air temperature or temporal rainfall distribution (as in the Iberian Peninsula (Denniston et al., 2018; Baldini et al., 2019) or moisture source changes (e.g., in parts of North America, Hardt et al., 2010; Oster et al., 2017), or a mixture of these processes (Asmerom et al., 2010; Lechleitner et al., 2018). The $\delta^{18}O_{precip}$ at the west coast of North America for example is influenced by temperature changes, a variable Pacific moisture source, and rainout dynamics (Oster et al., 2019). A comprehensive global study revealed that dripwater $\delta^{18}O$ mostly reflects amount-weighted $\delta^{18}O_{precip}$ in regions where the mean annual air temperature (MAAT) is <10 °C (Baker et al., 2019). The same study showed that in somewhat warmer climates (with MAAT between 10 °C and 16 °C) dripwater reflects a recharge-weighted $\delta^{18}O$ signal. This is evident in the Mediterranean, where caves can show pronounced winter season bias in recharge (Verheyden et al., 2008; Nehme et al., 2019). The composition of $\delta^{18}O_{precip}$ in alpine settings has been found to be particularly complex, showing a reversed $\delta^{18}O$-T relationship due to significant contribution of snow melt to the recharge (Lechleitner et al., 2018).

From a hydrological point of view, seasonal growth of speleothems is highly dependent on cyclical (normally annual) water supply. The amount of dripwater and dissolved ions in the water feeding the speleothems is a major parameter that influences growth rate (Fairchild and Baker, 2012; Hartmann and Baker, 2017). However, in-cave water supply is not simply controlled by the total amount of precipitation, but also by processes in the soil and epikarst. The effective precipitation is also an important factor in adjusting the cave's response to climate variability. Other parameters, such as seasonal variability of cave ventilation (thus cave air pCO_2) (Sherwin and Baldini, 2011; Noronha et al., 2017), cave air temperature (Casteel and Banner, 2015) and calcium concentrations (PCP) in the drip water (Baker et al., 2016) add further complexity to the relation between speleothem growth and the isotope signals included. The processes that control effective infiltration in the sub-soil and epikarst are controlled mainly by the local geology. The infiltrating water passes the bedrock either as matrix flow, which describes intra-granular permeability, or as fracture flow, which is water movement along bedding plane partings and joints (Baldini et al., 2006). The relative importance of each flow type determines the residence time of dripwater in the bedrock, and hence its isotopic (and also its elemental) composition (Fairchild and Baker, 2012; Nava-Fernandez et al., 2020). The response time (lag) of a given drip to infiltration can vary from hours to years (Mawmluh Cave: <1 month (Breitenbach et al., 2015), Golgotha Cave: ca. 6 months lag (Mahmud et al., 2018), Soreq Cave: 26–36 years (Kaufman et al., 2003)). The sensitivity of drips to rainfall (lag response) is vital for the achievable signal fidelity in the associated speleothem. A fast drip response makes the drip site more sensitive to individual rain events but increases the background noise in drip rate and $\delta^{18}O$ signal (Mahmud et al., 2018). A lag of several months might allow for thorough mixing of the dripwater and loss of seasonal dynamics (e.g., in Bleßberg Cave (Breitenbach et al., 2019)). For recording a seasonal signal, a drip response of a few weeks to one month is ideal to allow for seasonal variability to be recorded with limited background noise (e.g., Mawmluh Cave (Breitenbach et al., 2015)). Ideally, the seasonal cycle in surface precipitation $\delta^{18}O$ is transmitted into the cave and establishes a similar signal in the isotopic composition of the dripwater (e.g., Asmerom et al., 2010; Denniston et al., 2018). The seasonal response strongly depends on the residence time of water in the epikarst and monitoring is vital to establish in-cave dynamics.

In many (sub-)tropical regions, caves are characterised by intra-annual changes in water supply, dominated by a pronounced rainy season, while air temperature is nearly constant (Cruz et al., 2007; Breitenbach et al., 2015; Denniston et al., 2018). In these regions, $\delta^{18}O$ can be biased towards the season of recharge, which is mostly during the wet season (Baker et al., 2019). However, it is important to understand processes controlling $\delta^{18}O$ in precipitation first, before unravelling the processes at work inside the cave and during calcite deposition. Under favorable circumstances (seasonal climate, fast signal transfer from surface to cave, high speleothem deposition rates) ultra-high resolution sampling in the range of 10–50 μm can be used to extract seasonal stable isotope signals. Secondary ion mass spectrometry (SIMS) has successfully been used on stalagmites from Soreq Cave, Israel, to extract information on $\delta^{18}O$ changes at monthly resolution (Orland et al., 2009, 2012, 2014). In another study, computer-aided micromilling was used to build decades-long seasonally-resolved stable isotope time series of hydrological changes associated with ENSO events in Mesoamerica (Frappier et al., 2002), or monsoonal India (Myers et al., 2015). Such ultra-high resolved datasets are increasingly used to track seasonality not only in (sub-)modern times, but for many hundreds of years (Ridley et al., 2015) or the last interglacial (Orland et al., 2019). A detailed discussion of sampling techniques can be found in the review of Baldini et al. (2021).

Once the driver of seasonal variability in stable isotope ratios of surface and dripwater is identified, it is important to keep in mind that isotope fractionation affects the final $\delta^{18}O$ signal during carbonate precipitation. Oxygen isotope fractionation is inversely related to temperature (ca. −0.24 ‰/ °C at 20 °C, −0.22 ‰/ °C at 10 °C (O'Neil et al., 1969)). A cave-specific water-calcite oxygen isotope fractionation across a range of temperatures and cave environments has been observed (Tremaine et al., 2011), with $\Delta\delta^{18}O/\Delta T = -0.177$ ‰/ °C. Thus, speleothem $\delta^{18}O$ reflects the effects of all three regimes: atmosphere, epikarst and carbonate deposition within the cave (McDermott, 2004; Lachniet, 2009). This also means that speleothem $\delta^{18}O$ can either be negatively or positively related to temperature, or be independent if the two relationships (air temperature-rainfall and water-carbonate fractionation) cancel each other out. A study from Han-sur-Lesse Cave, Belgium, revealed how $\delta^{18}O$ loses sensitivity due to water mixing in the epikarst, whereas $\delta^{13}C$ showed a much stronger seasonal signal (Vansteenberge et al., 2020).

5.1.4. Parameters influencing stalagmite $\delta^{13}C$ and preservation of seasonality

The prospect of the oxygen palaeothermometer developed by Urey (1948), Epstein et al. (1951), Emiliani (1955) and many others resulted in a focus on the oxygen isotope ratio in speleothems (Thompson et al., 1976; Gascoyne, 1992), while the enthusiasm to understand the carbon isotope ($\delta^{13}C$) signal remained limited (Dorale et al., 1992; Holmgren et al., 1995). Interest in speleothem $\delta^{13}C$ gained ground with the realization that $\delta^{18}O$ is influenced by a range of hard-to-decipher processes and that the $\delta^{13}C$ signal contains equally significant environmental information (Baker et al., 1997; Bar-Matthews et al., 1997; Hellstrom and McCulloch, 2000) and can sometimes be more easily interpreted than $\delta^{18}O$ (Fohlmeister et al., 2020). Carbon isotopes have frequently been used as a proxy for vegetation changes (proportion of C_3 vs. C_4 plants (Dorale et al., 1992), or hydroclimate (Genty and Massault, 1999; Genty et al., 2001), although it has often been noted that the $\delta^{13}C$ signal might be influenced by a number of interlinked processes (Rudzka et al., 2011; Fohlmeister et al., 2020). These processes include mixing of CO_2 from the atmosphere with soil-derived CO_2, the latter being affected by root and microbial respiration (Fohlmeister et al., 2010), and degassing dynamics in the epikarst and cave. The CO_2 supply into the epikarst can be continuous (open system) or limited (closed system). The latter can occur under drier conditions with insufficient water supply (Lechleitner et al., 2016). Preferential loss of ^{12}C during CO_2 degassing in the epikarst or in-cave leads to PCP (Fairchild et al., 2000; Lechleitner et al., 2016; Oster et al., 2017) and higher speleothem $\delta^{13}C$ values. Thus, the speleothem $\delta^{13}C$ signal is largely the result of the CO_2 dynamics of the soil-epikarst-cave system and related to both local temperature and moisture variability (Genty et al., 2003; Rudzka et al., 2011; Fohlmeister et al., 2020). Under favorable conditions, $\delta^{13}C$ can act as a very sensitive tracer of local hydrological changes (Ridley et al., 2015; Lechleitner et al., 2017; Asmerom et al., 2020). In regions with a pronounced seasonal climate (e.g., in monsoonal regions) and where signal transport from surface to cave is sufficiently fast, speleothem $\delta^{13}C$ can reflect seasonal hydrological and/or cave ventilation changes and the sensitivity of speleothem $\delta^{13}C$ at seasonal to multi-annual timescales has been shown in numerous studies (Frappier et al., 2002; Johnson et al., 2006; Mattey et al., 2008; Ridley et al., 2015; Asmerom et al., 2020; Vansteenberge et al., 2020). Environmental monitoring and comparison of multiple proxies helps to bolster the interpretation of the $\delta^{13}C$ signal (Oster et al., 2015; Ridley et al., 2015; Lechleitner et al., 2017).

Jamieson et al. (2016) highlighted the advantage of using $\delta^{13}C$ together with trace element data to reveal seasonal hydro-climatic variability. A $\delta^{13}C$ record from Yok Balum Cave in southern Belize had previously been shown to inform on seasonal rainfall dynamics (Ridley et al., 2015). Adding U/Ca ratios (Jamieson et al., 2016) showed that both proxies reflect seasonal dynamics, with lower $\delta^{13}C$ and higher U/Ca values being linked to wetter conditions, while drier seasons result in higher $\delta^{13}C$ and lower U/Ca values. The joint use of $\delta^{13}C$ and PCP-sensitive U/Ca thus provides a powerful tool to reconstruct hydrological changes associated with seasonal shifts of moisture supply.

5.1.5. Organic matter in speleothems

When exposed to ultraviolet light, stalagmites often show distinct fluorescent lamination, which originates from organic matter in the overlying soil and epikarst, e.g., fulvic and humic acids, bacterial remains, or even pollen grains (Baker et al., 1993; Genty and Quinif, 1996; van Beynen et al., 2001; Proctor et al., 2002; Orland et al., 2012, 2014; Quiers et al., 2015). Organic fluorescent layers can be used for layer counting (Shopov et al., 1994), and as independent proxies of past environmental conditions (Baker et al., 2002). The formation of organic layers has been shown to reflect seasonal changes in vegetation or soil microbial activity, which in turn are linked to temperature or precipitation variations (Baker et al., 1993, 1999). Seasonal changes in soil moisture, and related export of organic matter from the soil, can result in annual banding in stalagmites, which has successfully been used to establish counting chronologies. Complications can arise if repeated flushing of organic matter from the soil leads to formation of multiple (intra-annual) bands (Baker et al., 2002; Martin-Chivelet et al., 2017). Understanding the mechanistic link between surface, epikarst and cave can sharpen fluorescence and luminescence as important tools for the reconstruction of various aspects of past seasonal variability.

5.2. Seasonal bias

An important first-order question refers to the potential seasonal bias of stalagmites and their proxies. Unlike a proxy that shows a simple seasonal amplitude change, a seasonally-biased proxy predominantly records a certain part of each year. Such seasonal bias can be introduced either (i) because the stalagmite is isolated during a certain season by, e. g. a frozen water supply Fig. 7 or flooding or (ii) because the proxy is recorded only during certain times of the year (e.g. dust, infiltration, soil-derived elements). Both scenarios still contain a climatic signal, but their intensity (how cold?, length of freezing?, how strong is the soil flush?) is not recorded. Seasonal biases are therefore difficult to detect and even harder to be quantified for the past. Monitoring of cave hydrology and meteorology, together with assessment of geomorphological parameters helps identifying potential complications through seasonal biasing, and sampling can be adjusted depending on the research question, e.g. flood-prone samples can be avoided, or seasonal samples can be targeted on purpose (Tadros et al., 2016).

To highlight the importance of environmental monitoring for identifying the seasonal bias, we discuss the unusual case of seasonal dripwater freezing, which is of particular importance for cave sites with near zero air temperatures (Fig. 7). In continental, high altitude or high latitude locations, cave ventilation can lead to the seasonal development of cave ice (Breitenbach et al., 2014). In southern Siberia, precipitation is highly seasonal, with a maximum during summer (Kostrova et al., 2020). Due to high evapotranspiration in summer and strong frost in winter only a fraction of the total precipitation reaches the sub-soil level as effective infiltration, which feeds drips in caves. Further, strong continentality with mean annual and cave air temperatures near zero (Zhang et al., 2001; Vaks et al., 2013) resulting in extended periods of ground freezing. Under these conditions, infiltration is only available during a short spring interval and autumn. Positive cave air temperatures are established with a cave-specific lag during summer and allow stalagmite growth, but in late autumn, cave ventilation lowers air temperatures below zero, which leads to freezing of infiltrating dripwater as ice stalagmites. Stalagmite growth is thus inhibited in winter (Fig. 7) and only resumes with warming of the cave during late spring and summer. Even small changes of mean annual air temperature can dramatically change the window of stalagmite growth, and thus the season recorded in the speleothem. Seasonal bias is of particular importance for slow-growing speleothems, because interpreting a record that is biased towards one season would lead to incorrect conclusions. The recoverable seasonality signal from slow growing stalagmites depends on the sampling resolution, growth bias, and required analyte volumes.

5.3. Modelling assists extraction of seasonal information

The development of forward models can assist in quantifying the

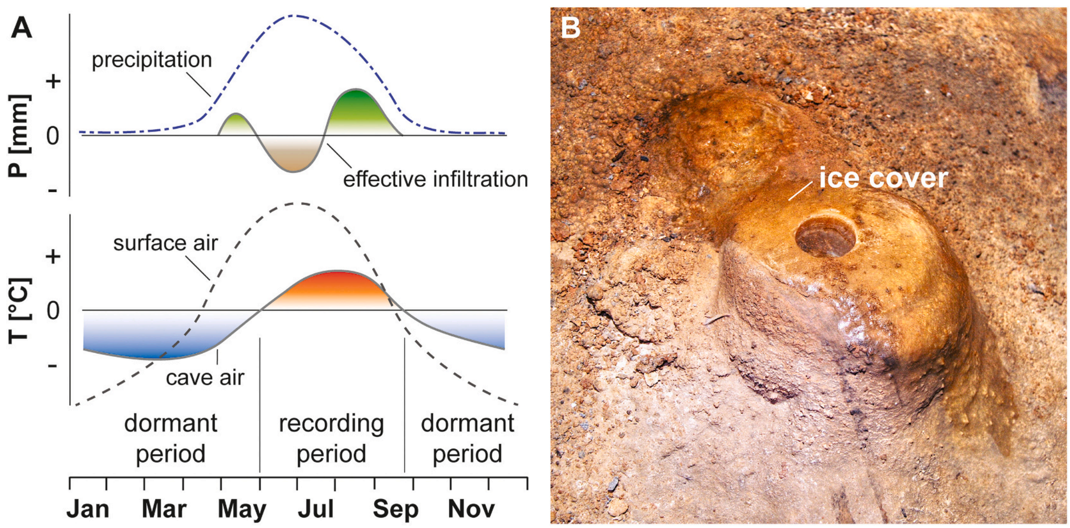

Fig. 7. Seasonal bias in a stalagmite due to seasonal freezing of dripwater. **A**: Schematic seasonal dynamics of key parameters governing the growth under near-freezing conditions. Only a fraction of total precipitation can infiltrate, and freezing conditions in the cave limit stalagmite growth to summer. **B**: Stalagmite with a cap of frozen dripwater in Okhotnichya Cave, Siberia. The drilled hole has a diameter of ca. 30 mm. Photo: SFMB.

sensitivity of proxies to the various climatic and karst processes that can act on a seasonal scale. Proxy system models (PSMs) simulate biological, physical, and geochemical impacts imparted on a climate signal by the cave environment (Evans, 2007; Ault et al., 2014; Dee et al., 2015; Wong and Breecker, 2015) and can translate the signal output from climate models (represented by time series of temperature or precipitation) to proxy space, generating forward-modeled "pseudo-proxy" time series of isotopic or geochemical variability in a stalagmite. PSMs can also facilitate the exploration of various climate scenarios, including seasonality dynamics, to be compared against speleothem proxy data (Baker et al., 2012). Many forward models investigate the evolution of specific proxies in karst and cave systems. For example, iSTAL is a forward model operated in Excel, that can be used to explore the influences of water-rock interactions and PCP on dripwater X/Ca ratios (Stoll et al., 2012). This model accounts for seasonal changes of cave air pCO_2 and can be used to evaluate the effects of seasonal rainfall on trace element proxies (e.g. Ronay et al., 2019). The PSM Karstolution (Treble et al., 2019) combines the karst process model KarstFor (Bradley et al., 2010; Baker and Bradley, 2010; Baker et al., 2013; Treble et al., 2013) with the isotope-enabled fractionation model ISOLUTION (Deininger et al., 2012). Python-based Karstolution accepts climate model time series (temperature, evaporation, $\delta^{18}O_{precip}$, allowing us to evaluate the influence of various processes, including rainfall, temperature, and pCO_2 seasonality, on speleothem $\delta^{18}O$ (Treble et al., 2019). The PHREEQC-based model CaveCalc (Owen et al., 2018) permits the investigation of processes influencing multiple proxies including $\delta^{18}O$, $\delta^{13}C$, and X/Ca. Among other things, CaveCalc can be used to evaluate the impact of seasonal changes in CO_2 gradients and fluid saturation on speleothem proxies. These are but a few examples of the forward models that inform us on how climate signals are modified in karst and cave systems. Such models offer an exciting path to exploring how seasonal bias and changes in seasonality may ultimately be recorded in speleothems.

5.4. Challenges & opportunities

Speleothems are extraordinary archives of past environmental conditions that offer, under favorable conditions, seasonal information. State-of-the-art analytical techniques allow extraction of this information at incredibly high resolution. Challenges remaining are (i) characterising surface-to-cave signal transfer, (ii) understanding and quantifying seasonal bias, and (iii) validation of the assumption that seasonality patterns remain similar to today (modern-analogue methodology). Slow-growing stalagmites from caves characterized by a slow response to surface conditions (i.e., significantly lagged response to surface conditions) and located in regions without clear seasonal changes in hydrology or temperature, might either not contain a seasonal signal or remain unsuitable with currently available instrumentation. Further, it remains challenging to interpret seasonal data from stalagmites in regions, that can be influenced by one of two strongly seasonal, and potentially overlapping climates (e.g., Westerlies and Indian Summer Monsoon in parts of Central Asia). Under conditions with such seasonal bias, only multi-archive/multi-proxy strategies might reveal past shifts of climatic regimes, because even modern long-term monitoring might not be helpful in understanding wholesale switches between different regimes. Seasonally growing stalagmites offer exciting opportunities to evaluate past seasonality, which might inform, and ultimately help improve, complex climate models. Multi-proxy studies at highest resolution (including SIMS, LA-ICPMS, synchrotron element mapping, or fluorescence microscopy) can be coupled with geochemical modeling to trace not only seasonality, but also erratic events, like earthquakes or long-term changes in host rock or soil composition.

6. Climate seasonality in dendrological records

6.1. Theoretical background

Tree stems accumulate wood (xylem) via a circumferential layer of meristematic cells underneath their bark named cambium (Fig. 8). Each year, trees act as living-sensors for a limited interval of time, during the vegetative season, when seasonal climatic conditions change and turn metabolic inactivity into a phase of plant growth, in general, and cambial cell division, in particular. Vegetative season ends when seasonal climatic conditions lower tree metabolic processes to minimal maintenance functions causing a season of cambial dormancy. Depending on the geographic location of a forest site, this dormant season can be initiated by cold periods (for example the winter season in mid to high latitude and mountainous regions), the dry season (in the subtropics and semi-arid regions), or through annually recurring flood events (e.g., in the Amazon river basin). The seasonal dynamics of cambial activity and dormancy are expressed in characteristic differences in the anatomy of wood cells allowing to identify different layers of wood produced each year, so called tree rings (Schweingruber, 1989). Hence, seasonality is the *conditio sine qua non* for the formation of tree

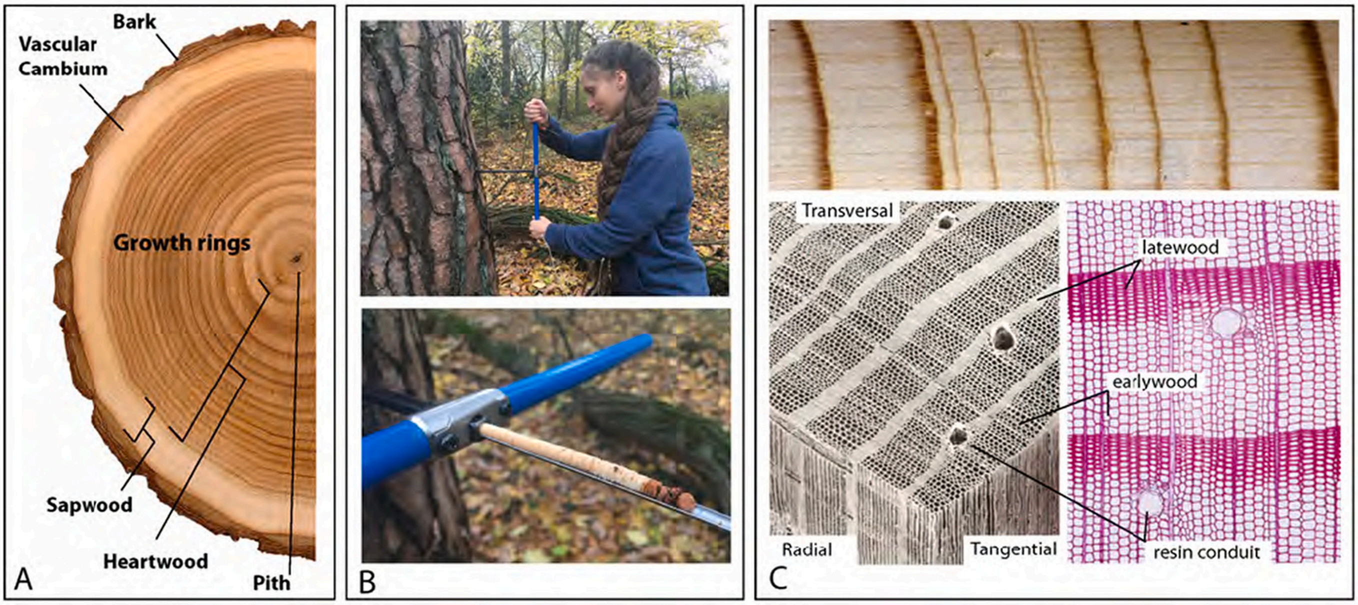

Fig. 8. Tree-ring sampling and preparation. **A**: Anatomical macrostructure of a tree trunk radial section. **B**: Increment borers are used to extract tree cores from living trees. **C**: Typical cores have a diameter of 0.4 cm, their surface is polished and cut with a microtome to expose the transversals section of wooden cells. Trees rings can be accurately counted, dated, measured and separated to chemically extract cellulose and obtain annually resolved time series of C, H, O stable isotope ratios. Preparation of transversal wood cross sections or thin sections enable the quantification of intra-annual cell anatomical parameters through microscopic scanning and image analysis.

rings and dendrochronological dating. During the vegetative season, tree-ring increment growth follows a sigmoid function starting slowly at the beginning of the growing season, followed by a phase of rapid and often almost linear accumulation, before it slows down again and levels off towards the end of the season. This is reflected in the anatomy of wood cells allowing to distinguish between earlywood and latewood (Fig. 8). In most species, earlywood is less dense than latewood. In conifers, this is because wood cells are larger, and their walls are thinner than those of latewood. Likewise, earlywood vessels of angiosperm trees are larger and usually more abundant in earlywood than in latewood. Tree rings can be identified because the dormant period evokes a sharp boundary between latewood of the previous and earlywood of the following tree ring. Within one growth season, however, the wood-anatomical transition from early- to latewood within a tree ring is rather gradual and a clear boundary is hard to define without quantitative measure of intra-ring wood structures (Creber and Chaloner, 1984). Also, the timing of the transition from early- to latewood is more dependent on tree species than on environmental conditions, e.g. earlywood formation of oak (*Quercus* sp.) is usually accomplished in spring before the leaves are fully expanded, i.e. at the time of none or negative net photosynthesis, when tree growth largely depends on reserves (Helle and Schleser, 2004). In contrast, most conifers start latewood formation in summer, induced by the seasonally decreased moisture supply and increased air temperatures which demand a reduction of wood hydraulic conductivity by adjusting the lumens of the water-conducting xylem cells. Hence, the ability of a tree ring to record seasonal environmental information depends on the rate of wood cell formation, but also the longevity of the cells. Within the vegetation period these two features are inversely related; while earlywood cells are formed at a high rate, they may only live for days up to a few weeks. Thick-walled latewood cells are built at very low rates, but may live up to several months and potentially integrate information on environmental or weather conditions over a much longer period of time (Schollaen et al., 2014). As a result, any inter- or intra-annual tree-ring parameter contains proxy information that is weighted by the non-linear seasonal dynamics of wood formation (Ljungqvist et al., 2020).

Trees cannot be viewed as passive physical recorders of environmental conditions. Climatic variability is usually recorded in the tree rings through indirect physiological reactions, rather than direct physical incorporation of a climate signal (Fig. 9). Internal drivers, such as species-specific physiology can constrain climatic significance of tree-ring parameters leading to frequently unstable relationships over time. This may be due to a change in the relative importance of the predominant climatic factor due to drastic changes in environmental boundary conditions and/or because trees may alter their behavior to improve their chances of survival.

Intra-seasonal dynamics of tree-ring formation as well as species-specific tree physiology are well taken into account in modern dendroclimatology. Firstly, by careful selection of tree sites and species (e.g., Schweingruber, 1996), secondly by modern calibration studies and monitoring of climate signal transfer from atmosphere into tree ring (Heinrich et al., 2018) and thirdly, by analyzing and combining a variety of inter- and intra-tree-ring parameters. This approach allows to produce high quality reconstructions of a wide range of different, seasonally changing meteorological variables with quantified precision (McCarroll and Loader, 2004). The suite of tree-ring parameters that can be measured to decipher year to year seasonal variability of climatic quantities begins with tree-ring width (TRW). It is easiest to measure and most frequently applied in reconstructions (Sheppard, 2010). Other parameters, like maximum latewood density (MXD), quantitative wood-cell anatomy (QWA) and stable isotopes (TRSI) of carbon, oxygen and hydrogen ($\delta^{13}C$, $\delta^{18}O$, $\delta^{2}H$) are more difficult to determine. However, QWA and TRSI are well established since several years now and not only allow to obtain inter-annual data, but also provide highly resolved intra-ring data patterns for assessing specific features of seasonality, such as length of a season or amplitude of seasonal fluctuations in temperature or precipitation. TRW and MXD variations have been used most successfully for climate reconstructions at sites where tree growth was limited by one principal climatic factor (Fritts, 1976). TRW and, even more so MXD, correlates best with summer season temperature for cold and moist high-latitude or high-elevation sites, where an increase in temperature in summer extends the growing season and allows for wider tree rings and more dense latewood. Under such site conditions QWA variables (cell wall thickness, cell lumen diameter, and -area) have

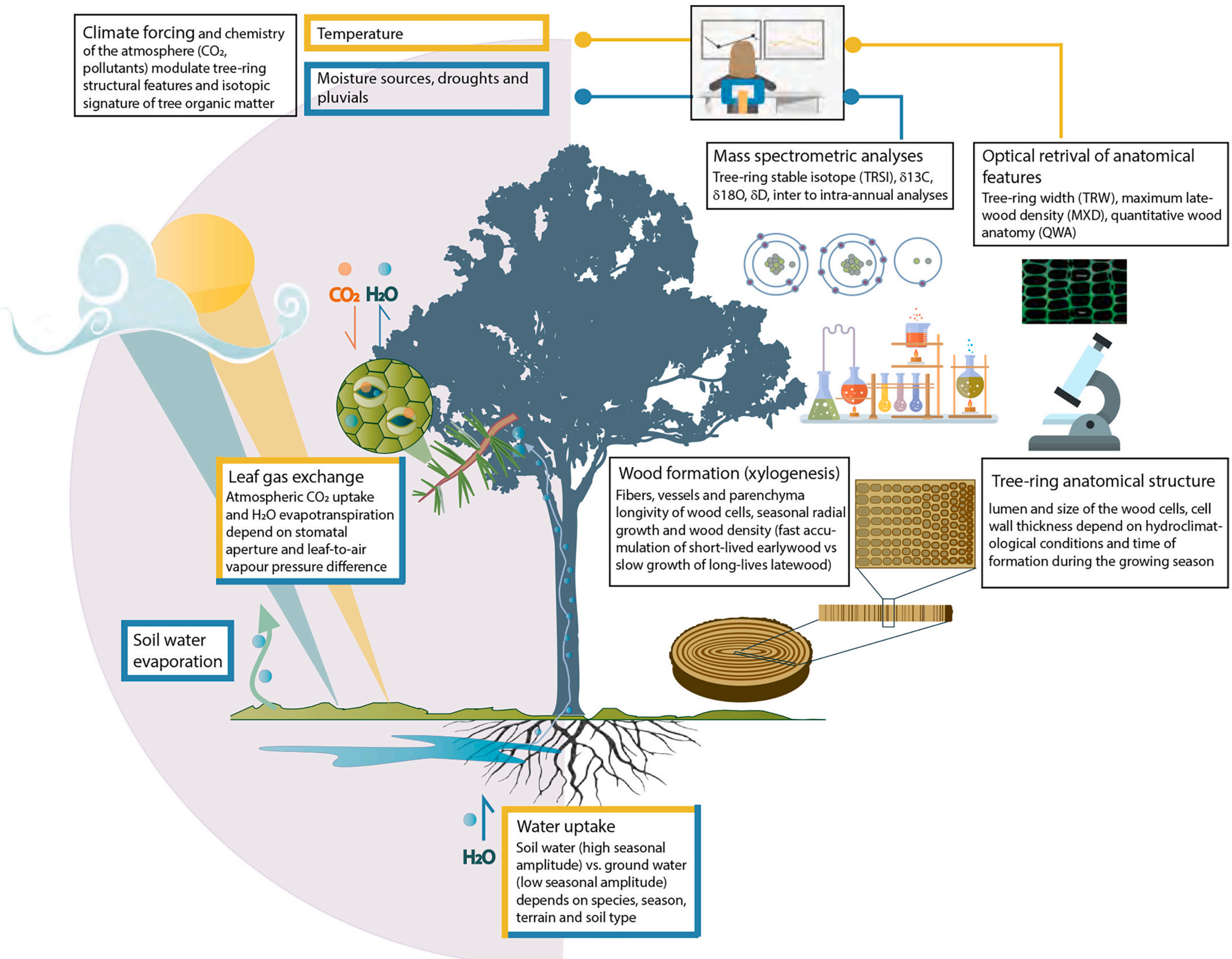

Fig. 9. Schematic illustrating the basic environmental factors and physiological processes affecting the chemical and physical properties of tree rings. These tree ring properties can be quantified by optical and mass spectrometric analyses for reconstructions of past climate variability at sub-annual to annual resolution and centennial to millennial time scales.

proven to provide additional information about seasonal precipitation which cannot be found in TRW and MXD (Pritzkow et al., 2014). A disadvantage of the use of MXD is its restriction to certain coniferous tree species (Bj“orklund et al., 2019). In this respect QWA analysis is of increasing importance as it can likewise be conducted on angiosperm wood (Fonti et al., 2010). Furthermore, QWA parameters revealed significant correlations with high confidence in relation to instrumental climate data at temperate sites, where climate-growth relationships are often diffuse and challenging to recover if proper site selection is not possible and a lack of knowledge of tree species and study region prevails (Drew et al., 2013).

6.2. What seasonal information can be recorded in trees?

Trees and woody shrubs are spread globally between ca. 70° N and 55° S. They occupy several ecological niches and their tree rings record a wide range of seasonal meteorological variables with temperature, precipitation amount and moisture (usually drought) being most frequently reconstructed from tree-ring chronologies.

Tree-ring samples from forest sites where temperature predominantly limits growth have been used extensively to reconstruct past temperature at various locations and regions around the world. Usually summer temperatures were reconstructed (in East Asia, Liu et al., 2020; South America, Lara et al., 2020; and the Mediterranean, Esper et al., 2020). Recently, several papers added to a growing body of cold season temperature reconstructions from China (Shi et al., 2017b) and Poland (Balanzategui et al., 2018).

Precipitation rates is also one of the most common features reconstructed from tree-ring archives as it is reflected both in fluctuations of tree ring width and/or cell lumen area, and in the isotopic signature of stem-cellulose. Because of this strong sensitivity, a large number of reconstructions is available from monsoon-dominated regions (China, He et al., 2019; India, Singh et al., 2009; and Thailand, Pumijumnong et al., 2020), where the south Asia monsoon provides the first order contribution to the annual water budget. Similarly, winter precipitation amount and variability are recorded by cellulose $\delta^{18}O$ in Central Asia (Foroozan et al., 2020), where the westerly disturbances deliver the bulk of annual precipitation. Tree ring growth and latewood also, have been used for reconstructing winter (monsoon) precipitation (e.g., North America, Griffin et al., 2013 or Fennoscandia, Linderholm and Chen, 2005). Generally, tree-ring width and wood-cell anatomy are underperforming in the tropics due to the lack of environmental limiting factors and the poorly understood climate-growth relationships, however tree-ring $\delta^{18}O$ shows negative relationship with precipitation volumes (Baker et al., 2016) and water supply in urban areas (Locosselli et al., 2020). Here, the historical perspective provided by the tree-ring archives can assist public policies related to management of water resources and climate change.

Besides precipitation rates, TRSI are also affected by moisture sources and/or different moisture pathways (Berkelhammer and Stott, 2008); recent studies combine ratios of stable oxygen isotopes in tree rings with Lagrangian moisture source diagnostic to reconstruct changes in the atmospheric circulation and moisture advection (Landshuter et al., 2020). Yet, antecedent precipitation is not always the dominant source of water supply reflected in tree-rings. Depending on their eco-hydrological setting, tree-ring records have been used to reconstruct time series of seasonal streamflow (e.g. Chen et al., 2019), and fluctuations of the water table (Zhou et al., 2019).

In conclusion, tree growth can proceed only as long and as fast as allowed by the primary environmental and physiological mechanism that restrict growth. The only geographical limitation to dendroclimatological investigations are treeless areas (oceans, deserts) and the lack of seasonal limiting factors (e.g., tropics). Ultimately, site-selection determines the strength and the nature of the archived climatic signal. In this sense, the wide spatial distribution of woody plants on the planet unlock powerful features to constrain climate seasonality. Large networks of trees with similar climate sensitivity allows to map how the seasonality of a given environmental forcing varies at the regional, up to continental scale (St George et al., 2010; Ballantyne et al., 2011). In contrast, the sharp changes of sensitivity of trees straddling steep climatic gradients (e.g., elevational transects) can be used to reconstruct different environmental variables and/or the same environmental variable at different times of the year, at the same location (Brunello et al., 2019; Szymczak et al., 2020).

6.3. Are tree rings unambiguously recording one climatic season?

The seasonal fluctuation of environmental parameters determines, at each forest site, the time and speed of tree growth. Calibration by empirical correlation and regression analysis with daily or monthly resolved climate records is traditionally used to indirectly infer the vegetative season of trees and thus the seasonal interval of the recorded climate signal. However, recent studies highlighted the complexity of the intra-seasonal signal preserved in individual tree-rings, which in some cases does not refer unambiguously to a single calendric season.

At the beginning of the vegetative season (spring) most deciduous trees (mostly broad-leaf trees) depend on sugar reserves stored as starch in the late summer of the previous year. This adaptive strategy, aiming at sustaining fast growth before the trees are capable of positive net photosynthesis, results in seasonally recurrent pattern of carbon isotope variations in cellulose of tree rings. Earlywood, built of stored carbon, is consequently relatively enriched in cellulose δ^{13}C compared to the depleted latewood which is built from currently produced carbohydrates (Helle and Schleser, 2004). Thus, some tree-ring parameters, like δ^{13}C, or TRW do usually show some significant auto-correlation between consecutive years and may dampen signals of seasonal changes and extremes (Xu et al., 2020).

Oxygen stable isotopes of tree rings are more promptly recorders seasonal climatic change (Nagavciuc et al., 2020). New insights into oxygen isotopes in Himalayan tree rings, come from a recent study by Brunello et al. (2019), which presents evidence that distinct seasonal water sources are recorded within the same tree ring. The gradual evolution of ambient conditions enables the trees to sustain a linear growth from March to October although the hydrological precipitation regime is characterized by the abrupt transition in mid-June from the pre-monsoon season, with locally recycled moisture and high δ^{18}O values, to the monsoon season, with an oceanic moisture and low δ^{18}O values. Thus, the interval of proxy sensitivity overlaps the relative contribution of two distinct hydro-meteorological seasons that cannot be individually deconvolved without validation with independent proxy records or highly resolved intra-annual TRSI studies (Schollaen et al., 2013).

Thus, most trees are characterized by a periodic radial growth rate. Whether this periodicity matches a scientifically sound definition of season remains to be assessed prior to interpretation. High-resolution intra-annual investigations on tree rings using the microtome or more sophisticated laser ablation techniques is progressively unlocking a retrospective view on plant physiological processes underlying woody plant response to intra-annual environmental changes (Belmecheri et al., 2018).

6.4. Seasonality of discrete events

Tree rings are not only useful to investigate annually or seasonally resolved climate variability, but also abrupt events likes fires, earthquakes and volcanic eruptions. The greatest advantage in using tree rings lies in the tight age control, which can resolve the frequency of events occurring in the past and precisely date the time of the year (or season) in which these events occurred.

Provided the onset and timing of the local growing season of trees is known, perturbations can generate growth anomalies within a tree ring that can be used to refine the dating of the event. As injuries, bordering callus tissue and tangential rows of resin ducts (Fig. 8) are being produced by the tree almost immediately after an event, which allows for more accurate dating, down to monthly resolution (Stoffel and Bollschweiler, 2008). Intra-seasonal dating has been used to infer the periods of increased rockfall activity (Schneuwly and Stoffel, 2008) or the reconstruction of past debris-flow events (Stoffel and Beniston, 2006). Fire scar positions in tree rings agree well with independent records of lightning and ignitions (Caprio and Swetnam, 1995) and provide useful information on the variability of fire seasonality (Rother et al., 2018). This has allowed centennial-long reconstructions of fire season and its length, and fire recurrence dynamics (Stambaugh et al., 2018). High groundwater levels and river overflow events have been documented by identifying multi-year intervals of strongly reduced annual growth (Jansma, 2020); the spatial distribution of trees allows to track the synchronicity of these events in adjacent regions to assess the extent of the floods and thus the scale of the natural forcing responsible for them.

The timing of abrupt changes in local hydroclimate, such as changes in the seasonal moisture sources or the inflow of extreme highly convective cyclonic events can be obtained from high-resolution δ^{18}O analyses. Li et al. (2011) unraveled the onset of tropical cyclone activities that are characterized by abrupt decline in δ^{18}O values, with a "V-shape" pattern in tree-ring latewood. Similarly, the intra-seasonal variation in δ^{18}O of cellulose in tree rings from the Quinghai-Tibetan Plateau reflects variation in the δ^{18}O of precipitation associated with incursion of the Indian summer monsoon (Zeng et al., 2016), the authors suggest that the minimum intra-seasonal tree ring δ^{18}O value might be used to infer and reconstruct the timing of the local monsoon onset. Distinct subseasonal isotope patterns seem indicative for years with heavy rainfall events from pre-monsoonal cyclones in Oman (Slotta et al., 2021), so that cyclonic activity can be potentially tracked back for hundreds of years (Berkelhammer and Stott, 2008).

In summary, in temperate regions with distinct seasons, modern tree ring analysis techniques allow to identify the frequency and the intensity of seasonally recurrent natural processes. These analyses deepen our understanding of the nature, magnitude and frequency of small-scale natural hazards with unmatched chronological control.

6.5. Concluding remarks

Trees constitute a remarkable archive with a wealth of ecological and environmental information and that allows insight into past changes at multi-annual to sub-seasonal level. Tree ring chronologies capture only a fraction of the total climate variability and their response is often limited to specific seasonal "windows". Additionally, within this active window, tree-ring proxies may not respond to a single environmental variable, or may be disproportionately dominated by a subset of the entire growing season. In this sense, tree rings may not record, at each location, the variables and seasons of greatest climatological interest. However, tree rings are high-fidelity multi-proxy archives, where structural and chemical proxies enable palaeo-environmental reconstructions in a wide range of locations around the world. Tree ring width, earlywood/latewood ratios, wood density, cell-wood anatomy, and stable isotope ratios ($\delta^{13}C$, $\delta^{18}O$, $\delta^{2}H$) exhibit distinct sensitivity to environmental variables and can be used to obtain distinct climatic information. Ultimately, the most promising and powerful approach would be to combine the information from all of these proxies within each ring to jointly constrain environmental conditions throughout the record. Such multi-proxy approach could be best interpreted in the frame of a unified bio-physical model, which could be obtained by developing and conditionally combining the mechanistic transfer-functions referring to each proxy (Brunello et al., 2019 and references therein).

The recent advances in analytical techniques enable us to analyze progressively smaller samples, (quantitative wood-cell anatomical features as well as intra-seasonal isotopic measurements) resulting in substantial gain in seasonal specificity and detection of discrete, abrupt events. The combination of highly robust chronologies, spatial coverage and signal replication, as well as robust physical understanding of wood formation and isotope fractionation in plants, makes tree rings a unique and powerful tool to investigate climate seasonality, providing long-term information on climate, ecology and archaeology as far back as thousands of years.

7. Varves – seasonally resolved sediment archives

Lakes, estuaries and oceans have the potential to record seasonal climate variability expressed as changes in the productivity, mineral precipitation or supply of material when deposition site is sheltered from currents, wave activity, turbidity flows, or bioturbation (anoxic or suboxic conditions). Annually laminated sediments - varves, are one of the most pronounced manifestations of seasonal changes within sedimentary archives. Per definition a varve is a sequence of layers, deposited in an aquatic environment within a single year. A varve comprises at least two distinguishable laminae, a couplet, each formed in response to seasonal fluctuation of physical, biological or chemical processes ultimately related to temperature or precipitation change. Varved sediments are found in a wide range of environments from marine to lacustrine and at all latitudes (see reviews by Schimmelmann et al. (2016) and Zolitschka et al. (2015) on marine and lacustrine varves, respectively). Continuous varve records can reach back thousands of years and cover abrupt climate changes of the last glacial and deglaciation (Bronk Ramsey et al., 2012; Zolitschka et al., 2000; Hughen et al., 1996), transition to Younger Dryas and the entire Holocene (Brauer et al., 2008). The seasonal resolution coupled with multitude of proxies, from lamina thickness and composition to geochemical signatures, make varve records one of the most detailed continental archives of past climatic and environmental change (Brauer et al., 2015; Zolitschka et al., 2015).

7.1. How varves record seasonal signals

The seasonal variability in temperature and precipitation causes change in physical, biological and chemical processes in the catchment (availability and supply of detrital material and nutrients) and in the water body (presence of aquatic components, e.g., algae, diatoms, minerals precipitating in surface water). Consequently, varve types fall in one of the three classes; (i) clastic, (ii) biogenic and (iii) chemical (endogenic varves *sensu* (Zolitschka et al., 2015)) or their combination (Fig. 10). Clastic varves consist of sand to coarse silt lamina deposited in response to vigorous inflow, and fine silt to clay sized particles deposited from suspension during limited inflow. Such varve type is common in Arctic and Alpine glacially fed lake systems (Hardy et al., 1996; Gilbert and Lamoureux, 2004; Amann et al., 2015). Biogenic varves form due to seasonal changes in biogenic production in the water column and/or on land. Such varves are found in lacustrine and marine environments in temperate, subtropical and tropical climates and only rarely in boreal (Saarni et al., 2015; Støren and Dahl, 2012) or arctic lakes (Chutko and Lamoureux, 2009). Typically, biogenic varve comprises a lamina consisting of diatom frustules or algae related to spring and summer blooms and a fall/winter lamina consisting of degraded plant detritus, amorphous organic matter and often metal sulfide or siderite precipitating at the lake bottom in anoxic conditions (Schimmelmann et al., 2016; Zolitschka et al., 2015; Brauer et al., 2008; Leng et al., 2013). Seasonal changes are mediated into chemical varves when the solubility of dissolved ions, such as calcium, magnesium or sulphate, in surface water is exceeded. This happens due to evaporative concentration (physical trigger) or following rapid changes in CO_2 and pH related to phytoplankton (biological trigger). Gypsum and halites are typical components of chemical varves in arid or semiarid climates (Ben Dor et al., 2019), while carbonates (calcite and/or aragonite) prevail in temperate climates (Dean et al., 2015; Mangili et al., 2010). In case of chemical varves two laminae might differ in crystal size, or a laminae composed of minerals precipitated in surface water follows a laminae of detrital, allochthonous material. In modern lakes and in fossil record, combinations of two or even all of the three types are common. For example, clastic-biogenic varves are typical from boreal to arctic environments while chemical varves often contain biogenic or organic laminae (biochemical varves, Zander et al., 2021). Last but not least, the prevalent type of varves can change through time (Ben Dor et al., 2019).

7.2. How varves are used to reconstruct seasonal signals

The key to ensure the fidelity of the varve record and its seasonal signal is the thorough understanding of the depositional environment. In particular, similar laminae can be formed by several, very different processes. In Arctic regions the clastic laminae result from temperature

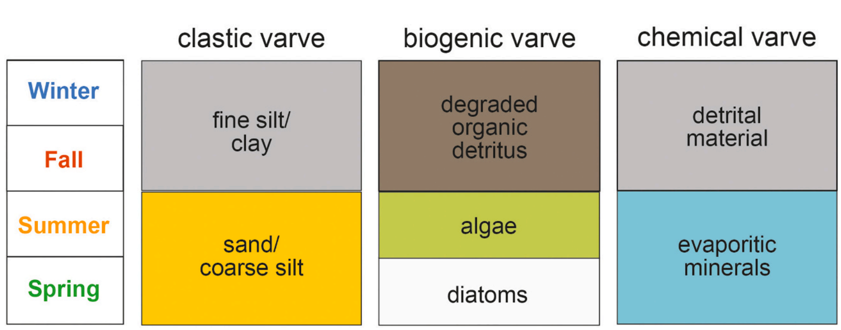

Fig. 10. Simplified models of deposition of clastic, biogenic and chemical varves. For comparison check (Roeser et al., 2021; Zolitschka et al., 2015) who provide complex and detailed models.

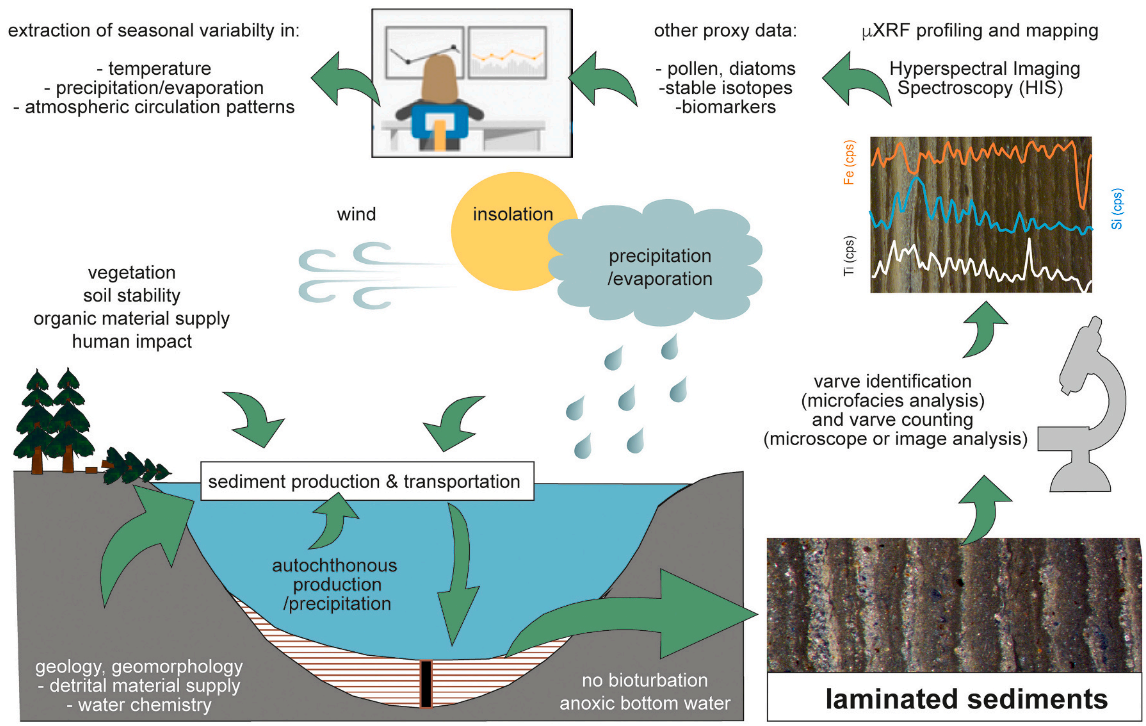

Fig. 11. Schematic illustration of how environmental conditions are reflected in the composition of laminated sediments, and how these features can be quantified to reconstruct past climate variability at inter-annual to millennial time scales.

increase and ice melting in summer, while in boreal zone with snow-rich winters a clastic laminae results from catchment erosion following the melting of snow in spring (Ojala et al., 2013; Saarni et al., 2016). In lower latitudes chemical laminae often form as a consequence of rainy (Hughen et al., 1996; Romero-Viana et al., 2008) or windy (Chu et al., 2009) season, when waters with contrasting properties are mixed, but spring algae blooms or summer evaporation might also trigger mineral precipitation (McCormack et al., 2019). Further, it is possible that a similar kind of lamina is formed several times within the same year. This can occur due to several pulses of glacier melting at arctic/alpine environments, multiple floods in spring and fall at mid latitudes, or multiple algal blooms in a single growing season (e.g., spring and autumn). While several models of varve formation exist, understanding local in-catchment processes and response to climatic forcing is essential for accurate interpretations. Taking into account these unknowns and uncertainties, interpretation of varve records requires calibration – a detailed identification of laminae-forming processes, optimally through combination of monitoring meteorological parameters, chemical profiling of lake water column, and sediment trap- and surface sediment sampling (e.g., Dean et al., 2015; Roeser et al., 2021, Fig. 11). Moreover, in case of sedimentary records independent dating method (e.g., tephrochronology, radiometric, or palaeomagnetic methods) is essential in confirming the annual nature of the laminae and ensuring a true 'varve' status (Fig. 11).

The modern methods applied to varve records include investigation of physical, (including optical), and chemical properties. Physical investigations are mostly non-destructive and involve qualitative analyses like microfacies analyses which is a description of components and structures, but also semi-quantitative analyses like micro X-Ray Fluorescence (μXRF) elemental profiling and mapping (Davies et al., 2015) and Hyperspectral Imaging Spectroscopy (HIS) (Butz et al., 2015). μXRF provides estimation of major element concentration in the sediment (Al, Si, S, K, Ca, Ti, Mn and Fe) which might be related to allochthonous input, biological activity or mineral precipitation, while HIS is an indicator of pigments which might be traced to specific biomarkers. Further, application of color software to digital images of sediment surface or to X-radiographs produces gray values which in turn can help to define seasonal laminae semi-automatically (Petterson et al., 1999) and aid in varve counting, and in measuring varve thickness and thickness of individual laminae (Fig. 11). Variations in varve thickness might be translated to changes in a seasonal process leading to respective laminae formation. For example: clastic laminae thickness might inform on runoff/ erosion intensity and serve as a proxy of the length/ amplitude of rainy or flood season (including floods due to snow or glacier melting) (Romero-Viana et al., 2008). Biological laminae thickness might inform on oxic/anoxic conditions at the lake bottom and serve as a proxy for windiness or productivity (Brauer et al., 2008).

Traditional microfacies analyses performed on thin sections can be implemented by Scanning Electron Microscope (SEM) imaging providing excellent documentation of sedimentary micro-structures and components (Brauer et al., 2015; Zolitschka et al., 2015). Recent instrumental advances, the increased precision and resolution with decreasing amount of required material further facilitate multi-proxy approach for seasonally laminated material and allow destructive but quantitative geochemical analyses of individual varves (Mangili et al., 2010; Zander et al., 2021). Geochemical analyses such as stable carbon and oxygen isotope composition, total carbon, total organic and inorganic carbon, total sulphur and total nitrogen are applied to explore annual-to-seasonal signals of productivity, precipitation/evaporation, temperature and water-column mixing (Mangili et al., 2010; Zander et al., 2021).

7.3. Challenges: incorrect assumptions, seasonal bias and changes in proxy sensitivity

The methods listed above are powerful tools to extract signal from both varved, and non-laminated sediments. The obvious advantage of varved material is its resolution, but the interpretation should be still cautious. Recent calibration studies from Polish lakes challenge traditional mechanisms of biochemical, in particular calcareous, varve formation and suggest that both, timing and the trigger of precipitation might be at odds with generally accepted assumptions. Roeser et al.

(2021) documented presence of triplets rather than couplets, with additional varve sub-layer consisting of re-suspended carbonate material. Zander et al. (2021) found a relation between a dominant varve type and meteorological conditions, in particular either wind strength or temperature prompting precipitation of calcite.

Beyond monitoring, careful examination sedimentary material is also important. Depending on the sedimentation rate physical sampling of individual year or season is not always feasible. Integrating several years in one sample might mix material from seasons or depths different than assumed. Such mixing might considerably influence geochemical signature of analyzed material (Mangili et al., 2010; McCormack and Kwiecien, 2021).

When juxtaposing varve structures to meteorological time series it must be taken into account that varve year is not exactly comparable to calendar years. The beginning of the varve year is related to the change of season while calendar year changes in the mid-winter (summer) on the northern (southern) hemisphere. Hence, the accumulation of the seasonal laminae does not necessarily reflect the conditions of the ongoing season, but like for example in case of boreal varves, the clastic lamina is deposited rapidly during spring, although the intensity of catchment erosion is related to the snow accumulation during the previous winter (Ojala et al., 2013). The amount of snow controls the amount of water released during melting period and consequently controls the intensity of spring flood and the volume of catchment erosion.

Environment-proxy relationship established by calibration between proxy data and instrumental and observational time-series might have changed over time. In case of multi-millennial varve records, the possible change of proxy sensitivity is a relevant question (Brauer et al., 2008; Martin-Puertas et al., 2012). External and internal forcing changes, internal feedbacks and anthropogenic activities in the catchment can modify the way how the lake reacts to seasonal changes and how these are translated into sedimentary record.

8. Seasonality in continental ice bodies

Continental ice is a powerful climate archive that directly preserves numerous proxies that inform on seasonal changes in atmospheric conditions. Major efforts have been undertaken to utilize continental ice to reconstruct past climate on various spatial and temporal scales. Of particular importance are the ice sheets of Greenland and Antarctica, but also polar and mountain glaciers, and numerous ice cores have been drilled since the middle of the 20th century. More recently, continental ice preserved in caves and permafrost has been recognized as a valuable archive of past climate and environment.

Here, we briefly review the potential of glacier ice, cave ice, and permafrost ground ice to reveal seasonal information. We strongly focus on stable isotopes of water as proxies for temperature and moisture sources.

8.1. Polar and mountain glaciers

Ice cores are arguably the single most important archives in the efforts to decipher late-Quaternary climate variability, due their outstanding time resolution and preservation of various proxies of past environmental conditions, including atmospheric gas composition. Ice cores have been drilled in high altitude and latitude ice caps and glaciers (Jouzel, 2013), in ground ice (Porter and Opel, 2020), and cave ice deposits (Perşoiu et al., 2017), yielding information on past temperature, precipitation, and atmospheric chemistry, to name just a few.

By far the most successful are the polar and glacier ice cores, in which a variety of physical and chemical parameters inform on past environmental variability: layer thickness and presence of melt layers; water δ^{18}O, δ^{2}H, and deuterium excess ($d = \delta^{2}H - 8 * \delta^{18}O$) (Dansgaard, 1964), major ion concentrations, gases (including CO_2 and NH_4) from fossil air, or cosmogenic isotopes. Several of these parameters vary cyclically throughout a year, but only a handful capture climatic information. We have grouped these into 1) proxies capturing seasonal dynamics of selected climatic parameters (water δ^{18}O and δ^{2}H) and 2) proxies reflecting season-specific climatic elements (water δ^{18}O and δ^{2}H, Na^{+}, K^{+}, melt layers), and below we discuss these in more detail.

The ice-core basics are well known and will only be marginally touched upon here. Ice formed through the diagenesis of continuously accumulating snow preserves the regional climatic history at time scales reaching several hundred thousand years (Augustin et al., 2004). While mid-to-low latitude glaciers preserve a predominantly *cold season* climatic signal, polar ice caps and ice sheets accumulate snowfall year-round, thus preserving *annual and potentially seasonal* information.

The seasonal dynamics of climatic parameters are preserved by water δ^{18}O and δ^{2}H from high accumulation sites in Greenland (Vinther et al., 2010; Sjolte et al., 2020) and the Tibetan Plateau (Thompson et al., 2018), but are generally missing in glaciers from winter-only accumulation sites at lower latitudes and the low accumulation sites in Antarctica. In precipitation, δ^{18}O and δ^{2}H have clear annual cycles, with a summer maximum and a winter minimum. Ideally these cycles are preserved and offer a clear picture of summer and winter air temperature changes on annual scales (Vinther et al., 2010). However, several problems plague the simple interpretation of δ^{18}O and δ^{2}H as proxies of past air temperature (Jouzel et al., 1997). These arise from changes at/of the moisture sources and tracks, changes in the seasonality of precipitation, changes in the strength of the inversion layer and effects of post-depositional processes.

Before the δ^{18}O of precipitation is locked in ice, it already carries with it a full history of weather and climate variability, including moisture source, rainout and precipitation dynamics. Initially, δ^{18}O of polar ice was used as proxy for mean annual air temperature (MAAT), but later work suggested that MAAT variability is better captured by winter δ^{18}O only (Vinther et al., 2010). In Greenland, winter precipitation δ^{18}O is strongly linked to W Greenland temperatures, while summer precipitation δ^{18}O carries a temperature signal of W Iceland (Vinther et al., 2010). Thus, while the seasonality of δ^{18}O in precipitation can be reconstructed from ice cores, this will not necessarily represent the annual cycle of air temperature at the site (or any other). Complex interactions (Holme et al., 2019) between seasonally distinct large-scale atmospheric patterns (e.g., winter-dominating North Atlantic Oscillation vs. summer-dominating Atlantic Multidecadal Oscillation) and oceanic processes (sea ice export, position of sea ice edge) modulate δ^{18}O in precipitation over polar ice sheets (Delaygue et al., 2000; Steen-Larsen et al., 2014). Moisture source changes also influence the stable isotope composition of oxygen and hydrogen in precipitation feeding mountain glaciers (Fisher et al., 2004; Perşoiu et al., 2017), resulting in changes similar to those induced by local temperature changes and/or changes in the season of precipitation.

Apart from these processes induced by seasonally varying influences, *changes in the seasonality of precipitation amount* (i.e., variations in warm *vs.* cold season precipitation amount) modulate precipitation δ^{18}O and δ^{2}H and ultimately, ice (Jouzel et al., 1997). As the δ^{18}O in precipitation is strongly influenced by seasonally distinct precipitation amount-weighted temperature (Crawford et al., 2014), changes in seasonal amount of precipitation modify the δ^{18}O signal in addition to changes in air temperatures.

Changes in the strength of the inversion layer leave a distinct seasonal imprint on δ^{18}O and δ^{2}H of precipitation (Fisher, 1992). Inversion layers above (mainly) ice caps and ice sheets results in higher temperatures at which precipitation forms compared to those near the surface. Such inversions are more frequent in winter and influenced by temperature changes, becoming more frequent in recent decades (Shahi et al., 2020). Strong inversion situations could have played an important role during cold periods (Cuffey et al., 1995), potentially affecting the comparability of seasonality of cold and warm periods.

Both, structure and stable isotope geochemistry of the snow pack are altered by *post-depositional processes* (Casado et al., 2018). Wind scouring removes part (or entirety) of the annual accumulation, leaving annual layers biased towards one (summer) season, or missing altogether. Diffusion in the firn can smooth out the annual cycle (Johnsen, 2007), while condensation and sublimation can add or remove ice crystals from the snow pack, further modifying the original $\delta^{18}O$ and $\delta^{2}H$ signals (Stenni et al., 2016).

In summary, ice cores drilled in areas with high accumulation rates preserve seasonally-distinct precipitation $\delta^{18}O$ and $\delta^{2}H$, but these are not easily translated into local seasonal variability. Large-scale circulation patterns, changes of moisture sources and paths to the site, and factors active during and after precipitation play important roles in forming seasonally-distinct imprints of the final $\delta^{18}O$ and $\delta^{2}H$ values in ice.

A final complication that strongly affects ice core $\delta^{18}O$ and $\delta^{2}H$ surface melting, percolation of water through the snow mass, and subsequent freezing. These processes are accompanied by isotopic exchange and kinetic fractionation that alters the original $\delta^{18}O$ and $\delta^{2}H$ values (Koerner, 1997). However, the melt layers formed by these processes in the ice could be used as indicators of the frequency of summer melt events (Grinsted et al., 2006).

Several other chemical and physical parameters reveal seasonal climate variability. Sea-sourced sodium ($ssNa^{+}$) and continental-sourced potassium ($nssK^{+}$) are transported onto polar ice sheets in a seasonally variable manner, with $ssNa^{+}$ peaking in winter and $nssK^{+}$ in spring (Legrand and Mayewski, 1997). Thus, these chemical species can indicate seasonal atmospheric circulation patterns, and inform, for example, on the strength of the Siberian high-pressure system (Meeker and Mayewski, 2002).

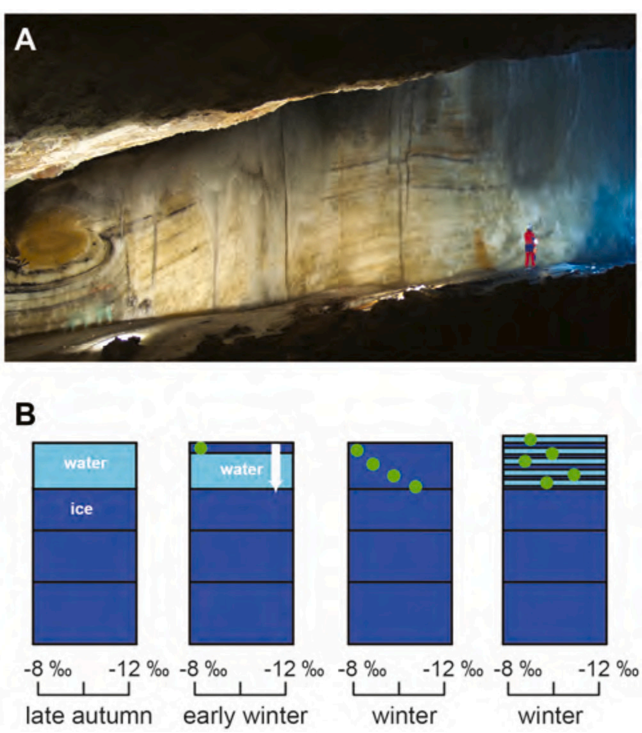

Fig. 12. **A**: The vertical profile of the ice block in Scărişoara Ice Cave. Annual layers are visible, rich in either surface-derived organic matter (black) or cryogenic cave carbonate (white). **B**: Conceptual model of development of $\delta^{18}O$ values in annual layers in cave ice. In autumn, a layer of ice forms on top of the existing ice (1st column). In early winter (2nd column) a layer of ice (enriched in ^{18}O) forms atop the water column. Arrow indicates freezing direction. Subsequent freezing of the water layer (3rd column) will result in successive layers with decreasing $\delta^{18}O$ values. Freezing of dripwater will result in thin layers of ice (4th column), each preserving the $\delta^{18}O$ of parent water.

8.2. *Cave ice*

Perennial ice deposits in caves occur in regions where the combination of cave morphology and favorable climatic conditions result in the accumulation and preservation of snow and ice. With very few exceptions, these conditions are met in low-to-high altitude mountains in the temperate zone, and as such, ice caves are ideally located to preserve seasonally-specific (i.e., winter) information on past environmental changes, frozen in ice and time. The various climatic and environmental proxies in cave ice include the isotopologues of water (Perşoiu et al., 2017) and cryogenic cave carbonate (CCC, Žák et al., 2008), several chemical species (Kern et al., 2011), pollen and macrofossils (Leunda et al., 2019), and microorganisms (Paun et al., 2019). Of these, the stable isotopes of hydrogen and oxygen offer the best prospect to reconstruct past climate – and potentially seasonal – information. However, contrary to the processes responsible for the formation of polar ice sheets and glaciers (see above), the specific processes of cave ice formation require careful examination. Perennial cave ice deposits form when snow and frozen water accumulate annually in single-entrance, descending caves, to grow into large (up to 150,000 m^3) underground glaciers that can host millennial-scale records of past climate variability (Perşoiu et al., 2017; Sancho et al., 2018; Bădăluţă et al., 2020; Fig. 12A).

There are two main processes by which snow and ice accumulate in caves: i) snow trapping and ii) infiltration water freezing. *Snow trapping* at the bottom of (sub)vertical shafts in mid-to-high altitude mountains forms deposits up to 80 m thick (Perşoiu et al., 2019). This is not enough to compress the snow beyond the firn-ice transition (0.83 g/cm^3, Langway et al., 1993). Partial melting of the upper layers in the warm season results in meltwater percolation and subsequent re-freezing inside the snow deposit. The thermal inversion of these snow traps limits the extent of melting and the small volumes of liquid water quickly re-freeze near the top of the snow deposit, thus limiting further melting. Consequently, these deposits form layered bodies of snow, firn and ice, with densities in the range of 0.5–0.9 g/cm^3, incorporating both allochthonous (atmospheric dust, organic debris, pollen, soil) and autochthonous (CCC, rock breakdown) sediments. While usually the annual mass balance at the top of these deposit is positive, extreme summer precipitation events or prolonged heatwaves could lead to rapid ablation and obliteration of the annual layering.

The second main mechanism of cave ice formation is the *freezing of liquid water* in caves. Cold air avalanches, triggered by the higher density of external cold air compared to cave air, can lead to undercooling of the cave environment and subsequent freezing of water. Given suitable cave geometry, cold air lakes form that can exist in dynamic equilibrium with snow ice for millennia. Freezing in such cold traps might occur in two distinct stages, one in late autumn and early winter, and the second throughout the cold season, depending on the timing of cooling and water availability (Persoiu et al., 2011). In the first stage, liquid water derived from dripwater accumulates in shallow pools atop of an existing ice body and freezes from top to bottom to form a layer of so-called “lake ice”, up to 20–25 cm thick. During freezing, CCC is precipitated from the carbonate-rich solution to form a layer of CCC at the bottom of the pool, and thereby incorporated into the ice as the entire water column freezes. Sporadic inflow of snowmelt during the winter months will freeze on top of this ice layer as thin sheets of ice – termed “floor ice” – resembling aufeis (naled) formed in high-latitude regions (Lauriol and Clark, 1991). With the onset of melting in summer, these layers of floor ice usually melt. Consequently, cave ice deposits formed through the freezing of water are build-up by layers of dense (approaching 0.917 g/cm^3) and usually lake ice, alternating with CCC-rich ones (sometimes mixed with allochthonous sediments).

The season-specific genetic processes described above lead to the formation of cave glaciers, hosting a record of the stable isotope composition of parent water. As these glaciers form in winter only, the stable isotope composition of cave ice will reflect that of winter precipitation (depending on altitude and latitude, between September and March) and thus constitutes a season-specific proxy of past climate conditions. However, the complex mechanisms involved in ice formation translate in similarly complex fractionation processes affecting oxygen and hydrogen isotopes. The latter require a meticulous sampling strategy in order to extract the targeted climatic information. This approach first requires disentangling the two different types of ice that build up the studied glaciers – snow/firn and ice.

Snow/firn ice will retain the initial stable isotope composition of parent snow, even if percolating water will re-freeze inside the snow deposit. Melting of the snow at the surface, percolation through the remaining snow deposit and subsequent freezing are accompanied by both kinetic and equilibrium fractionation (Arnason, 1969; Jouzel and Souchez, 1982; Koerner, 1997; Persoiu et al., 2011; Pu et al., 2020) that affect the original δ^{18}O and δ^{2}H values. While melting usually proceeds without fractionation, isotopic exchange between snow and ice and freezing are accompanied by strong equilibrium and kinetic fractionation, respectively. However, due to the geometry and morphology of the snow deposits (Kern et al., 2018; Bădăluță et al., 2020) the meltwater will percolate and freeze in its entirety inside the snow deposit so that the final δ^{18}O and δ^{2}H values in snow and ice (after melting and refreezing) are similar to the initial ones. Consequently, the stable isotope composition of cave ice formed through (partial) diagenesis of snow will retain the climatic signal carried by the isotopic composition of precipitation water, not unlike ice cores recovered from glaciers affected by summer melt (Koerner, 1997; Isaksson et al., 2003).

Opposing this, cave ice deposits built up by the freezing of water require a different approach. Freezing of water to form both floor and lake ice (see above) is accompanied by strong kinetic fractionation (Persoiu et al., 2011), albeit with different consequences on the δ^{18}O and δ^{2}H values. Floor ice forms as very thin (sub-millimeter) layers of water flow on top of the existing cave glaciers, and a distinctive δ^{18}O and δ^{2}H gradient develops along the flow path (Fig. 12B). However, owing to the very small amounts of water involved (freezing conditions outside would prevent melting) and the very short flow paths, an isotopically homogeneous layer of ice can be assumed. Further, melting in the warm season could possibly remove this layer of floor ice (with site-specific variations induced by cave and ice morphology) and consequently, any ice body formed through freezing of water will be composed of lake ice only. The kinetic fractionation processes (Jouzel and Souchez, 1982) active as lake ice forms through top-down freezing of shallow water pools will result in a clear gradient of δ^{18}O and δ^{2}H values, with the upper (first to form) layers being enriched in ^{18}O and ^{2}H (compared to the parent water). Consequently, consecutive layers of ice would show a succession of high and low δ^{18}O and δ^{2}H values, not reflecting the original stable isotope composition of water (Persoiu et al., 2011). To circumnavigate this problem, entire layers (regardless of their thickness) must be integrated and analyzed. A different approach is based on the observation that samples from a layer of frozen water align along a straight line in a δ^{18}O/δ^{2}H diagram (Jouzel and Souchez, 1982). The intersection of this line and the Local Meteoric Water Line (LMWL) will give the δ^{18}O and δ^{2}H values of water before freezing (assuming that the original water is derived from local precipitation). This approach has been shown to be effective (Persoiu et al., 2011) although in practice it demands that each ice layer be thick enough to allow for at least three aliquots to be extracted, and the LMWL must be known (and assumed to have been stable through the entire times span of ice accumulation). Recent studies of cave ice deposits formed through freezing of water revealed that, despite potential issues related to kinetic fractionation and melting of ice, the water isotopes retain useful information of past winter climate conditions (Perşoiu et al., 2017; Sancho et al., 2018). Partial melting of the annual layers and/or complete melting of several years' equivalent of ice accumulation dampens the annual signal. Still, decadal to millennial scale changes can be reconstructed.

While seasonality (i.e., a seasonal cycle) is not registered by δ^{18}O and δ^{2}H in cave ice *per se*, a seasonally distinct climatic signal is. The δ^{18}O and δ^{2}H values register cold season (winter) air temperature changes and the derived deuterium excess records changes in relative humidity at the moisture source. Recently, deuterium excess (d-excess) in cave ice has been interpreted as indicating changes in the source regions delivering moisture to the cave sites (Perşoiu et al., 2017), allowing for the reconstruction of large-scale atmospheric circulation patterns. Consequently, cave ice δ^{18}O and δ^{2}H could be used in conjunction with warm season (summer) sensitive proxies of past climate variability to reconstruct past changes of regional annual air temperature amplitudes. Promising proxies for the summer season are δ^{18}O and δ^{13}C in tree rings, which have been shown to record changes in summer air temperature and/or summer droughts (Nagavciuc et al., 2019).

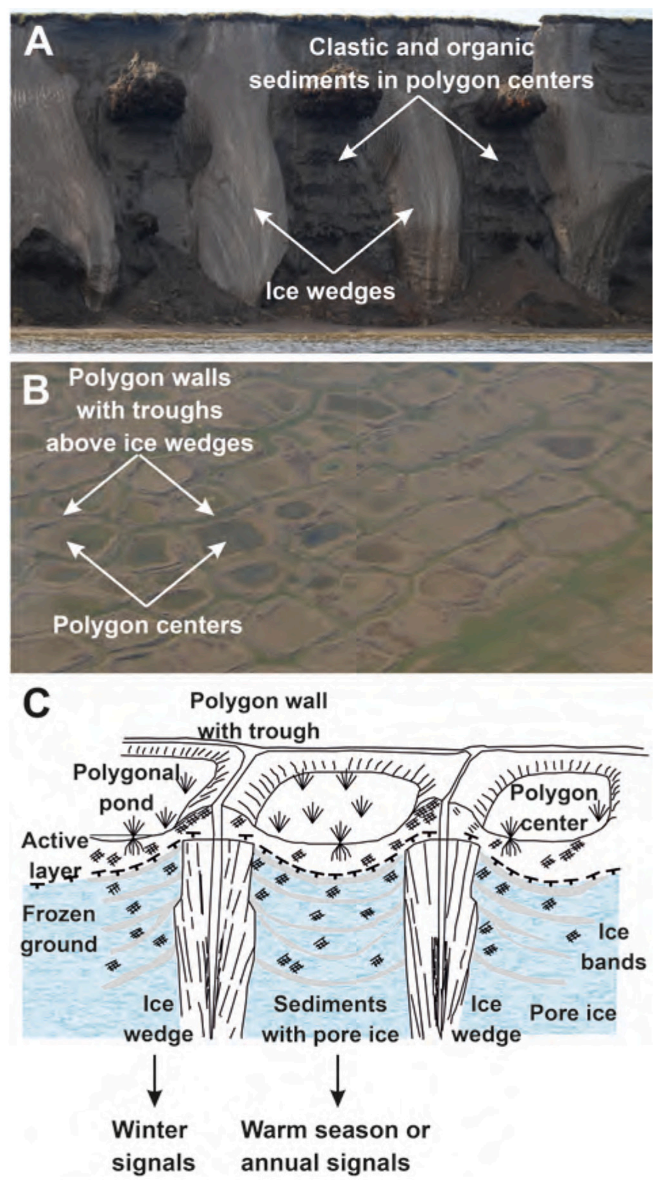

Fig. 13. Ground ice in permafrost landscapes. **A**: Permafrost cliff at Sobo-Sise Island in the Lena river delta (Siberia) showing about 20 m high ice wedges and in between polygon centers with clastic and organic sediments. **B**: Polygonal permafrost landscape shaped by ice-wedge growth. **C**: Schematic overview of ice-wedge polygons including ice wedges and pore ice, which can be used as seasonal climate archives. Photos by TO.

8.3. *Permafrost ground ice (ice wedges and pore ice)*

Ground ice from the non-glaciated high latitude permafrost regions holds important information on seasonal-scale palaeoclimate. A detailed assessment of seasonal temperature and moisture dynamics in the high latitudes is particularly important for holistic palaeoclimate reconstructions due to the highly seasonal climate forcing leading to long winters, short summers and short shoulder seasons. Ground ice comprises all forms of ice in permafrost – ground that remains frozen for at least two consecutive years - irrespective of the form or origin of the ice.

Ground ice can be formed in numerous ways and, thus, can be found in many variations such as buried glacier ice, intrusive ice, pool ice, dilution crack ice, ice wedges, and intrasedimental (i.e. pore and segregated) ice (Murton, 2013). Given the wide distribution of permafrost which underlies about 24 percent of the northern hemisphere landmass (Nitze et al., 2018), ground ice is a characteristic of arctic and sub-arctic regions across different climate and vegetation zones.

Here, we focus on the two types of ground ice with the highest palaeoclimatic potential, and in particular with regard to season-specific information due to their specific formation conditions, i.e. (1) ice wedges, and (2) pore ice (Fig. 13). Similar to glacier and cave ice (see above), ground ice based palaeoclimate studies use mainly stable isotopes of water, i.e. $\delta^{18}O$, δ^2H and deuterium excess of precipitation (e.g., Meyer et al., 2015; Opel et al., 2018; Porter and Opel, 2020). While $\delta^{18}O$ and δ^2H in ice are long regarded as sensitive proxies for local temperatures (Dansgaard, 1964), deuterium excess provides information on moisture source conditions (Merlivat and Jouzel, 1979). As a peculiarity of ground ice, δ values, deuterium excess, as well as slope and intercept of the $\delta^{18}O$-δ^2H relationship have to be carefully examined in tandem to assess the formation conditions of ground ice and post-depositional processes related to melt and refreezing in the snowpack and in the seasonally thawing uppermost soil layer (active layer) before fixation in the permafrost (Porter and Opel, 2020).

8.3.1. *Ice wedges*

Ice wedges are the most studied type of ground ice with regard to palaeoclimatology (Porter and Opel, 2020) and are mostly sampled at nearly vertical coastal or riverine outcrops providing natural access to the full width of ice wedges (Fig. 13). Ice wedges record a distinct cold season seasonality, i.e. they record explicitly climate information for the period characterized by snow cover (Opel et al., 2018).

This winter signal originates from the ice wedge formation processes: Ice wedges form when winter cold deeply penetrates the ground, causing thermal contraction cracks that are then filled predominantly by snowmelt in spring, even though minor contributions of snow and hoar frost may occur. Melt water refreezes immediately due to sub-zero temperatures of the permafrost and forms a vertical ice vein, which preserves the integrated stable isotope composition of the winter snow pack (Fig. 14). The repetition of frost crack infill over several tens to thousands of years results in the formation of massive wedge-shaped ice bodies consisting of many individual ice veins with the oldest at the margins and the youngest in the center of an ice wedge, each representing the precipitation of a particular cold season. Hence, ice wedges represent the extended winter season in the high latitudes, i.e. the meteorological winter and spring seasons (*ca.* December to May) (Meyer et al., 2015). It should be noted that the cold season snowpack is subject to multiple processes that may alter its internal stratigraphy and isotopic composition, including depth hoar formation, repeated melting and refreezing, snow drift erosion and accumulation, and sublimation (Opel et al., 2018).

However, numerous recent studies (Holland et al., 2020; Meyer et al., 2015; Opel et al., 2017, 2019; Vasil'chuk et al., 2018) show that

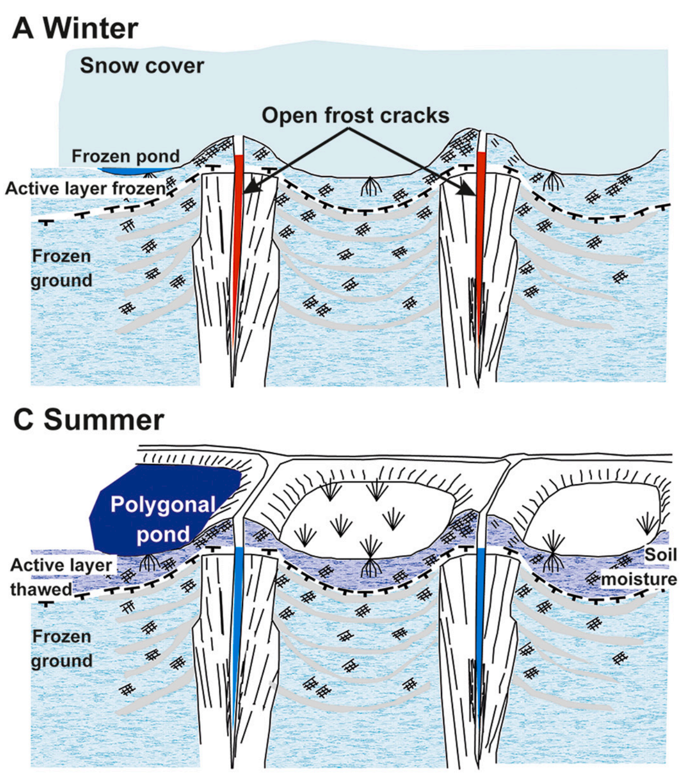

Fig. 14. Schematic overview of relevant seasonal processes leading to the formation of ice wedges and pore ice as climate archives. **A**: Winter. Accumulation of snow cover subject to sublimation and wind drift, frost cracks open. **B**: Spring. Snowmelt refreezes in frost cracks and forms new ice veins. **C**: Summer. Soil moisture in the thawed active layer integrates melt water and precipitation subject to evaporation. **D**: Fall. Active layer freezes and soil moisture turns into pore ice, initial snow cover.

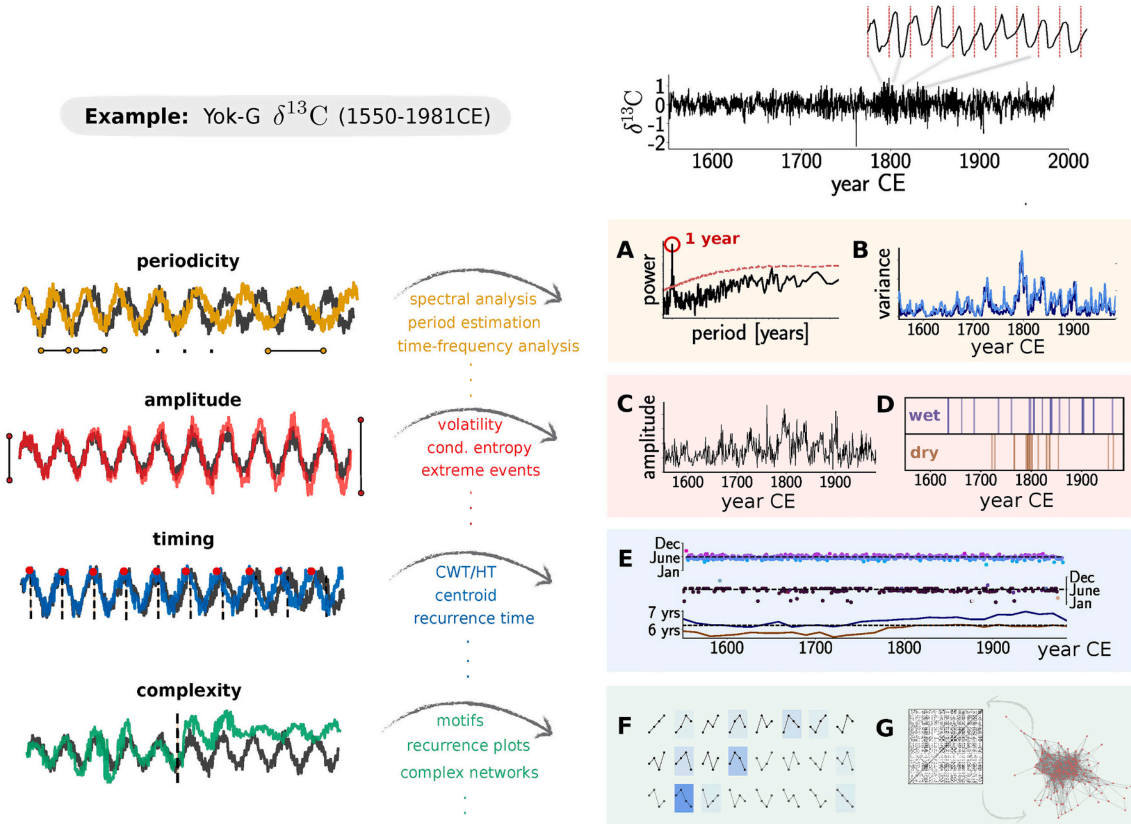

Fig. 15. Four features of seasonal variations with schematic illustrations on the left and examples for their analysis on the right, i.e. periodicity, amplitude, timing and complexity. The δ^{13}C variability measured on stalagmite Yok-G from Yok Balum cave, Belize, offers very high resolution and a layer-counted chronology (Ridley et al., 2015). The detrended record (using a Gaussian kernel filter) confines the analysis to seasonal-scale changes (upper right panel). Annual periodicity is extracted via a Lomb-Scargle periodogram (**A**) and studied over time by means of a continuous wavelet scale average around the annual period (dark blue) and sliding Gaussian kernel window variance analysis (bright blue) (**B**). Seasonal amplitude is computed as difference between annual maxima and minima (**C**) and an event series of extreme dry/wet seasons is obtained by a peaks-over-threshold approach with a 99%-quantile threshold (**D**). Timing of the wet season is extracted as the centroid of subannual patterns (upper panel) and exceedance times of the average wet season δ^{13}C value for each individual year (center panel). Average recurrence times between δ^{13}C values of distinct wet (dry) seasons are shown in the bottom panel in blue (brown) (**E**). Seasonal patterns are encoded as ordinal patterns ($l = 4$). The blue shading indicates their frequency in the (linear interpolated) record (**F**). Complexity of irregularly sampled seasonal patterns are characterized by a recurrence plot/recurrence network, based on a computation of the edit distance measure.

ice wedge stable isotope compositions are often close to the Global and/or Local Meteoric Water Line. This indicates that the ice wedge isotope compositions have not substantially altered during ice wedge formation, and still preserves the climate information of cold season precipitation. Thus, the wedge ice isotopes are suitable for the reconstruction of past winter temperatures (derived from δ^{18}O, δ^{2}H) and moisture source and transport properties (using deuterium excess). More recently, also marine aerosols trapped in ice wedges have been studied and interpreted in terms of past sea ice cover dynamics even though their seasonal attribution is not fully constrained yet (Iizuka et al., 2019).

Knowledge gaps and challenges regarding ice wedge-based palaeoclimate and seasonality reconstructions concern ice wedge formation processes (i.e. frost cracking and infilling dynamics), and the origin and preservation of the stable isotope signal, both requiring detailed monitoring studies. Other issues to address relate to ice wedge dating and time series development (Opel et al., 2018). Ice wedge chronologies are mainly constrained by radiocarbon dating of particulate organic matter such as plant macro remains, animal coprolites or dissolved organic carbon incorporated in the ice. Ice wedge time series are then generated by age-distance modelling between individual ages or by "stacking" paired age and proxy information (Meyer et al., 2015).

Unfortunately, the fact that ice-rich permafrost is sensitive to thaw means that we often deal with incomplete stratigraphies and complex chronologies. Hence, ice wedges predating the last interglacial are rare and most ice wedge-based winter palaeoclimate records date from the last glacial (i.e., MIS 3 and MIS 2) and the Holocene (Porter and Opel, 2020). However, the oldest known ice wedges are more than 700 ka old (Froese et al., 2008), indicating that ice wedges (and more generally permafrost) can survive several interglacials.

The palaeoclimate potential of ice wedges is determined by their ability to provide millennial to centennial-scale time series of information on atmospheric conditions during winter, a season not or only inadequately covered by most other high-latitude climate archives. For instance, ice wedge stable isotopes revealed a pronounced winter cooling during the Younger Dryas cold event in Northern Alaska, formerly believed to be only limited, or completely absent in this region (Meyer et al., 2010). However, ice wedge palaeoclimate records gained more attention when they helped to close the gap between Holocene palaeoclimate and model data, frequently referred to as Holocene temperature conundrum (Liu et al., 2014). Meyer et al. (2015) for the first time reconstructed an Arctic Holocene winter warming trend for the Lena river delta, driven mainly by increasing winter (November to April) insolation. This long-term trend is in stark contrast to most other high-latitude records, which show cooling related to the decreasing summer insolation (Kaufman et al., 2020; Marcott et al., 2013). The evidence of long-term winter warming is in line with annual climate model simulations that show only minor changes or even a warming over the Holocene (Liu et al., 2014). Subsequent ice wedge studies from Siberia (Opel et al., 2017) and Canada (Holland et al., 2020) confirmed this Holocene Arctic winter warming, and highlighted the strongly seasonal climate forcing in the high latitudes.

Ice wedge stable isotope records with their strict winter signal have the potential to close existing seasonal and spatial gaps of Arctic palaeoclimate reconstructions. Their seasonal specifics help reconstructing the differential impact of highly seasonal climate forcing in the high latitudes.

8.3.2. Pore ice

Pore ice fills the pores of frozen soils and sediments and holds the grains together (Fig. 13). Pore ice can best be sampled by drilling vertical boreholes into sediment-rich permafrost. The sediment may also contain organic material for radiocarbon dating as well as palaeoecological proxies including pollen and plant macro remains for independent seasonal palaeoclimate studies.

Compared to ice wedges, pore ice has a less well expressed seasonal signal that heavily depends on local site characteristics (Porter and Opel, 2020). Pore ice in syngenetic permafrost originates from water in the seasonally thawed active layer (Fig. 14). Syngenetic permafrost is aggrading with the rising permafrost table (the permafrost surface at the base of the active layer) due to the accumulation of surface sediment. The pore water freezes in pores at the base of the active layer, thereby becoming part of the permafrost. It may comprise a mix of meltwater from fresh snow and active layer pore ice of previous years as well as warm-season precipitation (Porter and Opel, 2020). Depending on local climate, relief, and soil properties the active layer water represents a blend of warm-season (Porter et al., 2019) or rather annual (Schwamborn et al., 2006) precipitation. The isotopic composition of water in the active layer can be altered by a number processes, including evaporation and freeze-thaw cycles (Fig. 14). The constant enrichment of pore ice in heavy isotopes during final freezing and incorporation into permafrost must be taken into account for interpretations (Porter et al., 2019).

The pore ice-based isotope records of Porter et al. (2019) from a peatland in Yukon, Canada, represent the first full-Holocene summer temperature reconstruction from pore ice. These reconstructions reveal deglacial warming, an Early Holocene Maximum, long-term cooling in response to deceasing summer insolation, as well as abrupt modern warming. The results are generally consistent with other regional multi-proxy compilations (Kaufman et al., 2016) and shed new light on yet contrasting Early Holocene temperature reconstructions. While pollen-based reconstructions indicate a cold Early Holocene, midge- and pore ice-based reconstructions reveal a warm Early Holocene.

However, as there exist only a few pore ice reconstructions at all, more studies are required to further constrain pore ice isotope formation conditions and the respective seasonal signals.

In summary, ground ice, including both wedge ice and syngenetic pore ice, records season-specific climate information that can substantially contribute to holistic palaeoclimate reconstructions in the high latitudes. Taking advantage of the individual seasonal signals of both archives, the combination of ice wedge and pore ice data, and where possible classic palaeo-ecological proxies (such as pollen) from host sediments can enable a full characterization of past seasonal dynamics.

9. Numerical tools for extracting seasonality changes from palaeoenvironmental time series

As the previous sections show, seasonality expresses itself in different fashions in each environmental archive, and is accompanied with individual challenges and limitations. Seasonality reconstruction is concerned with the extraction of prominent features which closely link to the respective notion of seasonality, such as periodicity, seasonal amplitude, timing/duration or complexity (see Box 7) of seasonal patterns (Fig. 15). In order to characterize seasonal variability, quantitative time series analysis methods allow extraction of various features related to seasonality and to gain confidence in their statistical significance. Here we give an overview of how systematic application of numerical tools can help to extract and substantiate the reconstruction of seasonality in presence of data-related obstacles.

While well-dated proxy records allow for direct assessment of subannual or seasonal variations (Ridley et al., 2015; Felis et al., 2015), lower resolved time series may contain valuable information on variability that is linked to seasonal variability. Some records reflect information related to different seasons, others only yield a specific response to a single season (Meyer et al., 2015, see Sections 5 and 8) (see Box 7). In some records, the most prominent and valuable information on seasonality might be found in extreme excursions from the baseline (Chu et al., 2012; Yi et al., 2012). In all these cases, nonstationarity (see Box 5) in the underlying geophysical and geochemical processes can render the recorded seasonal features highly variable over time. Numerically extractable information goes beyond detecting changes in an annual cycle; even in the presence of a stable annual cycle throughout a time series. Not only can the 'seasonal amplitude' vary significantly, but also timing and duration of seasons are distinct features that become detectable (see Box 1), e.g., as phase shifts (Fig. 15). Where the underlying forcing mechanisms are well understood, proxy data can be linked to a specific season even in lower resolved time series (Meyer et al., 2015).

Obstacles for retrieving seasonality include (among others) limited temporal resolution and lacking reproducibility (de Winter et al., 2021). Frequently, standard methods (e.g., periodograms) must be adapted before they can be used to extract seasonality from irregularly sampled time series (Musial et al., 2011). Further, the sampling integration (i.e., the time integrated in each discrete sample) is vitally important when assessing the suitability of a time series for seasonality analysis. Unambiguous differentiation between an actual seasonal cycle and noise can be challenging even in well-dated records, with remaining age uncertainty obscuring the significance of a present seasonal fingerprint. Archives with lower-than-annual resolution can only yield seasonality-related information when a clear mechanism links proxies to environmental parameters, and/or to a specific season (see Section 8) (see Box 5). Therefore, the mechanism that embeds seasonal signals in an archive decides upon which method is ultimately best suited to extract them.

This chapter is intended as overview of statistical methods to extract information on seasonality from palaeoenvironmental archives. We first summarize methods frequently used in palaeoclimatology, then we briefly discuss recently developed tools that help scrutinizing diverse seasonality archives across disciplines.

Box 7
Glossary for statistical terms

- **Boostrapping** is a nonparametric statistical technique that allows to estimate confidence bounds or prediction errors for a signal through resampling. Based on an empirical estimate of a system's probability distribution, n values from this distribution are randomly drawn with replacement in each of N_b bootstrap runs.
- **Complexity** of a signal comprises a range of features that are typically encountered in the study of nonlinear and nonstationary systems. Measuring the complexity of a signal complements and exceeds characterization of strictly linear signals, e.g. by reflecting their tendency to exponentially deviate from a given value or the degree of irregularity in their variability. Even systems which predominately exhibit regular, periodic behaviour may show episodic bursts of irregular, chaotic dynamics that can be best captured by complexity measures. In seasonal climate signals, this can be expressed as a superposition of variations in periodicity, amplitude, and timing as well as in abrupt shifts from predictable to stochastic or intermittent dynamics (e.g., caused by a changing influence of semi-stochastic large scale atmospheric patterns).
- **Continuous Wavelet Transform (CWT)** is a signal decomposition into small oscillations with specific frequency. Each oscillation is represented by a shifted and scaled version of a *Mother Wavelet*. CWT is a powerful tool to track signal cycle changes through time (e.g., the annual cycle). They are similar to a time series power spectrum but allow for better reconstruction of the signal in time.
- **Dynamic Time Warping** allows matching signals of varying length and with distinct sampling. Its application to proxy records can be interesting for comparing signals with very different temporal resolution. It can inform on optimal signal alignment and provides a (dis) similarity measure.
- **Entropy** is a universal concept in thermodynamics that can be interpreted as the amount of information that is associated with state of a system. In applications to (nonlinear) time series, it is commonly utilized as a complexity measure. Many different definitions are possible (Shannon entropy, permutation entropy, …) while each of them requires the empirical estimation of a probability distribution. It is often also loosely interpreted as an indicator of how 'disordered' a system behaves.
- **Exceedence times** are time instances at which a time series $x(t)$ has a larger than pre-specified value a: $x(t) > a$. For palaeoseasonality, a characteristic value (e.g., mean wet season rainfall, see fig. 15 in main text) can be computed in order to study at which time t_i this value is first exceeded in an given year. Decreasing exceedance times would then indicate a trend towards an earlier wet season onset.
- **Granger causality** is a prediction-based concept of statistical causality. If a signal X_1 causes a signal X_2, then past values of X_1 should allow to predict future X_2 values beyond the information contained in past X_2 values alone. The mathematical formulation of Granger causality is based on linear regression modelling of stochastic processes (Granger, 1969).
- **Hilbert-Huang analysis, Empirical mode decomposition and Singular Spectrum Analysis** are distinct methods that are used to decompose a signal into *intrinsic modes*. If a signal contains significant variability at multiple timescales, each mode may represent this scale-specific variability. In contrast to CWT, decomposition does not rely on a specific type of function.
- **Hilbert-transformation (HT)** is a mathematical transformation of a signal that allows to extract its *instantaneous frequency and phase*. It is related to the Fourier transform. When studying an annual cycle, the instantaneous phase of a signal reflects *how much is cycle is shifted forwards and backwards for different episodes in time*.
- **Independence** of a signal is a common prerequisite for applying statistical analyses and means that the studied signal does not exhibit any serial dependence, implying an absence of trends, cycles or stochastic long-range dependence.
- **Kolmogorov-Smirnov distance** measures similarity between probability distribution functions (PDF). It is used to test whether an empirical PDF is compatible with a known reference distribution (e.g. a normal distribution) or if two empirically estimated PDFs could be generated from the same reference distribution. It may yield spurious results if many extreme values are included in the empirical sample.
- **Least-squares based wavelet approach** allows extraction of cycles through time. Least-squares optimization aims at minimizing the squared deviation between a result and the optimal result. When applied to wavelets, this approach can obtain a near-optimal wavelet representation of a cycle through time, despite uneven sampling.
- **Nonstationarity** in a signal can indicate that an external process affects the studied system such that it, e.g., results in a continuous change of the mean in a time series. Other nonstationary signal variations include shifts in variance, extreme events, or continuous variations in dominant cycles.
- **Non-rectangular, smooth kernel function** apply weights to neighboring observed data in a time series. Often used in sliding-window analyses, e.g. moving averages. A window function is chosen that decays smoothly towards the edges of the time window of specified width h. Smooth kernel windows allow better temporal localization of the covered time series segment, thereby limiting spurious artefacts in spectral analysis compared to sliding window analyses. A popular example are normal-weighed Gaussian kernel windows.
- **Normality** refers to the notion that the empirical estimate of a signal's probability density function can be well approximated by a normal distribution.
- **Quantiles** are statistical values that characterize a probability distribution. For empirical data a quantile is a specific value that splits the sample of all values into one fraction p that is smaller and one fraction $1 - p$ that is larger than the quantile. This value is referred to as the (empirical) p-quantile of the sample. Quantiles are often used to report confidence intervals.
- **Return periods** are periods in which a time series returns to a similar or equivalent magnitude it has visited before. In extreme value analysis, a certain extremely high (low) magnitude is specified as *return level*. The return time corresponding to this return level denotes the time interval typically passed between two events above (below) this return level. It is estimated from a model description of the time series called *generalized extreme value distribution*.
- **Seasonality indicators** are standardized, quantified characterizations of one or more seasonal features. They allow to enhance comparability between different expressions of seasonality in distinct archives and help multi-proxy palaeoseasonality studies. Often focussed on quantifying a single feature of seasonal change.

9.1. Statistical tools

The broad spectrum of methods that can be subsumed under the term *statistical tools* ranges from simple seasonal averaging to extreme value analysis and linear correlations. A suitable combination of these tools can help to tackle some of the challenges related to seasonality detection and move towards quantitative analysis.

9.1.1. Descriptive statistics

A first step towards quantifying seasonality is related to estimating statistical properties of a record's frequency distribution. The frequencies can be found by binning histograms or by estimating kernel density representations. For sufficiently long records, histograms for distinct episodes or (non)overlapping time windows can give a statistical estimate of temporal seasonality evolution (Emile-Geay et al., 2016). Empirical distributions may then be compared, e.g., between different study sites or time periods by means of suitable similarity measure, such as Kolmogorov-Smirnov distance (Marozzi, 2013).

The estimation of statistical properties, like sample average, variance or quantiles, reveal tendencies (trends) if computed for time periods that characterize distinct seasons. For instance, analyzing the δ^{18}O signal of limpet shells, Wang et al. (2012) detected a cooling trend in the seasonal temperature for the Late Holocene from 3300–2500 BP to the Roman Warm Period (2500–1600 BP) by means of varying seasonal averages. Computing statistical properties on sliding windows can help tracking seasonality changes (Wirth et al., 2013), and the use of basic statistics can substantiate the interpretation of seasonality dynamics beyond qualitative analysis (Feranec et al., 2009). Testing seasonal amplitude or seasonal vs. non-seasonal patterns can also be carried out with more sophisticated measures like conditional entropy. Entropy generally quantifies the 'informativeness' of a distribution (e.g., a subannual rainfall distribution), resulting in higher values in case of more complex and more contrasted distributions (Feng et al., 2013). Although specifically designed statistical tests can characterize a record's seasonality (De Jager et al., 1989; Nwogu et al., 2016; Freedman, 1979; Davey and Flores, 1993), they remain rarely applied because they often do not account for the full complexity in proxy time series. Restrictions like independence or normality often pose significant limitations to the scope of basic hypothesis tests. Yet, meaningful seasonality-related properties can be extracted by combining multiple suitable tests and careful, case-specific definition of the null-hypothesis. Bootstrapping techniques (Bischoff et al., 2017; Mudelsee, 2013) offer a parameter-free approach to compute confidence limits by resampling a time series, without the need to make assumptions with respect to the data.

Seasonality indicators are often based on basic statistical measures to make specific statements about seasonality, e.g., to compare seasonality at different geographical locations (Cook et al., 2010) or between modeled and empirical proxy data (Schneider et al., 2010). A popular definition is established by the contrast of temperature or rainfall between seasons, expressed by differences or ratios (Emile-Geay et al., 2016; Felis et al., 2015) ('seasonal amplitude', Fig. 15C). For example, rainfall seasonality has been characterised by dividing values for strong by such for low rainfall season (Walsh and Lawler, 1981), whereas — for instance — the difference between maximum and minimum monthly coral Sr/Ca and δ^{18}O values has been used to quantify seasonality in temperature the Caribbean at the end of the last interglacial (Felis et al., 2015). Fig. 15C shows an example of variations in the seasonal amplitude derived from δ^{13}C variations measured at very high resolution on annually laminated stalagmite Yok-G over the last 400 years. In this case, it is defined as the difference between maximum and minimum proxy values for a given year and reflects seasonality of local rainfall. Such a characterization is yet not able to define the timing of seasons, e.g., how the subannual rainfall distribution changes from year to year (see Fig. 15E). If subannual resolution can be assessed, seasonality indicators should always account for the different manifestations of seasonality in the data and not be limited to a single seasonal property. For example, variable approaches have been considered to quantify variability of seasonal timing (Pascale et al., 2014). Annually laminated archives are particularly useful to extract information on seasonal timing, e.g., as shown in Fig. 15E: here, timing of the wet season was extracted by deriving centroids ('center of mass') from the subannual rainfall distributions and computing exceedance times of a pre-defined value for each year (upper and center panel). Recurrence times between dry/wet seasons of distinct years can also unveil intriguing information on the seasonal cycle (lower panel).

The definition of a seasonality indicator benefits from such diverse approaches. Thackeray and Fitchett (2016) define a seasonality index using multiple regression on fossil records and distinguish summer and winter rainfall regimes in South Africa. Feng et al. (2013) give a spatial characterization of distinct seasonal rainfall regimes across the tropics based on how complex subannual rainfall distributions are rendered in terms of their seasonal amplitude, timing and duration. Also indicators of extreme weather have been used to characterize seasonality dynamics (Yi et al., 2012; Nicault et al., 2008; Chu et al., 2012) (see below). Consequent application of seasonality indicators across disciplines could improve inter-comparability of independent proxy archives. Combining multiple methods enhances the interpretational value of seasonality reconstructions.

Nonstationary extreme value analysis can characterize events found in palaeoclimate proxy records, like floods, droughts, extreme precipitation, which can be season-specific (De Haan and Ferreira, 2007; Naveau and Ammann, 2005). Extreme events have significant repercussions for agricultural, social and ecological dynamics (Mannshardt et al., 2013), making their analysis particularly worthwhile when studied along with historical proxy archives (see also chapter 2). As climate is inherently nonstationary, suitable methods and implementations are employed (Cheng et al., 2014), whereby two basic approaches can be distinguished, i.e., the computation of block maxima/minima, and the so called peak-over-threshold approach (De Haan and Ferreira, 2007).

The *block maxima/minima* approach splits time series into consecutive blocks and computes maxima and minima, e.g., seasonal maxima in proxy data. For instance, an extensive analysis of 26 bivalve shell surfaces from the North Atlantic revealed that seasonal climatic extremes had an impact on the evolution of Norse colonies during warm and cold periods (Patterson et al., 2010). Time series with lower than seasonal resolution may be split into larger blocks. Since droughts for example occur within a specific season, some trends regarding the intensity (i.e., number of extreme events) of that season can be estimated. Using estimates of extreme value distribution (or their parameters) in a multi-proxy framework can give insights into spatio-temporal recurrence of extreme climate conditions (Mannshardt et al., 2013).

The *peak-over-threshold* approach analyses the frequency of amplitudes above or below a threshold (often a quantile of the dataset). The frequency of threshold exceedances and return periods are useful to understand the temporal variability in the occurrence of season-related extreme conditions (Xoplaki et al., 2005). Fig. 15D shows series of season-specific extreme events extracted from δ^{13}C values based on the 99%-quantile of the full time series. The same approach also helped to identify phases of stationary and nonstationary hydroclimatic changes in the Western Mediterranean in a 2800 year long seasonally-resolved lake record (Corella et al., 2016). Evaluating exceedance and recurrence probabilities of extreme precipitation events, this study found that the modern frequency of heavy rainfall events is normal in a historical perspective, but likely to increase under future warming conditions. If an event time series is suspected to contain periodicities, these can be identified, e.g., by computing the Rayleigh measure: for example, Peavoy and Franzke (2010) test a time series characterized by Dansgaard–Oeschger cycles for periodicity in a Bayesian framework which also helps evaluation of seasonal-scale dynamics. Individual proxy time series can be embedded in larger proxy ensembles from different locations and the co-occurrence of extreme events can be studied using synchronization measures between events (Malik et al., 2012; Ozken et al., 2018) while accounting for proxy-specific uncertainties. Some proxy time series may entail immediate implications linked to seasonal extreme weather, like droughts in Spain since 1506 C.E. that are identified in accounts of religious ceremonies (Domínguez-Castro et al., 2008).

Detrending and frequency filtering is a standard pre-processing step when focusing on variability on single timescales in a proxy record (Wu et al., 2007). After subtracting a trend from the original time series, the effectiveness of this decomposition should be evaluated, e.g., using spectral analysis and signal-to-noise ratio. As a basic approach, moving averages yield trends of intrinsic variability of time series. However, the degree of smoothing is only controlled by the applied window width.

Importantly, moving averages can result in spurious trend characterizations and their frequency response makes them vulnerable to erroneous high-frequency variations (Mudelsee et al., 2012). Non-rectangular, smooth kernel functions are more appropriate for sliding window statistics and have been used in an uncertainty-aware regression approach to estimate trends in proxy time series. Local or global polynomial and spline regression can be employed to extract trends of varying complexity and can also be combined with kernel functions.

Another widely used technique is band-pass filtering, or applying a filter-bank to a time series. For example, Hardt et al. (2010) low-pass filtered a stalagmite-based isotope record and extracted seasonal strength that they were able to link to multi-decadal summer NAO variability. These approaches should be used carefully, since band-pass filters are neither designed for irregularly spaced or chronologically 'uncertain' data, nor accounting for above-mentioned intricacies surrounding moving averages. Seasonal and Trend decomposition using LOESS (STL decomposition) extracts smooth components of a time series by using local regression (Cleveland et al., 1990) which has, for example, been applied to extract smooth long-term trends from palaeoclimate records (Westerhold et al., 2020).

Mode decomposition approaches such as Singular Spectrum Analysis (SSA) and Empirical Mode Decomposition (EMD) capture nonlinear oscillatory modes and trends (Huang and Wu, 2008; Vautard and Ghil, 1989; Ghil et al., 2002). Modifications for time series with missing data exist (Kondrashov and Ghil, 2006; Musial et al., 2011) and some applications to palaeoclimate data have been carried out (Olafsdottir et al., 2013). These approaches offer the advantage that they capture the intrinsic variability of the time series, can yield higher modes of variability, and account for nonlinear oscillations. In summary, every detrending approach involves the risk of eliminating variability so that the remainder is spuriously interpreted as a seasonal component despite of its actual insignificance or that seasonal variability is unintentionally eliminated.

Linear correlations are a popular tool in time series analysis to characterize relations between multiple time series or the serial dependence of a time series when the data is normally distributed. Being limited to detecting linear relations, linear correlations do not account for more complex or causal relationships often found in (palaeo)climate data. (Non-)linear correlations can greatly improve significance of statements compared to simple visual inspection ('wiggle-matching'), which is still popular (Cheng et al., 2012). With regard to seasonality extraction, correlations are applied to confirm seasonal proxy interpretation (Medina-Elizalde et al., 2010; Lachniet et al., 2012; McKay and Kaufman, 2014), to test model validity between empirical and simulated seasonal signals (Büntgen et al., 2017), or studying lead-lag effects. Multiple approaches allow the computation of correlations for irregularly sampled proxy time series (Rehfeld et al., 2011; Hu et al., 2017). Statistical testing for significant correlations can also be designed such that it includes the dating uncertainties of a record (Haam and Huybers, 2010). Each of these is preferable against aggregating or interpolating the time series on a regular time axis without accounting for uncertainty since this introduces statistical biases that can hardly be controlled (Schulz and Stattegger, 1997). A kernel-based approach (Rehfeld et al., 2011) together with an estimate for confidence limits (Roberts et al., 2017) can be considered a robust method to detect linear correlations in irregularly sampled records. Finally, causality (directionality) between irregularly sampled, age uncertain proxy records can also be tested based on measures that are conceptually inspired by Granger causality (Granger, 1969; Smirnov et al., 2017). These methods might help identify drivers of seasonally variable strength.

With multiple and spatially distributed proxies that are known to record the same climatological parameter, seasonality can generally be detected beyond a regional scale and be compared between single proxies (Abram et al., 2007). In this context, spatio-temporal mode decomposition approaches allow for extraction of a limited number of dominant modes that encompass a certain part of the variability from such spatial data. The most popular approach in this range is the Empirical Orthogonal Functions technique which is also frequently employed in climate field reconstructions (Riedwyl et al., 2009) and is effectively applied to instrumental climate data (Buizert et al., 2018) and proxy data with uncertainties (Deininger and McDermott, 2016). Some applications show that the climate field perspective unveiled by mode decomposition approaches allows for detection of season-specific reconstructions on (pan-)regional scales (Neukom et al., 2011, 2014; Tan et al., 2019). Shi et al. (2017a) reconstruct the May-September precipitation field of China for the past 500 years using a dataset comprising 479 proxy records and identify three dominant modes with different spatio-temporal dynamics by means of ensemble empirical mode decomposition.

Regression techniques help to determine how multiple proxies or spatially distinct archives depend on each other by regarding them as a set of a dependent and multiple independent variables. They can be flexibly adapted to many problems and can help to detect seasonality. If a suitable measure for seasonality can be established, a linear regression can be computed to quantify the dependence of seasonality on the variability at other timescales or links to other proxy records. For example, Emile-Geay et al. (2016) employed a linear regression on a multi-proxy, multi-site coral and mollusc dataset while accounting for uncertainties. Contrasting standard assumptions presumed in PMIP3 models, they uncover a positive relation between ENSO variance and seasonality. Linear regression is also used to validate proxy interpretation. For example, Boldt et al. (2015) use uncertainty-aware linear regression against instrumental data to support their interpretation of the chlorophyll content in a sediment core as proxy for regional summer temperature.

Uncertainty propagation in statistical analysis significantly enhances confidence in extracted (seasonal) characteristics. Accounting for dating uncertainties is particularly important when the significance of an annual period (see Section 9.2) or seasonal timing is evaluated. Many frameworks allow for such a characterization of age uncertainty that can be propagated through period estimation techniques for stalagmite proxy records, ranging from Bayesian approaches (Franke et al., 2018; Boers et al., 2019; Parnell et al., 2011; Goswami et al., 2014) to Monte Carlo sampling-based techniques (Scholz and Hoffmann, 2011; Breitenbach et al., 2012; Duesing et al., 2021). Whenever seasonality in high resolution records is to be aligned with records from other locations that are characterised by different climatic conditions, integrating multiple proxies with variable temporal resolution in presence of uncertainties arises as significant issue. Li et al. (2010) combined multiple proxies to reconstruct temperature using a Bayesian hierarchical model, accounting for uncertainty and coherently integrating multiple proxies despite distinct temporal resolutions.

9.2. Spectral analysis

Spectral analysis is a powerful tool to find seasonal cycles in temporally sufficiently resolved proxy records, and to test their significance. Even if a record does not allow the detection of annual or sub-annual cyclicities due to sparse temporal sampling, spectral analysis can provide valuable insights into the modulation of signals related to seasons or longer periods that can affect seasonal patterns, e.g., ENSO. Periodogram approaches are probably the most popular technique to study which periods are present (Came et al., 2007; Carolin et al., 2016; Jones et al., 2006; Hubeny et al., 2006; Asmerom et al., 2007; Sinha et al., 2015). Based on the Fourier transform of the studied time series, regular periodogram-based methods are somewhat limited: straight-forward application is only viable for constantly sampled records without related uncertainty since irregular sampling intervals result in a loss of structure in Fourier peaks (VanderPlas, 2018; Babu and Stoica, 2010). Intricacies like high-frequency noise, dating uncertainties, limited record length, and measurement artefacts need to be considered when interpreting identified periods (see below). In the following, methods that are designed to estimate periods in such records are discussed. Subsequently, we give an overview of how this can be achieved in presence of nonstationarity.

Period estimation techniques are of increasing interest in seasonality studies. Unfortunately, no automated or optimal strategy for estimating periods in proxy records exists and each method requires a systematic evaluation of significance.

A prominent method to estimate periods in unevenly sampled records with dating uncertainties is the Lomb–Scargle (LS) periodogram (Scargle, 1982, 1989). Similar to the classical periodogram, it can be understood as a least squares fit of sinusoids at each frequency which uses a $\mathcal{X}^2$–expression to minimize the residuals. It can account for dating uncertainties by including Gaussian errors around each proxy value (Scargle, 1989). Often the LS periodogram is applied together with the estimation of AR(1)-spectra to assess significance (REDFIT, Schulz and Mudelsee, 2002; Mudelsee et al., 2009), although the robustness of this approach has recently been questioned (Xu, 2019). Fig. 15A shows a LS periodogram for the Yok-G δ^{13}C record using the REDFIT algorithm to evaluate the significance of the identified annual spectral peak. In order to integrate uncertainties, periodograms can be computed for different realizations of an age-modelled proxy whereas each realization is compatible with the dating uncertainties (Berkelhammer et al., 2010). When tasked with detecting seasonal periods, potential aliasing must be considered: if the sampling frequency of an irregularly sampled record episodically falls below half the annual frequency, seasonality can no longer be reliably extracted (Nyquist theorem). Specifying a frequency grid to prevent aliasing may thus be impeded (Mudelsee, 2013).

Although still relatively rare, spectral estimates are used in seasonality studies. For example, de Winter et al. (2017) have reconstructed late Cretaceous annual cycles using high resolution isotope and trace element records from fossil shells. Others studies have used LS periodograms to relate wet/dry cycles in varved lake sediments to Indian summer monsoon changes even in the absence of sub-annual resolution of the proxy record (Jones et al., 2006). LS periodograms have also helped to identify the influence of orbital forcing on seasonal strength (Oliveira et al., 2017). To generalize classical LS periodograms and improve frequency detection or significance testing, spectral density can be combined with other methods (Zechmeister and Kürster, 2009; Lenoir and Crucifix, 2018b). For highly resolved records, Welch overlapping segment averaging (Welch, 1967) might be particularly useful, as smoother periodograms can be estimated. Another approach that is based on a windowed representation of a time series is the Multitaper method (Percival et al., 1993; Chave, 2019). Methods specifically designed to estimate periods in irregularly sampled records furthermore include Gaussian kernel-based spectra (Rehfeld et al., 2011), phase-folding techniques and Bayesian approaches (Shi and Gallagher, 2019; Stoica and Sandgren, 2006; Graham et al., 2013; VanderPlas, 2018); depending on the specific application, these are sometimes superior to classic methods.

In multiple proxy records, cross-spectral analysis allows identification of shared spectral power within the same frequency band, similar to LS periodograms (Ólafsdóttir et al., 2016) or Gaussian kernel approaches (Rehfeld et al., 2011). Cross-power spectra have successfully been use to test the influence of solar forcing on droughts (Yu and Ito, 1999), or to study Holocene rainfall seasonality (Deng et al., 2014).

Time-frequency (TF) analysis extends classic period estimation techniques and evaluates the presence of periodicities through time (Tary et al., 2014). As an arbitrarily accurate determination of both frequency and time is impossible, respective methods need to offer a compromise. ontinuous Wavelet Transform (CWT) (Torrence and Compo, 1998) does so while yielding a clear graphical output and standardized significance testing (Maraun et al., 2007). It is efficient in retrieving low and high frequencies as well as nonstationary features of a time series (such as frequency variations). Instantaneous phase estimates can be made by the Hilbert-transformation (HT) of a time series. By tracking the mutual spectral power between multiple time series through time via cross-wavelet or wavelet coherence analysis (Grinsted et al., 2004), significant periods of different intertwined processes can also be extracted (e.g., from instrumental records (Ghil et al., 2002; Lau and Weng, 1995; Rossi et al., 2011)). The increasingly frequent application of CWT on bivalves, speleothems, and tree rings highlights the popularity of this method for seasonality studies (Schöne and Fiebig, 2009; Asmerom et al., 2020; Labotka et al., 2016; Ronay et al., 2019). For instance, the authors of (Ronay et al., 2019) support their hypothesis that a strategically located speleothem reflects dry rather than monsoon season infiltration as an often overlooked interpretation by applying CWT to the proxy record. Still, irregular sampling remains rarely addressed. Often, spline or polynomial interpolation methods are used that are known to introduce artefacts, especially in the high-frequency bands. Fig. 15B displays variance in the annual band of a CWT (Wavelet scale average) for the Yok-G stable isotope record (dark blue), whereby linear interpolation was used to regularize the time axis. In comparison, a Gaussian kernel variance estimate (Rehfeld et al., 2011) with suitable bandwidth that naturally accounts for irregular sampling is shown (bright blue), showcasing how distinctiveness of the seasonal cycle can be tracked through time.

Several approaches have addressed a solution to account for irregular sampling in CWT: Foster's Morlet Weighted Wavelet Z-Transform method (Foster, 1996) has contributed to the definition of Wavelets for irregularly sampled astronomical time series. It has also found some application in the palaeoclimate literature (Bazzicalupo et al., 2020) whereas some studies take uncertainty into account as well (Witt and Schumann, 2005). Using this method, Prasad et al. (2009) found evidence for seasonality changes in varved sediments from Lake Holzmaar, including winter cooling, summer rainfall intensity, and changes in season onsets/offsets during the 8.2 ka event. An extension to cross wavelet analysis is available and was, e.g., employed to capture how spatial coherence of periodic components in proxy time series is restructured throughout the Holocene by analysis of a global multiproxy data set (Wirtz et al., 2010). Inspired by the LS periodogram, a least-squares based wavelet approach has also been put forward (Ghaderpour and Pagiatakis, 2017). Another direction has been approached using projection methods where first applications remain to be carried out as of now (Lenoir and Crucifix, 2018a). Work on related TF-analysis techniques has also partially been directed towards treatment of irregular sampling (Thakur et al., 2013). Significance testing (see Section 9.3) can be applied by randomization of wavelet coefficients, retaining wavelet-related properties of the underlying time series (Keylock, 2007). Finally, alternative techniques like Hilbert-Huang and Singular Spectrum Analysis remain less frequently used in palaeoclimatological contexts, likely due to a more intricate mathematical background (Huang and Wu, 2008; Lambert et al., 2021; Ghil et al., 2002). Effectiveness in application to both seasonal climate data (Ghil and Mo, 1991a,b) and palaeoclimate records (Taricco et al., 2015) has been demonstrated, yielding performance comparable to CWT analysis (Taricco et al., 2015).

9.3. Nonlinear time series analysis

The fundamental processes that constitute seasonal proxy signals are often highly nonlinear, comprising nonlinear feedbacks, non-Gaussian distributions and nonlinear interrelations. For instance, abrupt transitions result from nonlinear threshold responses of interconnected climate subsystems (Denton et al., 2005b). Rather than representing simple sinusoidal signals, seasonal variability and cycles with higher periods in broadband records consist of nonlinear oscillations. A comprehensive description of such systems requires application of well-established nonlinear time series analysis methods. Several techniques allow to test time series for nonlinear features (Theiler et al., 1991). If the seasonal signal in a proxy record is modulated by a range of frequencies, we can test if nonlinear oscillations can adequately describe these dynamics (Vejmelka and Paluš, 2009). Surrogate testing is a powerful, non-parametric approach where ‘surrogate’ realizations of a time series are generated to test for certain features, e.g., nonlinearity. An ensemble of random realizations mimics the scrutinized signal with respect to some of its specific features by preserving them in a constrained randomization procedure (Schreiber and Schmitz, 2000). For instance, simple random shuffling can be performed with the goal of significance testing, either on the time series itself (with the null-hypothesis of absent serial dependence) or on estimated phases to preserve power spectral density (e.g. with the null-hypothesis of different TF characteristics) (Venema et al., 2006).

Nonlinear correlation measures are often better suited to study interdependencies between multiple records, like mutual information or event synchronization (Rehfeld et al., 2011; Paluš, 2007; Ramos et al., 2017; Boers et al., 2014), rather than relying on linear correlations. Dynamic Time Warping (DTW) (Berndt and Clifford, 1994) helps in estimating similarities between records of different length. For example, Hausmann et al. (2019) use DTW to demonstrate a significant correlation between the Mg/Ca record and water temperatures in molluscs and highlight their importance as archives of seasonality. Marwan et al. (2002) employ a recurrence plot based technique with the similar goal of matching unaligned rock magnetic data of two different sediment cores.

Recurrence analysis is a very flexible technique and can be applied to irregularly sampled and age-uncertain records (Ozken et al., 2018; Marwan et al., 2018; Goswami et al., 2018). Where seasonal changes can be linked to abrupt transitions, their detection is often based on some measure of complexity or anomaly detection (Garland et al., 2018b,a). Recurrence plots stand out as a simple-to-implement albeit powerful tool (Marwan et al., 2007), as they cannot only detect rapid shifts, but can also estimate periods, provide information on the underlying dynamics, and identify nonlinear relationships in multivariate data sets (Donges et al., 2011; Marwan and Kurths, 2015; Zbilut and Marwan, 2008; Ramos et al., 2017). Fig. 15G shows a recurrence plot based on the edit distance approach proposed in (Ozken et al., 2018) and illustrates the possibility to transform it into a complex (recurrence) network.

Symbolic dynamics represents an additional means to detect abrupt shifts and characterize recurring patterns in nonlinear time series. By encoding a time series as a sequence of symbols (motifs or ‘words’), it is well applicable to data with relatively high levels of noise and can deal with irregular or low sampled nonlinear time series (Sakellariou et al., 2016; McCullough et al., 2016). A possible choice for such symbols are ordinal patterns as displayed in Fig. 15F: given a pattern length of 4, 24 distinct patterns can be distinguished and the computation of their frequency in the (linearly interpolated) Yok-G $\delta^{13}C$ record allows for statements on the seasonal-scale complexity.

Information theoretical methods exhibit yet another perspective on seasonality extraction, often facilitating estimation of periods in nonlinear time series that are noisy and irregularly sampled (Cincotta et al., 1995; Garland et al., 2018a). While many applications to irregularly sampled astronomical records exist (Huijse et al., 2011), palaeoclimate studies that often address similar objectives remain to be carried out with such methods.

Complex time series networks (Fig. 15G) and (palaeo-)climate spatial networks (Oster and Kelley, 2016) can finally provide quantitative frameworks that improve confidence in the fidelity of proxy records as reflectors of regional seasonality and its teleconnectivity (McRobie et al., 2015; Eroglu et al., 2016).

9.4. Methodological challenges and strategies

Despite the availability of a range of tools, sole visual inspection of proxy records is still a common strategy. It appears that many studies focus on the challenging task of reconstructing climate variability from proxy evidence, thereby limiting their efforts of additional, more complex, analyses. Many recent studies highlight the great potential of effective collaboration between researchers from both the proxy and methodological domains. Innovation on both fronts – proxy development and calibration, and statistical approaches to high-resolution irregularly sampled data – is essential for accurate reconstruction of seasonal dynamics.

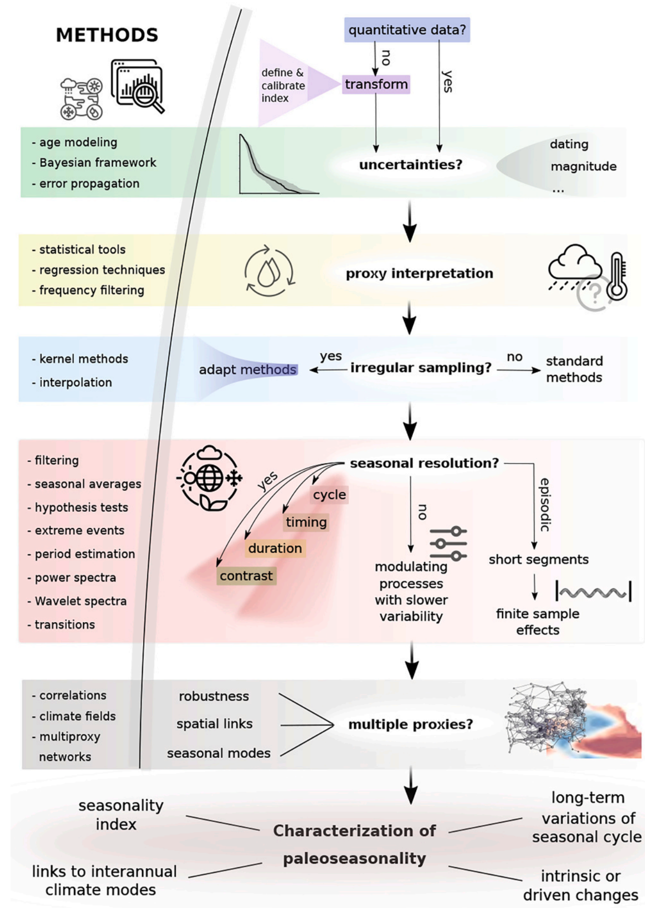

Fig. 16. Schematic illustration of how seasonality can be extracted from a palaeoenvironmental archive. Each box represents a typical proxy-specific challenge that may need to be accounted for. Numerical methods that are well-suited to extract and quantify seasonality are displayed in the left part of the flow chart.

We highlight several challenges in this endeavor: (a) **Shortness of records** limits the applicability of most standard time series analysis methods. (b) **Uncertainties** – both related to proxy values and dating – need to be propagated in thorough statistical analyses; accounting for uncertainties is vital for palaeoseasonality studies as they are often on the same order of magnitude as the proxy value or sampling frequency. (c) **Irregular sampling** poses a major challenge for extracting seasonal information. Only a few methods beyond spectral analysis account for non-uniform sampling intervals. Statistical biases may dominate records resolved at sub-annual timescale, especially when the number of samples per year undergoes significant variations. (d) **Signal-to-noise ratios** are critical for highly-resolved proxy data as very few archives record an unambiguous climate signal. Fig. 16 summarizes how these challenges can be approached when palaeoseasonality is targeted using numerical methods.

One suggestion which might facilitate methodological soundness of analyses and trans-disciplinary collaboration, is supplementing innovative methods with well-documented and easily accessible open-source software.

Including local seasonal records from different, and spatially dispersed, archives will improve the understanding of regional climate dynamics, but only under the premise that uncertainties at both, the data/results and the interpretational level are taken into consideration

(Peyron et al., 2011). Such scrutiny is feasible only if adequate assumptions and statistical methods are in place. On the other hand, the application of transdisciplinary multi-archive and multi-proxy approaches harbors enormous potential to refine seasonality detection across archives and environments; related phenomena often encompass a broad range of semi-stochastic phenomena (see Box 3) (Abram et al., 2007).

Consequently, combining different archives in palaeoseasonality studies will encourage more universal definitions of seasonality indicators that account for a broader set of ubiquitous seasonal features (see Fig. 15). Variations in palaeoseasonality are best represented by standardized indicators which consider more than one seasonal feature, are designed to compare seasonality across archives, and are based on a mathematically sound definition that effectively tackles above listed technical challenges.

10. Summary and outlook

10.1. Compositional make-up of climate seasonality

Seasonal changes in our environment are periodic and global, happening at the temporal scale of human behavior. This, and the fact that seasonal dynamics are perceptible over human live spans, makes the reconstruction of past changes in seasonality of paramount importance for the study of past human-environment interactions.

The concept of seasonality is rooted in the annual march of the Earth around the Sun, and the nonlinear response of the physical climate system (and human adaptation) to regular changes in solar forcing. The regional and local expression of seasonal changes is always a consequence of (semi-)stochastic internal feedbacks that are superimposed on predictable external solar forcing. Accordingly, the range of annual temperature and precipitation changes varies notably even along the same latitude. The most important factors modulating the seasonal signal are continentality and altitude, both (relatively) constant over longer time scales, and large-scale atmospheric circulation patterns that vary periodically but not regularly (semi-stochastically). Further, archive-specific sensitivity and sampling approaches have the potential to modulate proxy signals.

10.2. Relevance of trans- and multidisciplinary approaches

Recent years revealed the importance of close collaboration between disciplines, including (palaeo-)climatology, (palaeo-)ecology, history, physics, archaeology, and anthropology, when tackling pressing questions in Earth Sciences. Finding a common language in such transdisciplinary studies is a vital, but often challenging, prerequisite for communicating results and ideas across scientific communities, and the public. Similarly, acknowledging archive- and proxy-specific limitations and analytical uncertainties allows for assessing data quality and provides robust input for statistical approaches, which often reveal and quantify hidden information better than the naked eye. Choosing adequate statistical method(s) is challenging, and providing scrupulous interpretations and relevant outcomes calls for informed, close collaboration between palaeoenvironmental scientists and statisticians.

Recurring, archive-independent challenges relate to a) precise high-resolution sampling of often fragile, not linearly-grown or -accumulated, and size-limited material to capture the full range of seasonal variability, b) establishing the environment-proxy relationship that is constant over time and related to only one variable (e.g., only temperature, or only precipitation), c) quantifying seasonal change in terms of physical units (° C, mm, number of days, etc.).

Continuous instrumental developments, and detailed monitoring and calibration efforts allow for addressing these challenges at least at a local scale. At regional or global scales, the most inconvenient issue is a deficiency of long, radiometrically-dated and seasonally-resolved records whose spatial and temporal coverage permits broader-scale inferences. The compilation and compare & contrast approach across different archives is essential in overcoming this inconvenience. At the same time a stringent quality assessment of each individual archive in its own merit and with its own limitations – age uncertainty, recorded season, qualitative or quantitative information and analytical error propagation – is critical. Simple, or more sophisticated statistical methods help in extracting the seasonal signal, assuring data quality, and juxtaposing seasonally resolved data in their own domain(s).

10.3. Proposed framework

Misconceptions and challenges in interpreting true or purported seasonal signals often originate from integrating data that were not/poorly quality-checked, or produced using different scientific practices and uncertainty propagation strategies. Below, we propose a framework that might be beneficial when targeting seasonal signals in palaeoenvironmental archives:

- examine the archive(s) critically, including sampling resolution, age control (both layer-counted and, if available, radiometric), proxy sensitivity or bias towards a certain season, and adapt the most adequate sampling strategy.
- try to identify climate variable (temperature, precipitation) that has changed, and the direction of this change (increase or decrease in annual amplitude) rather than refer to 'change in seasonality'. Note that if the sampling is not continuous or sequential, but 'bulk', a change in baseline might appear as a 'change in amplitude'.
- keep in mind that environmental archives only rarely can inform on the timing and duration of seasonal precipitation. Over longer timescales, the amount of precipitation might stay constant but its distribution may change.
- compare the direction of the documented change(s) with the one predicted by insolation forcing. Discrepancies in the expected direction of change might reveal more details and a deeper insight into environmental evolution and response to insolation forcing than a simple admission that such a change has happened.
- in some cases, particularly when talking about rainfall or the combination of temperature and rainfall changes, several scenarios might be possible. Clearly articulating and justifying these (often contradictory) scenarios provides an explicit step in disentangling external forcing factors and internal feedbacks, and help completing the mosaic of past environments and human societies.
- while comparing seasonal signals from different archives keep in mind individual archive-specific limitations.

The transparency of communicating results gains in importance in trans-disciplinary projects. Different environments, and human societies within them, might react differently to the same forcing, the former depending on their natural architecture, the latter on their societal structure, vulnerability, conditioning, and resilience. Yet, admitting the heterogeneity of possible responses is as important as identifying the factors dictating this heterogeneity. A careful approach involving quality-controlled data and in-depth consideration of internal feedbacks operating in a given natural or anthropogenic environment will provide profound insights into how regional and local conditions adjusted to external forcing. Such insights are of critical importance as they inform the predictions of the effects of anthropogenic climate change on local to regional environments.

Declaration of Competing Interest

The authors declare that they have no known competing financial interests or personal relationships that could have appeared to influence the work reported in this paper.

Acknowledgements

Chris Jazwa received financial support for the data collection from the National Science Foundation (grant NSF BCS-1724639). Tobias Braun received financial support from the Deutsche Forschungsgemeinschaft in the context of the DFG project MA4759/11-1 'Nonlinear empirical mode analysis of complex systems: Development of general approach and application in climate'. Aurel Perşoiu was supported by a grant of the Romanian Ministry of Education and Research, CNCS - UEFISCDI, project number PN-III-P4-ID-PCE-2020-2723, within PNCDI III. Monica Ionita was supported by Helmholtz Association through the joint program "Changing Earth - Sustaining our Future" (PoF IV) program of the AWI.

References

Abram, N.J., Gagan, M.K., Liu, Z., Hantoro, W.S., McCulloch, M.T., Suwargadi, B.W., 2007. Seasonal characteristics of the Indian Ocean Dipole during the Holocene epoch. Nature 445, 299.

Caprio, A.C., Swetnam, T.W., 1995. Historic fire regimes along an elevational gradient on the west slope of the Sierra Nevada, California. United States Department of Agriculture Forest Service General Technical Report Int.

Acosta, V.G., Zevallos, J.M.P., Del Villar, A.M., 2003. Desastres agrícolas en México: catálogo histórico, vol. 2. CIESAS.

Aggarwal, P.K., Romatschke, U., Araguas-Araguas, L., Belachew, D., Longstaffe, F.J., Berg, P., Schumacher, C., Funk, A., 2016. Proportions of convective and stratiform precipitation revealed in water isotope ratios. Nat. Geosci. 9, 624–629.

Aharon, P., Rasbury, M., Murgulet, V., 2006. Caves of Niue Island, South Pacific: speleothems and water geochemistry. In: Perspectives on Karst Geomorphology, Hydrology, and Geochemistry - A Tribute Volume to Derek C. Ford and William B. White. Geological Society of America, pp. 283–295.

Aldeias, V., Gur-Arieh, S., Maria, R., Monteiro, P., Cura, P., 2016. Shell we cook it? An experimental approach to the microarchaeological record of shellfish roasting. Archaeol. Anthropol. Sci. 11, 389–407.

Amann, B., Szidat, S., Grosjean, M., 2015. A millennial-long record of warm season precipitation and flood frequency for the North-western Alps inferred from varved lake sediments: implications for the future. Quat. Sci. Rev. 115, 89–100.

Andrus, C., 2011. Shell midden sclerochronology. Quat. Sci. Rev. 30, 2892–2905.

Araguás-Araguás, L., Froehlich, K., Rozanski, K., 1998. Stable isotope composition of precipitation over southeast Asia. J. Geophys. Res.: Atmos. 103, 28721–28742.

Arnason, B., 1969. The exchange of hydrogen isotopes between ice and water in temperature glaciers. Earth Planet. Sci. Lett. 6, 423–430.

Asmerom, Y., Baldini, J.U.L., Prufer, K.M., Polyak, V.J., Ridley, H.E., Aquino, V.V., Baldini, L.M., Breitenbach, S.F.M., Macpherson, C.G., Kennett, D.J., 2020. Intertropical convergence zone variability in the neotropics during the common Era. Sci. Adv. 6.

Asmerom, Y., Polyak, V., Burns, S., Rassmussen, J., 2007. Solar forcing of Holocene climate: new insights from a speleothem record, southwestern United States. Geology 35, 1–4.

Asmerom, Y., Polyak, V.J., Burns, S.J., 2010. Variable winter moisture in the southwestern United States linked to rapid glacial climate shifts. Nat. Geosci. 3, 114–117.

Augustin, L., Barbante, C., Barnes, P.R.F., Marc Barnola, J., Bigler, M., Castellano, E., Cattani, O., Chappellaz, J., Dahl-Jensen, D., Delmonte, B., Dreyfus, G., Durand, G., Falourd, S., Fischer, H., Flückiger, J., Hansson, M.E., Huybrechts, P., Jugie, G., Johnsen, S.J., Jouzel, J., Kaufmann, P., Kipfstuhl, J., Lambert, F., Lipenkov, V.Y., Littot, G.C., Longinelli, A., Lorrain, R., Maggi, V., Masson-Delmotte, V., Miller, H., Mulvaney, R., Oerlemans, J., Oerter, H., Orombelli, G., Parrenin, F., Peel, D.A., Petit, J.R., Raynaud, D., Ritz, C., Ruth, U., Schwander, J., Siegenthaler, U., Souchez, R., Stauffer, B., Peder Steffensen, J., Stenni, B., Stocker, T.F., Tabacco, I.E., Udisti, R., van de Wal, R.S.W., van den Broeke, M., Weiss, J., Wilhelms, F., Winther, J.G., Wolff, E.W., Zucchelli, M.p.a.l.a., 2004. Eight glacial cycles from an Antarctic ice core. Nature 429, 623–628.

Ault, T.R., Cole, J.E., Overpeck, J.T., Pederson, G.T., Meko, D.M., 2014. Assessing the risk of persistent drought using climate model simulations and paleoclimate data. J. Climate 27, 7529–7549.

Babu, P., Stoica, P., 2010. Spectral analysis of nonuniformly sampled data-a review. Digtal Sig. Process. 20, 359–378.

Bailey, G., 2007. Time perspectives, palimpsests and the archaeology of time. J. Anthropol. Archaeol. 26, 198–223.

Bailey, G., Craighead, A., 2003. Late Pleistocene and Holocene coastal palaeoeconomies: a reconsideration of the Molluscan evidence from northern Spain. Geoarchaeology 18, 175–204.

Baker, A., Bradley, C., 2010. Modern stalagmite δ18o: Instrumental calibration and forward modelling. Global Planet. Change 71, 201–206.

Baker, A., Bradley, C., Phipps, S., Fischer, M., Fairchild, I., Fuller, L., Spötl, C., Azcurra, C., 2012. Millennial-length forward models and pseudoproxies of stalagmite δ 18o: an example from NW Scotland. Climate Past 8, 1153–1167.

Baker, A., Bradley, C., Phipps, S.J., 2013. Hydrological modeling of stalagmite δ18o response to glacial-interglacial transitions. Geophys. Res. Lett. 40, 3207–3212.

Baker, A., Flemons, I., Andersen, M.S., Coleborn, K., Treble, P.C., 2016. What determines the calcium concentration of speleothem-forming drip waters? Global Planet. Change 143, 152–161.

Baker, A., Hartmann, A., Duan, W., Hankin, S., Comas-Bru, L., Cuthbert, M.O., Treble, P. C., Banner, J., Genty, D., Baldini, L.M., Bartolomé, M., Moreno, A., Pérez-Mejías, C., Werner, M., 2019. Global analysis reveals climatic controls on the oxygen isotope composition of cave drip water. Nat. Commun. 10, 2984.

Baker, A., Ito, E., Smart, P.L., McEwan, R.F., 1997. Elevated and variable values of 13c in speleothems in a British cave system. Chem. Geol. 136, 263–270.

Baker, A., Mockler, N.J., Barnes, W.L., 1999. Fluorescence intensity variations of speleothem-forming groundwaters: implications for paleoclimate reconstruction. Water Resour. Res. 35, 407–413.

Baker, A., Proctor, C.J., Barnes, W.L., 2002. Stalagmite lamina doublets: a 1000 year proxy record of severe winters in northwest Scotland? Int. J. Climatol. 22, 1339–1345.

Baker, A., Smart, P.L., Edwards, R.L., Richards, D.A., 1993. Annual growth banding in a cave stalagmite. Nature 364, 518–520.

Balanzategui, D., Knorr, A., Heussner, K.U., Wazny, T., Beck, W., Slowinski, M., Helle, G., Buras, A., Wilmking, M., Van Der Maaten, E., Scharnweber, T., Dorado-Linan, I., Heinrich, I., 2018. An 810-year history of cold season temperature variability for northern Poland. Boreas 47, 443–453.

Balasse, M., Ambrose, S.H., Smith, A.B., Price, T., 2002. The seasonal mobility model for prehistoric herders in the South-western Cape of South Africa assessed by isotopic analysis of sheep tooth Enamel. J. Archaeol. Sci. 29, 917–932.

Baldini, J., Lechleitner, F., Breitenbach, S., van Hunen, J., Baldini, L., Wynn, P., Jamieson, R., Ridley, H., Baker, A., Walczak, I., Fohlmeister, J., 2021. Detecting and quantifying palaeoseasonality in stalagmites using geochemical and modelling approaches. Quat. Sci. Rev. 254, 106784.

Baldini, J., McDermott, F., Fairchild, I., 2006. Spatial variability in cave drip water hydrochemistry: implications for stalagmite paleoclimate records. Chem. Geol. 235, 390–404.

Baldini, J.U.L., 2010. Cave atmosphere controls on stalagmite growth rate and palaeoclimate records. Geol. Soc. London, Special Publications 336, 283–294.

Baldini, L.M., Baldini, J.U., McDermott, F., Arias, P., Cueto, M., Fairchild, I.J., Hoffmann, D.L., Mattey, D.P., Müller, W., Nita, D.C., Ontañón, R., Garciá-Moncó, C., Richards, D.A., 2019. North Iberian temperature and rainfall seasonality over the Younger Dryas and Holocene. Quat. Sci. Rev. 226, 105998.

Ballantyne, A.P., Baker, P.A., Chambers, J.Q., Villalba, R., Argollo, J., 2011. Regional differences in south American monsoon precipitation inferred from the growth and isotopic composition of tropical trees. Earth Interac. 15.

Ban, F., Baker, A., Marjo, C.E., Duan, W., Li, X., Han, J., Coleborn, K., Akter, R., Tan, M., Nagra, G., 2018. An optimized chronology for a stalagmite using seasonal trace element cycles from Shihua Cave, Beijing, North China. Sci. Rep. 8, 4551.

Banner, J., Guilfoyle, A., James, E., Stern, L., Musgrove, M., 2007. Seasonal variations in modern speleothem calcite growth in Central Texas, U.S.A. J. Sediment. Res. 77, 615–622.

Bar-Matthews, M., Ayalon, A., Kaufman, A., 1997. Late quaternary paleoclimate in the eastern Mediterranean region from stable isotope analysis of speleothems at Soreq Cave, Israel. Quat. Res. 47, 155–168.

Barthel, S., Isendahl, C., 2013. Urban gardens, agriculture, and water management: sources of resilience for long-term food security in cities. Ecol. Econ. 86, 224–234. Sustainable Urbanisation: A resilient future.

Bazzicalupo, P., Maiorano, P., Girone, A., Marino, M., Combourieu-Nebout, N., Pelosi, N., Salgueiro, E., Incarbona, A., 2020. Holocene climate variability of the Western Mediterranean: surface water dynamics inferred from calcareous plankton assemblages. Holocene 30, 691–708.

Beckers, B., Berking, J., Schütt, B., 2013. Ancient water harvesting methods in the drylands of the mediterranean and Western Asia. eTopoi. J. Ancient Stud. 2, 145–164.

Belli, R., Borsato, A., Frisia, S., Drysdale, R., Maas, R., Greig, A., 2017. Investigating the hydrological significance of stalagmite geochemistry (Mg, Sr) using Sr isotope and particulate element records across the Late Glacial-to-Holocene transition. Geochim. Cosmochim. Acta 199, 247–263.

Belmecheri, S., Wright, W.E., Szejner, P., Morino, K.A., Monson, R.K., 2018. Carbon and oxygen isotope fractionations in tree rings reveal interactions between cambial phenology and seasonal climate. Plant Cell Environ. 41, 2758–2772.

Ben Dor, Y., Neugebauer, I., Enzel, Y., Schwab, M.J., Tjallingii, R., Erel, Y., Brauer, A., 2019. Varves of the dead sea sedimentary record. Quat. Sci. Rev. 215, 173–184.

Berkelhammer, M., Sinha, A., Mudelsee, M., Cheng, H., Edwards, R.L., Cannariato, K., 2010. Persistent multidecadal power of the Indian Summer Monsoon. Earth Planet. Sci. Lett. 290, 166–172.

Berkelhammer, M.B., Stott, L.D., 2008. Recent and dramatic changes in pacific storm trajectories recorded in delta o-18 from bristlecone pine tree ring cellulose. Geochem. Geophys. Geosys. 9.

Berndt, D.J., Clifford, J., 1994. Using dynamic time warping to find patterns in time series.. In: KDD Workshop, Seattle, WA, pp. 359–370.

Bicho, N., Haws, J., 2008. At the land's end: marine resources and the importance of fluctuations in the coastline in the prehistoric hunter-gatherer economy of Portugal. Quat. Sci. Rev. 27, 2166–2175.

Bischoff, T., Schneider, T., Meckler, A.N., 2017. A conceptual model for the response of tropical rainfall to orbital variations. J. Climate 30, 8375–8391.

Bj“orklund, J., von Arx, G., Nievergelt, D., Wilson, R., Van den Bulcke, J., G”unther, B., Loader, N.J., Rydval, M., Fonti, P., Scharnweber, T., Andreu-Hayles, L., Büntgen, U., D'Arrigo, R., Davi, N., De Mil, T., Esper, J., G” artner, H., Geary, J., Gunnarson, B.E., Hartl, C., Hevia, A., Song, H., Janecka, K., Kaczka, R.J., Kirdyanov, A.V., Kochbeck, M., Liu, Y., Meko, M., Mundo, I.,

Nicolussi, K., Oelkers, R., Pichler, T., Sánchez-Salguero, R., Schneider, L., Schweingruber, F., Timonen, M., Trouet, V., Van Acker, J., Verstege, A., Villalba, R., Wilmking, M., Frank, D., 2019. Scientific Merits and Analytical Challenges of Tree-Ring Densitometry.
Blatrix, R., Roux, B., Béarez, P., Prestes-Carneiro, G., Amaya, M., Aramayo, J.L., Rodrigues, L., Lombardo, U., Iriarte, J., de Souza, J.G., Robinson, M., Bernard, C., Pouilly, M., Durécu, M., Huchzermeyer, C.F., Kalebe, M., Ovando, A., McKey, D., 2018. The unique functioning of a pre-Columbian Amazonian floodplain fishery. Sci. Rep. 8, 5998.
Bliege Bird, R., Bird, D.W., Codding, B.F., Parker, C.H., Jones, J.H., 2008. The "fire stick farming" hypothesis: Australian aboriginal foraging strategies, biodiversity, and anthropogenic fire mosaics. Proc. Natl. Acad. Sci. 105, 14796–14801. https://www.pnas.org/content/105/39/14796.full.pdf.
Boch, R., Spötl, C., Frisia, S., 2011. Origin and palaeoenvironmental significance of lamination in stalagmites from Katerloch Cave, Austria. Sedimentology 58, 508–531.
Boers, N., Goswami, B., Ghil, M., 2019. A complete representation of uncertainties in layer-counted paleoclimatic archives. Climate Past 13, 1169–1180.
Boers, N., Rheinwalt, A., Bookhagen, B., Barbosa, H.M., Marwan, N., Marengo, J., Kurths, J., 2014. The south American rainfall dipole: a complex network analysis of extreme events. Geophys. Res. Lett. 41, 7397–7405.
Boldt, B.R., Kaufman, D.S., McKay, N.P., Briner, J.P., 2015. Holocene summer temperature reconstruction from sedimentary chlorophyll content, with treatment of age uncertainties, Kurupa Lake, Arctic Alaska. Holocene 25, 641–650.
Borsato, A., Frisia, S., Fairchild, I.J., Somogyi, A., Susini, J., 2007. Trace element distribution in annual stalagmite laminae mapped by micrometer-resolution X-ray fluorescence: Implications for incorporation of environmentally significant species. Geochim. Cosmochim. Acta 71, 1494–1512.
Bougeois, L., De Rafélis, M., Reichart, G., de Nooijer, L., Dupont-Nivet, G., 2016. Mg/Ca in fossil oyster shells as palaeotemperature proxy, an example from the Palaeogene of Central Asia. Palaeogeogr. Palaeoclimatol. Palaeoecol. 441, 611–626.
Bourke, P., Willan, R., 2009. '*Anadara granosa*' (Mollusca: Bivalvia: Arcidae) discovered live in darwin harbour, with implications for understanding climate change in northern Australia. Beagle: Rec. Museums Art Gall. North. Territ. 25, 115–118.
Bova, S., Rosenthal, Y., Liu, Z., Godad, S.P., Yan, M., 2021. Seasonal origin of the thermal maxima at the holocene and the last interglacial. Nature 589, 548–553.
Bowen, G.J., Cai, Z., Fiorella, R.P., Putman, A.L., 2019. Isotopes in the water cycle: regional- to global-scale patterns and applications. Annu. Rev. Earth Planet. Sci. 47, 453–479.
Boyce, M.S., 1979. Seasonality and patterns of natural selection for life histories. Am. Nat. 114, 569–583.
Bradley, C., Baker, A., Jex, C.N., Leng, M.J., 2010. Hydrological uncertainties in the modelling of cave drip-water δ18o and the implications for stalagmite palaeoclimate reconstructions. Quat. Sci. Rev. 29, 2201–2214.
Braje, T.J., Erlandson, J.M., Rick, T.C., Davis, L., Dillehay, T., Fedje, D.W., Froese, D., Gusick, A., Mackie, Q., McLaren, D., et al., 2020. Fladmark 40: what have we learned about a potential pacific coast peopling of the americas? Am. Ant. 85, 1–21.
Branscombe, T.L., Bosch, M.D., Miracle, P.T., 2020. Seasonal shellfishing across the east adriatic mesolithic-neolithic transition: oxygen isotope analysis of *Phorcus turbinatus* from Vela Spila (Croatia). Environ. Archaeol. 0, 1–14.
Brasseur, P., Beckers, J., Brankart, J., Schoenauen, R., 1996. Seasonal temperature and salinity fields in the Mediterranean Sea: climatological analyses of a historical data set. Deep Sea Res. Part I: Oceanograph. Res. Pap. 43, 159–192.
Brauer, A., Dulski, P., Mangili, C., Mingram, J., Liu, I., 2015. The potential of varves in high-resolution paleolimnological studies. PAGES News 17, 96–98.
Brauer, A., Haug, G.H., Dulski, P., Sigman, D.M., Negendank, J.F.W., 2008. An abrupt wind shift in western Europe at the onset of the Younger Dryas cold period. Nat. Geosci. 1, 520–523.
Brázdil, R., 2002. History of weather and climate in the Czech Lands: instrumental meteorological measurements in Moravia up to the end of the eighteenth century, vol. 5. Masaryk University.
Brázdil, R., Kiss, A., Rezníčková, L., Barriendos, M., 2020. Droughts in historical times in europe, as derived from documentary evidence. Palaeohydrology. Springer, pp. 65–96.
Brázdil, R., Pfister, C., Wanner, H., Von Storch, H., Luterbacher, J., 2005. Historical climatology in Europe – the state of the art. Climatic Change 70, 363–430.
Breitenbach, S.F., Lechleitner, F.A., Meyer, H., Diengdoh, G., Mattey, D., Marwan, N., 2015. Cave ventilation and rainfall signals in dripwater in a monsoonal setting – a monitoring study from NE India. Chem. Geol. 402, 111–124.
Breitenbach, S.F., Plessen, B., Waltgenbach, S., Tjallingii, R., Leonhardt, J., Jochum, K.P., Meyer, H., Goswami, B., Marwan, N., Scholz, D., 2019. Holocene interaction of maritime and continental climate in Central Europe: new speleothem evidence from Central Germany. Global Planet. Change 176, 144–161.
Breitenbach, S.F.M., Cai, Y., Kwiecien, O., Osinzev, A., Tan, L., Zhang, H., 2014. A high-altitude cave as example for active karstification in the eastern Tibetan Plateau. Cave Karst Sci. 41, 132–137.
Breitenbach, S.F.M., Rehfeld, K., Goswami, B., Baldini, J.U., Ridley, H.E., Kennett, D.J., Prufer, K.M., Aquino, V.V., Asmerom, Y., Polyak, V.J., et al., 2012. Constructing proxy records from age models (copra). Climate Past 8, 1765–1779.
Bricker, H.M., Bricker, V.R., 2020. A Comparison of historical evidence for droughts in the pre-columbian maya codices with climatological evidence for droughts during the early and late classic periods. Ethnohistory 67, 97–126.
Britton, C.E., 1938. A meteorological chronology to AD 1450. Ciel Et Terre 54, 332.
Brocas, W.M., Felis, T., Gierz, P., Lohmann, G., Werner, M., Obert, J.C., Scholz, D., Kölling, M., Scheffers, S.R., 2018. Last interglacial hydroclimate seasonality reconstructed from tropical atlantic corals. Plaeocean. Paleoclimatol. 33, 198–213.
Bronk Ramsey, C., Staff, R.A., Bryant, C.L., Brock, F., Kitagawa, H., van der Plicht, J., Schlolaut, G., Marshall, M.H., Brauer, A., Lamb, H.F., Payne, R.L., Tarasov, P.E., Haraguchi, T., Gotanda, K., Yonenobu, H., Yokoyama, Y., Tada, R., Nakagawa, T., 2012. A complete terrestrial radiocarbon record for 11.2 to 52.8 kyr B.P. Science 338, 370–374.
Brook, G.A., Rafter, M.A., Railsback, L.B., Sheen, S.W., Lundberg, J., 1999. A high-resolution proxy record of rainfall and ENSO since AD 1550 from layering in stalagmites from Anjohibe Cave, Madagascar. Holocene 9, 695–705.
Brunello, C.F., Andermann, C., Helle, G., Comiti, F., Tonon, G., Tiwari, A., Hovius, N., 2019. Hydroclimatic seasonality recorded by tree ring δ18O signature across a Himalayan altitudinal transect. Earth Planet. Sci. Lett. 518, 148–159.
Bădăluță, C.A., Perşoiu, A., Ionita, M., Piotrowska, N., 2020. Stable isotopes in cave ice suggest summer temperatures in east-central Europe are linked to Atlantic Multidecadal Oscillation variability. Climate Past 16, 2445–2458.
Buisman, J., Van Engelen, A.F., 1995. Duizend jaar weer, wind en water in de lage landen, deel 1 tot 1300. Van Wijnen. Franeker, the Netherlands (in Dutch).
Buizert, C., Sigl, M., Severi, M., Markle, B.R., Wettstein, J.J., McConnell, J.R., Pedro, J.B., Sodemann, H., Goto-Azuma, K., Kawamura, K., et al., 2018. Abrupt ice-age shifts in southern westerly winds and Antarctic climate forced from the north. Nature 563, 681.
Büntgen, U., Krusic, P.J., Verstege, A., Sang”uesa-Barreda, G., Wagner, S., Camarero, J.J., Ljungqvist, F.C., Zorita, E., Oppenheimer, C., Konter, O., et al., 2017. New tree-ring evidence from the Pyrenees reveals Western Mediterranean climate variability since medieval times. J. Climate 30, 5295–5318.
Burchell, M., Cannon, A., Hallmann, N., Schwarcz, H., Schöne, B., 2012. Refining estimates for the season of shellfish collection on the pacific northwest coast: applying high-resolution stable oxygen isotope analysis and sclerochronology. Archaeometry 55, 258–276.
Burke, A., Castanet, J., 1995. Histological observations of cementum growth in horse teeth and their application to archaeology. J. Archaeol. Sci. 22, 479–493.
Burkhardt, T., Hense, A., 1985. On the reconstruction of temperature records from proxy data in mid Europe. Arch. Meteorol. Geophys. Bioclimatol. Ser. B 35, 341–359.
Butler, P., Wanamaker, A., Scourse, J., Richardson, C., Reynolds, D., 2013. Variability of marine climate on the North Icelandic Shelf in a 1357-year proxy archive based on growth increments in the bivalve Arctica islandica. Palaeogeogr. Palaeoclimatol. Palaeoecol. 373, 141–151.
Butz, C., Grosjean, M., Fischer, D., Wunderle, S., Tylmann, W., Rein, B., 2015. Hyperspectral imaging spectroscopy: a promising method for the biogeochemical analysis of lake sediments. J. Appl. Rem. Sen. 9, 096031-1-096031-20.
Buzon, M.R., Bowen, G.J., 2010. Oxygen and carbon isotope analysis of human tooth enamel from the New Kingdom site of Tombos in Nubia. Archaeometry 52, 855–868.
Cai, Y., Chiang, J.C., Breitenbach, S.F., Tan, L., Cheng, H., Edwards, R.L., An, Z., 2017. Holocene moisture changes in western China, Central Asia, inferred from stalagmites. Quat. Sci. Rev. 158, 15–28.
Cai, Z., Tian, L., 2016. Atmospheric controls on seasonal and interannual variations in the precipitation isotope in the east Asian Monsoon Region. J. Climate 29, 1339–1352.
Came, R.E., Oppo, D.W., McManus, J.F., 2007. Amplitude and timing of temperature and salinity variability in the subpolar North Atlantic over the past 10 ky. Geology 35, 315–318.
Camenisch, C., Salvisberg, M., 2020. Droughts in Bern and Rouen from the 14th to the beginning of the 18th century derived from documentary evidence. Climate Past 16, 2173–2182.
Campana, S., 1999. Chemistry and composition of fish otoliths: pathways, mechanisms and applications. Mar. Ecol. Prog. Ser. 188, 263–297.
Camuffo, D., 1987. Freezing of the Venetian Lagoon since the 9th century A.D. in comparision to the climate of western Europe and England. Climatic Change 10, 43–66.
Cannon, A., Yang, D.Y., 2006. Early storage and sedentism on the pacific northwest coast: Ancient dna analysis of salmon remains from namu, British Columbia. Am. Ant. 71, 123–140.
Carolin, S.A., Cobb, K.M., Lynch-Stieglitz, J., Moerman, J.W., Partin, J.W., Lejau, S., Malang, J., Clark, B., Tuen, A.A., Adkins, J.F., 2016. Northern Borneo stalagmite records reveal West Pacific hydroclimate across MIS 5 and 6. Earth Planet. Sci. Lett. 439, 182–193.
Carré, M., Cheddadi, R., 2017. Seasonality in long-term climate change. Quaternaire 28, 173–177.
Carrel, W.K., 1994. Reproductive history of female black bears from dental cementum. In: Bears: Their Biology and Management, vol. 9, pp. 205–212.
Casado, M., Landais, A., Picard, G., Münch, T., Laepple, T., Stenni, B., Dreossi, G., Ekaykin, A., Arnaud, L., Genthon, C., Touzeau, A., Masson-Delmotte, V., Jouzel, J., 2018. Archival processes of the water stable isotope signal in east antarctic ice cores. Cryosphere 12, 1745–1766.
Casteel, R.C., Banner, J.L., 2015. Temperature-driven seasonal calcite growth and drip water trace element variations in a well-ventilated Texas cave: implications for speleothem paleoclimate studies. Chem. Geol. 392, 43–58.
Cáceres, J., Pelascini, F., Motto-Ros, V., Moncayo, S., Trichard, F., Panczer, G., Marín-Roldán, A., Cruz, J., Coronado, I., Martín-Chivelet, J., 2017. Megapixel multi-elemental imaging by Laser-Induced Breakdown Spectroscopy, a technology with considerable potential for paleoclimate studies. Sci. Rep. 7, 1–11.
Chave, A.D., 2019. A multitaper spectral estimator for time-series with missing data. Geophys. J. Inter. 218, 2165–2178.
Chen, F., Shang, H., Panyushkina, I.P., Meko, D.M., Yu, S., Yuan, Y., Chen, F., 2019. Tree-ring reconstruction of Lhasa River streamflow reveals 472 years of hydrologic change on southern Tibetan Plateau. J. Hydrol. 572, 169–178.

Chen, T., Cobb, K., Roff, G., Zhao, J., Yang, H., Hu, M., Zhao, K., 2018. Coral-derived western Pacific tropical sea surface temperatures during the last millennium. Geophys. Res. Lett. 45, 3542–3549.
Cheng, H., Zhang, P., Spötl, C., Edwards, R., Cai, Y., Zhang, D., Sang, W., Tan, M., An, Z., 2012. The climatic cyclicity in semiarid-arid central Asia over the past 500,000 years. Geophys. Res. Lett. 39.
Cheng, L., AghaKouchak, A., Gilleland, E., Katz, R.W., 2014. Non-stationary extreme value analysis in a changing climate. Climatic change 127, 353–369.
Chevalier, M., Davis, B.A., Heiri, O., Seppä, H., Chase, B.M., Gajewski, K., Lacourse, T., Telford, R.J., Finsinger, W., Guiot, J., Kühl, N., Maezumi, S.Y., Tipton, J.R., Carter, V.A., Brussel, T., Phelps, L.N., Dawson, A., Zanon, M., Vallé, F., Nolan, C., Mauri, A., de Vernal, A., Izumi, K., Holmström, L., Marsicek, J., Goring, S., Sommer, P.S., Chaput, M., Kupriyanov, D., 2020. Pollen-based climate reconstruction techniques for late quaternary studies. Earth-Sci. Rev. 210, 103384.
Chu, G., Sun, Q., Wang, X., Liu, M., Lin, Y., Xie, M., Shang, W., Liu, J., 2012. Seasonal temperature variability during the past 1600 years recorded in historical documents and varved lake sediment profiles from northeastern China. Holocene 22, 785–792.
Chu, G., Sun, Q., Zhaoyan, G., Rioual, P., Qiang, L., Kaijun, W., Han, J., Liu, J., 2009. Dust records from varved lacustrine sediments of two neighboring lakes in northeastern China over the last 1400 years. Quat. Inter. 194, 108–118.
Chuine, I., Yiou, P., Viovy, N., Seguin, B., Daux, V., Ladurie, E.L.R., 2004. Grape ripening as a past climate indicator. Nature 432, 289–290.
Chutko, K.J., Lamoureux, S.F., 2009. Biolaminated sedimentation in a High Arctic freshwater lake. Sedimentology 56, 1642–1654.
Cincotta, P.M., Mendez, M., Nunez, J.A., 1995. Astronomical time series analysis. I. A search for periodicity using information entropy. Astrophys. J. 449, 231.
Clark, I.D., Fritz, P., 2004. Environmental Isotopes in Hydrogeology. CRC Press.
Cleveland, R.B., Cleveland, W.S., McRae, J.E., Terpenning, I., 1990. Stl: A seasonal-trend decomposition. J. Offic. Stat. 6, 3–73.
Cobo, A., García-Escárzaga, A., Gutiérrez-Zugasti, I., Setién, J., González-Morales, M., López-Higuera, J., 2017. Automated measurement of magnesium/calcium ratios in gastropod shells using laser-induced breakdown spectroscopy for paleoclimatic applications. Appl. Spectrosc. 71, 591–599.
Coe, W., Fox, D., 1942. Biology of the California sea mussel (*Mytilus californianus*). J. Exp. Biol. 90, 1–30.
Colonese, A., Mannino, M., Mayer, D.Y., Fa, D., Finlayson, J., Lubell, D., Stiner, M., 2011. Marine mollusc exploitation in Mediterranean prehistory: an overview. Quat. Inter. 239, 86–103.
Colonese, A., Vetro, D., Landini, W., Di Giuseppe, Z., Hausmann, N., Demarchi, B., d'Angelo, C., Leng, M., Incarbona, A., Whitwood, A., Martini, F., 2018. Late Pleistocene-Holocene coastal adaptation in central Mediterranean: snapshots from Grotta d'Oriente (NW Sicily). Quat. Inter. 493, 114–126.
Comboul, M., Emile-Geay, J., Evans, M., Mirnateghi, N., Cobb, K., Thompson, D., 2014. A probabilistic model of chronological errors in layer-counted climate proxies: applications to annually banded coral archives. Climate Past 10, 825–841.
Conover, D.O., 1992. Seasonality and the scheduling of life history at different latitudes. J. Fish Bio. 41, 161–178.
Cook, E.R., Anchukaitis, K.J., Buckley, B.M., D'Arrigo, R.D., Jacoby, G.C., Wright, W.E., 2010. Asian monsoon failure and megadrought during the last millennium. Science 328, 486–489.
Corella, J.P., Valero-Garces, B.L., Vicente-Serrano, S.M., Brauer, A., Benito, G., 2016. Three millennia of heavy rainfalls in Western Mediterranean: frequency, seasonality and atmospheric drivers. Sci. Rep. 6, 38206.
Crawford, J., Hughes, C.E., Lykoudis, S., 2014. Alternative least squares methods for determining the meteoric water line, demonstrated using gnip data. J. Hydrol. 519, 2331–2340.
Creber, G.T., Chaloner, W.G., 1984. Influence of environmental factors on the wood structure of living and fossil trees. Botan. Rev. 50, 357–448.
Cross, J., 1988. Expanding the scope of seasonality research in archaeology. In: Huss-Ashmore, R. (Ed.), Masca Research Papers in Science and Archaeology, vol. 5, pp. 55–64.
Crowley, T.J., Short, D.A., Mengel, J.G., North, G.R., 1986. Role of seasonality in the evolution of climate during the last 100 million years. Science 231, 579–584.
Cruz, F.W., Burns, S.J., Jercinovic, M., Karmann, I., Sharp, W.D., Vuille, M., 2007. Evidence of rainfall variations in Southern Brazil from trace element ratios (Mg/Ca and Sr/Ca) in a Late Pleistocene stalagmite. Geochim. Cosmochim. Acta 71, 2250–2263.
Cuffey, K.M., Clow, G.D., Alley, R.B., Stuiver, M., Waddington, E.D., Saltus, R.W., 1995. Large arctic temperature change at the wisconsin-holocene glacial transition. Science 270, 455–458.
Dansgaard, W., 1964. Stable isotopes in precipitation. Tellus 16, 436–468.
Daux, V., Garcia De Cortazar-Atauri, I., Yiou, P., Chuine, I., Garnier, E., Le Roy Ladurie, E., Mestre, O., Tardaguila, J., 2012. An open-access database of grape harvest dates for climate research: data description and quality assessment. Climate Past 8, 1403–1418.
Davey, A., Flores, B., 1993. Identification of seasonality in time series: a note. Math. Comput. Mode. 18, 73–81.
Davies, S.J., Lamb, H.F., Roberts, S.J., 2015. Micro-XRF Core Scanning in Palaeolimnology: Recent Developments. In: Croudace, I.W., Rothwell, R.G. (Eds.), Micro-XRF Studies of Sediment Cores: Applications of a Non-Destructive Tool for the Environmental Sciences. Springer Netherlands, Dordrecht, pp. 189–226.
Day, C.C., Henderson, G.M., 2013. Controls on trace-element partitioning in cave-analogue calcite. Geochim. Cosmochim. Acta 120, 612–627.
De Haan, L., Ferreira, A., 2007. Extreme value theory: an introduction. Springer Science & Business Media.
De Jager, O., Raubenheimer, B., Swanepoel, J., 1989. A powerful test for weak periodic signals with unknown light curve shape in sparse data. Astron. Astrophys. 221, 180–190.
De Landa, D., Garibay Kintana Garibay, K., 1978. Relación de las cosas de Yucatán. Editorial Porrua.
De Vries, J., 1977. Histoire du climat et économie: des faits nouveaux, une interprétation différente. Ann. Histoire. Sci. Soc. 32, 198–226.
De Vynck, J.C., Cowling, R.M., Potts, A.J., Marean, C.W., 2016. Seasonal availability of edible underground and aboveground carbohydrate resources to human foragers on the cape south coast, south africa. Peer J. 4, e1679.
Dean, J.R., Eastwood, W.J., Roberts, N., Jones, M.D., Yigitbasioglu, H., Allcock, S.L., Woodbridge, J., Metcalfe, S.E., Leng, M.J., 2015. Tracking the hydro-climatic signal from lake to sediment: a field study from central Turkey. J. Hydrol. 529, 608–621.
Dee, S., Emile-Geay, J., Evans, M., Allam, A., Steig, E., Thompson, D., 2015. Prysm: an open-source framework for proxy system modeling, with applications to oxygen-isotope systems. J. Adv. Mode. Earth Sys. 7, 1220–1247.
Degroot, D., Anchukaitis, K., Bauch, M., Burnham, J., Carnegy, F., Cui, J., de Luna, K., Guzowski, P., Hambrecht, G., Huhtamaa, H., Izdebski, A., Kleemann, K., Moesswilde, E., Neupane, N., Newfield, T., Pei, Q., Xoplaki, E., Zappia, N., 2021. Towards a rigorous understanding of societal responses to climate change. Nature 591, 539–550.
Deininger, M., Fohlmeister, J., Scholz, D., Mangini, A., 2012. Isotope disequilibrium effects: the influence of evaporation and ventilation effects on the carbon and oxygen isotope composition of speleothems-a model approach. Geochim. Cosmochim. Acta 96, 57–79.
Deininger, M., McDermott, F., 2016. Coherency of european speleothem δ18o records linked to north atlantic ocean circulation. EGU General Assembly Conference Abstracts pp. EPSC2016-5031.
Delaygue, G., Jouzel, J., Masson, V., Koster, R.D., Bard, E., 2000. Validity of the isotopic thermometer in central antarctica: limited impact of glacial precipitation seasonality and moisture origin. Geophys. Res. Lett. 27, 2677–2680.
deMenocal, P.B., 1995. Plio-pleistocene african climate. Science 270, 53–59.
Deng, W., Wei, G., Yu, K., Zhao, J.x., 2014. Variations in the timing of the rainy season in the northern South China Sea during the middle to late Holocene. Paleoceanography 29, 115–125.
Denniston, R.F., Houts, A.N., Asmerom, Y., Wanamaker Jr., A.D., Haws, J.A., Polyak, V. J., Thatcher, D.L., Altan-Ochir, S., Borowske, A.C., Breitenbach, S.F.M., Ummenhofer, C.C., Regala, F.T., Benedetti, M.M., Bicho, N.F., 2018. A stalagmite test of North Atlantic SST and Iberian hydroclimate linkages over the last two glacial cycles. Climate Past 14, 1893–1913.
Denton, G.H., Alley, R.B., Comer, G.C., Broecker, W.S., 2005a. The role of seasonality in abrupt climate change. Quat. Sci. Rev. 24, 1159–1182.
Denton, G.H., Alley, R.B., Comer, G.C., Broecker, W.S., 2005b. The role of seasonality in abrupt climate change. Quat. Sci. Rev. 24, 1159–1182.
Dias, P., Beaini, T., Melani, R., 2010. Age estimation from dental cementum incremental lines and periodontal disease. J. Foren. Odonto-Stomatol. 28, 13–21.
Dobrovolný, P., Moberg, A., Brázdil, R., Pfister, C., Glaser, R., Wilson, R., van Engelen, A., Limanówka, D., Kiss, A., Halíčková, M., Macková, J., Riemann, D., Luterbacher, J., B“ohm, R., 2010. Monthly, seasonal and annual temperature reconstructions for Central Europe derived from documentary evidence and instrumental records since AD 1500. Climatic Change 101, 69–107.
Domínguez-Castro, F., Santisteban, J.I., Barriendos, M., Mediavilla, R., 2008. Reconstruction of drought episodes for central Spain from rogation ceremonies recorded at the Toledo Cathedral from 1506 to 1900: a methodological approach. Global Planet. Change 63, 230–242.
Donges, J.F., Donner, R.V., Trauth, M.H., Marwan, N., Schellnhuber, H.J., Kurths, J., 2011. Nonlinear detection of paleoclimate-variability transitions possibly related to human evolution. Proc. Natl. Acad. Sci. 108, 20422–20427.
Dorale, J.A., González, L.A., Reagan, M.K., Pickett, D.A., Murrell, M.T., Baker, R.G., 1992. A High-Resolution Record of Holocene Climate Change in Speleothem Calcite from Cold Water Cave. Northeast Iowa. Sci. 258, 1626–1630.
Doughty, C.E., Faurby, S., Svenning, J.C., 2016a. The impact of the megafauna extinctions on savanna woody cover in South America. Ecography 39, 213–222.
Doughty, C.E., Wolf, A., Morueta-Holme, N., Jørgensen, P.M., Sandel, B., Violle, C., Boyle, B., Kraft, N.J.B., Peet, R.K., Enquist, B.J., Svenning, J.C., Blake, S., Galetti, M., 2016b. Megafauna extinction, tree species range reduction, and carbon storage in Amazonian forests. Ecography 39, 194–203.
Piperno, Dolores R., Pearsall, Deborah M., 1998. The Origins of Agriculture in the Lowland Neotropics. Academic Press.
Drew, D.M., Allen, K., Downes, G.M., Evans, R., Battaglia, M., Baker, P., 2013. Wood properties in a long-lived conifer reveal strong climate signals where ring-width series do not. Tree Phys. 33, 37–47.
Druckenbrod, D.L., Mann, M.E., Stahle, D.W., Cleaveland, M.K., Therrell, M.D., Shugart, H.H., 2003. Late-eighteenth-century precipitation reconstructions from James Madison's Montpelier plantation. Bulletin Am. Meteorol. Soc. 84, 57–72.
Duesing, W., Berner, N., Deino, A.L., Foerster, V., Kraemer, K.H., Marwan, N., Trauth, M. H., 2021. Multiband wavelet age modeling for a 293 m (600 kyr) sediment core from chew bahir basin, southern ethiopian rift. Front. Earth Sci. 9, 35.
Durham, S., Gillikin, D., Goodwin, D., Dietl, G., 2017. Rapid determination of oyster lifespans and growth rates using LA-ICP-MS line scans of shell Mg/Ca ratios. Palaeogeogr. Palaeoclimatol. Palaeoecol. 485, 201–209.
Emile-Geay, J., Cobb, K.M., Carré, M., Braconnot, P., Leloup, J., Zhou, Y., Harrison, S.P., Correge, T., McGregor, H.V., Collins, M., et al., 2016. Links between tropical Pacific seasonal, interannual and orbital variability during the Holocene. Nat. Geosci. 9, 168.
Emiliani, C., 1955. Pleistocene Temperatures. J. Geol. 63, 538–578.

Epstein, S., Buchsbaum, R., Lowenstam, H., Urey, H.C., 1951. Carbonate-water isotopic temperature scale. GSA Bull. 62, 417–426.
Erlandson, J.M., Rick, T.C., Braje, T.J., Casperson, M., Culleton, B., Fulfrost, B., Garcia, T., Guthrie, D.A., Jew, N., Kennett, D.J., Moss, M.L., Reeder, L., Skinner, C., Watts, J., Willis, L., 2011. Paleoindian seafaring, maritime technologies, and coastal foraging on california's channel islands. Science 331, 1181–1185.
Eroglu, D., McRobie, F.H., Ozken, I., Stemler, T., Wyrwoll, K.H., Breitenbach, S.F., Marwan, N., Kurths, J., 2016. See-saw relationship of the Holocene East Asian-Australian summer monsoon. Nat. Commun. 7, 12929.
Esper, J., Klippel, L., Krusic, P.J., Konter, O., Raible, C.C., Xoplaki, E., Luterbacher, J., B”untgen, U., 2020. Eastern Mediterranean summer temperatures since 730 CE from Mt. Smolikas tree-ring densities. Climate Dyn. 54, 1367–1382.
Evans, M., 2007. Toward forward modeling for paleoclimatic proxy signal calibration: a case study with oxygen isotopic composition of tropical woods. Geochem. Geophys. Geosyst. 8.
Fairchild, I., Baker, A., 2012. Speleothem Science: From Process to Past Environment. Wiley-Blackwell, Chichester, UK.
Fairchild, I.J., Borsato, A., Tooth, A.F., Frisia, S., Hawkesworth, C.J., Huang, Y., McDermott, F., Spiro, B., 2000. Controls on trace element (Sr-Mg) compositions of carbonate cave waters: implications for speleothem climatic records. Chem. Geol. 166, 255–269.
Fairchild, I.J., Smith, C.L., Baker, A., Fuller, L., Spötl, C., Mattey, D., McDermott, F., E.I. M.F., 2006. Modification and preservation of environmental signals in speleothems. Earth-Sci. Rev. 75, 105–153.
Falkowski, T.B., Chankin, A., Diemont, S.A.W., Pedian, R.W., 2019. More than just corn and calories: a comprehensive assessment of the yield and nutritional content of a traditional Lacandon Maya milpa. Food Sec. 11, 389–404.
Fallah, B., Sodoudi, S., Russo, E., Kirchner, I., Cubasch, U., 2017. Towards modeling the regional rainfall changes over Iran due to the climate forcing of the past 6000 years. Quat. Inter. 429, 119–128.
Faulkner, P., 2013. Life on the Margins: An Archaeological Investigation of Late Holocene Economic Variability, Coastal Blue Mud Bay, Northern Australia. ANU E Press, Canberra.
Felis, T., Giry, C., Scholz, D., Lohmann, G., Pfeiffer, M., P“atzold, J., Kölling, M., Scheffers, S.R., 2015. Tropical Atlantic temperature seasonality at the end of the last interglacial. Nat. Commun. 6, 6159.
Felis, T., Lohmann, G., Kuhnert, H., Lorenz, S.J., Scholz, D., P“atzold, J., Al-Rousan, S.A., Al-Moghrabi, S.M., 2004. Increased seasonality in Middle East temperatures during the last interglacial period. Nature 164–168.
Feng, X., Porporato, A., Rodriguez-Iturbe, I., 2013. Changes in rainfall seasonality in the tropics. Nat. Climate Change 3, 811–815.
Feranec, R.S., Hadly, E.A., Paytan, A., 2009. Stable isotopes reveal seasonal competition for resources between late Pleistocene bison (Bison) and horse (Equus) from Rancho La Brea, southern California. Palaeogeo. Palaeoclimatol. Palaeoecol. 271, 153–160.
Ferguson, J.E., Henderson, G.M., Fa, D.A., Finlayson, J.C., Charnley, N.R., 2011. Increased seasonality in the Western Mediterranean during the last glacial from limpet shell geochemistry. Earth Planet. Sci. Lett. 308, 325–333.
Fiedel, S.J., 2000. The peopling of the new world: Present evidence, new theories, and future directions. J. Archaeol. Res. 8, 39–103.
Finstad, K., Ingram, B., Schweikhardt, P., Lightfoot, K., Luby, E., Coles, G., 2013. New insights about the construction and use of shell mounds from the geochemical analysis of mollusks: an example from the greater San Francisco Bay. J. Archaeol. Sci. 40, 2648–2658.
Fisher, D., Wake, C., Kreutz, K., Yalcin, K., Steig, E., Mayewski, P., Anderson, L., Zheng, J., Rupper, S., Zdanowicz, C., Demuth, M., Waszkiewicz, M., Dahl-Jensen, D., Goto-Azuma, K., Bourgeois, J., Koerner, R., Sekerka, J., Osterberg, E., Abbott, M., Finney, B., Burns, S., 2004. Stable isotope records from mount logan, eclipse ice cores and nearby jellybean lake. water cycle of the north pacific over 2000 years and over five vertical kilometres: Sudden shifts and tropical connections. Géogr. Phys. Quat. 58, 337–352.
Fisher, D.A., 1992. Stable isotope simulations using a regional stable isotope model coupled to a zonally averaged global model. Cold Reg. Sci. Tech. 21, 61–77.
Füllenbach, C., Schöne, B., Mertz-Kraus, R., 2015. Strontium/lithium ratio in aragonitic shells of Cerastoderma edule (Bivalvia) – a new potential temperature proxy for brackish environments. Chem. Geol. 417, 341–355.
Fohlmeister, J., Schröder-Ritzrau, A., Spötl, C., Frisia, S., Miorandi, R., Kromer, B., Mangini, A., 2010. The influences of hydrology on the radiogenic and stable carbon isotope composition of cave drip water, Grotta Di Ernesto (Italy). Radiocarbon 52, 1529–1544.
Fohlmeister, J., Voarintsoa, N.R.G., Lechleitner, F.A., Boyd, M., Brandtstätter, S., Jacobson, M.J., Oster, J.L., 2020. Main controls on the stable carbon isotope composition of speleothems. Geochim. Cosmochim. Acta 279, 67–87.
Fonti, P., Von Arx, G., García-González, I., Eilmann, B., Sass-Klaassen, U., G” artner, H., Eckstein, D., 2010. Studying global change through investigation of the plastic responses of xylem anatomy in tree rings. New Phytologist 185, 42–53.
Foroozan, Z., Griessinger, J., Pourtahmasi, K., Brauning, A., 2020. 501 years of spring precipitation history for the semi-arid northern iran derived from tree-ring delta o-18 data. Atmosphere 11.
Foster, G., 1996. Wavelets for period analysis of unevenly sampled time series. Astro. J. 112, 1709.
Franke, P.M., Huntley, B., Parnell, A.C., 2018. Frequency selection in paleoclimate time series: A model-based approach incorporating possible time uncertainty. Environmetrics 29, e2492.
Frappier, A., Sahagian, D., González, L.A., Carpenter, S.J., 2002. El Niño events recorded by stalagmite carbon isotopes. Science 298, 565–565.
Freedman, L., 1979. The use of a Kolmogorov-Smirnov type statistic in testing hypotheses about seasonal variation. J. Epdemiol. Commun. Health 33, 223–228.
Frisia, S., Borsato, A., 2010. Carbonates in continental settings: facies, environments, and processes. In: Alonso-Zarza, A., Tanner, L. (Eds.), Carbonates in Continental Settings: Facies, Environments, and Processes. Elsevier volume 61 of Developments in Sedimentology, p. iii.
Fritts, H., 1976. Tree Rings and Climate. Academic Press, London, 582 p.
Froese, D.G., Westgate, J.A., Reyes, A.V., Enkin, R.J., Preece, S.J., 2008. Ancient permafrost and a future, warmer arctic. Science 321, 1648–1648.
Gabitov, R.I., Watson, E.B., Sadekov, A., 2012. Oxygen isotope fractionation between calcite and fluid as a function of growth rate and temperature: an in situ study. Chem. Geol. 306-307, 92–102.
Gabriela, P.C., Takayuki, Y., Jean-Louis, D., Kélig, M., Philippe, B., 2021. Reconstructing freshwater fishing seasonality in a neotropical savanna: first application of swamp eel (*Synbranchus marmoratus*) sclerochronology to a pre-Columbian Amazonian site (Loma Salvatierra, Bolivia). J. Archaeol. Sci.: Rep. 37, 102880.
Galewsky, J., Steen-Larsen, H.C., Field, R.D., Worden, J., Risi, C., Schneider, M., 2016. Stable isotopes in atmospheric water vapor and applications to the hydrologic cycle. Rev. Geophys. 54, 809–865.
García-Escárzaga, A., Gutiérrez-Zugasti, I., Cobo, A., Cuenca-Solana, D., Martín-Chivelet, J., Roberts, P., González-Morales, M., 2019. Stable oxygen isotope analysis of *Phorcus lineatus* (da Costa, 1778) as a proxy for foraging seasonality during the Mesolithic in northern Iberia. Archaeol. Anthropol. Sci. 11, 5631–5644.
Garcia, R.R., Díaz, H.F., Herrera, R.G., Eischeid, J., Prieto, M.d.R., Hernández, E., Gimeno, L., Durán, F.R., Bascary, A.M., 2001. Atmospheric circulation changes in the tropical Pacific inferred from the voyages of the Manila galleons in the sixteenth-eighteenth centuries. Bull. Am. Meteorol. Soc. 82, 2435–2456.
Garland, J., Jones, T.R., Bradley, E., Neuder, M., White, J.W., 2018a. Climate entropy production recorded in a deep antarctic ice core. arXiv:1806.10936.
Garland, J., Jones, T.R., Neuder, M., Morris, V., White, J.W., Bradley, E., 2018b. Anomaly detection in paleoclimate records using permutation entropy. Entropy 20, 931.
Gascoyne, M., 1992. Palaeoclimate determination from cave calcite deposits. Quat. Sci. Rev. 11, 609–632.
Genty, D., Baker, A., Massault, M., Proctor, C., Gilmour, M., Pons-Branchu, E., Hamelin, B., 2001. Dead carbon in stalagmites: carbonate bedrock paleodissolution vs. ageing of soil organic matter. Implications for ^{13}C variations in speleothems. Geochim. Cosmochim. Acta 65, 3443–3457.
Genty, D., Blamart, D., Ouahdi, R., Gilmour, M., Baker, A., Jouzel, J., Van-Exter, S., 2003. Precise dating of Dansgaard-Oeschger climate oscillations in western Europe from stalagmite data. Nature 421, 833–837.
Genty, D., Massault, M., 1999. Carbon transfer dynamics from bomb- ^{14}C and $\delta^{13}C$ time series of a laminated stalagmite from SW France – modelling and comparison with other stalagmite records. Geochim. Cosmochim. Acta 63, 1537–1548.
Genty, D., Quinif, Y., 1996. Annually laminated sequences in the internal structure of some Belgian stalagmites; importance for paleoclimatology. J. Sediment. Res. 66, 275–288.
Ghaderpour, E., Pagiatakis, S.D., 2017. Least-squares wavelet analysis of unequally spaced and non-stationary time series and its applications. Math. Geosci. 49, 819–844.
Ghil, M., Allen, M., Dettinger, M., Ide, K., Kondrashov, D., Mann, M., Robertson, A.W., Saunders, A., Tian, Y., Varadi, F., et al., 2002. Advanced spectral methods for climatic time series. Rev. Geophys. 40, 3-1.
Ghil, M., Mo, K., 1991a. Intraseasonal oscillations in the global atmosphere. Part I: Northern Hemisphere and tropics. J. Atmos. Sci. 48, 752–779.
Ghil, M., Mo, K., 1991b. Intraseasonal oscillations in the global atmosphere. Part II: Southern Hemisphere. J. Atmos. Sci. 48, 780–790.
Gilbert, R., Lamoureux, S., 2004. Processes affecting deposition of sediment in a small, morphologically complex lake. J. Paleolimnol. 31, 37–48.
Gimmi, U., Luterbacher, J., Pfister, C., Wanner, H., 2007. A method to reconstruct long precipitation series using systematic descriptive observations in weather diaries: the example of the precipitation series for Bern, Switzerland (1760–2003). Theor. Appl. Climatol. 87, 185–199.
Glaser, R., Brázdil, R., Pfister, C., Dobrovolný, P., Vallvé, M.B., Bokwa, A., Camuffo, D., Kotyza, O., Limanówka, D., Rácz, L., 1999. Seasonal temperature and precipitation fluctuations in selected parts of Europe during the sixteenth century. Clim. Change 43, 169–200.
Golicz, A.A., Bayer, P.E., Barker, G.C., Edger, P.P., Kim, H., Martinez, P.A., Chan, C.K.K., Severn-Ellis, A., McCombie, W.R., Parkin, I.A.P., Paterson, A.H., Pires, J.C., Sharpe, A.G., Tang, H., Teakle, G.R., Town, C.D., Batley, J., Edwards, D., 2016. The pangenome of an agronomically important crop plant brassica oleracea. Nat. Commun. 7, 13390.
Gordon Childe, V.., 1936. Man makes himself. Nature 138, 699–700.
Goswami, B., Boers, N., Rheinwalt, A., Marwan, N., Heitzig, J., Breitenbach, S.F., Kurths, J., 2018. Abrupt transitions in time series with uncertainties. Nat. Commun. 9, 48.
Goswami, B., Heitzig, J., Rehfeld, K., Marwan, N., Anoop, A., Prasad, S., Kurths, J., 2014. Estimation of sedimentary proxy records together with associated uncertainty. Nonlin. Process. Geophys. 21, 1093–1111.
Graham, M.J., Drake, A.J., Djorgovski, S., Mahabal, A.A., Donalek, C., Duan, V., Maker, A., 2013. A comparison of period finding algorithms. Monthly Not. Royal Astro. Soc. 434, 3423–3444.
Granger, C.W., 1969. Investigating causal relations by econometric models and cross-spectral methods. Econ.: J. Econ. Soc. 424–438.
Griffin, D., Woodhouse, C.A., Meko, D.M., Stahle, D.W., Faulstich, H.L., Carrillo, C., Touchan, R., Castro, C.L., Leavitt, S.W., 2013. North American monsoon

precipitation reconstructed from tree-ring latewood. Geophys. Res. Lett. 40, 954–958.
Grinsted, A., Moore, J.C., Jevrejeva, S., 2004. Application of the cross wavelet transform and wavelet coherence to geophysical time series. Nonlin. Process. Geophys. 11, 561–566.
Grinsted, A., Moore, J.C., Pohjola, V., Martma, T., Isaksson, E., 2006. Svalbard summer melting, continentality, and sea ice extent from the lomonosovfonna ice core. J. Geophys. Res.: Atmos. 111.
Gutiérrez-Zugasti, I., García-Escárzaga, A., Martín-Chivelet, J., González-Morales, M., 2015. Determination of sea surface temperatures using oxygen isotope ratios from phorcus lineatus (Da Costa, 1778) in northern Spain: implications for paleoclimate and archaeological studies. Holocene 25, 1002–1014.
Gutiérrez-Zugasti, I., Suárez-Revilla, R., Clarke, L., Schöne, B., Bailey, G., González-Morales, M., 2017. Shell oxygen isotope values and sclerochronology of the limpet patella vulgata linnaeus 1758 from northern Iberia: implications for the reconstruction of past seawater temperatures. Palaeogeo. Palaeoclimatol. Palaeoecol. 484, 48–61.
Haam, E., Huybers, P., 2010. A test for the presence of covariance between time-uncertain series of data with application to the dongge cave speleothem and atmospheric radiocarbon records. Paleoceanography 25.
Hallmann, N., Burchell, M., Schöne, B., Irvine, G., Maxwell, D., 2009. High-resolution sclerochronological analysis of the bivalve mollusk saxidomus gigantea from Alaska and British Columbia: techniques for revealing environmental archives and archaeological seasonality. J. Archaeol. Sci. 36, 2353–2364.
Hao, Z., Wu, M., Zheng, J., Chen, J., Zhang, X., Luo, S., 2020. Patterns in data of extreme droughts/floods and harvest grades derived from historical documents in eastern china during 801-1910. Climate Past 16, 101–116.
Hardt, B., Rowe, H.D., Springer, G.S., Cheng, H., Edwards, R.L., 2010. The seasonality of east central North American precipitation based on three coeval holocene speleothems from southern west Virginia. Earth Planet. Sci. Lett. 295, 342–348.
Hardy, D.R., Bradley, R.S., Zolitschka, B., 1996. The climatic signal in varved sediments from lake C2, northern ellesmere Island, Canada. J. Paleolimnol. 16, 227–238.
Hartland, A., Zitoun, R., 2018. Transition metal availability to speleothems controlled by organic binding ligands. Geochem. Perspec. Lett. 8, 22–25.
Hartmann, A., Baker, A., 2017. Modelling karst vadose zone hydrology and its relevance for paleoclimate reconstruction. Earth-Sci. Rev. 172, 178–192.
Hassan, F.A., 2007. Extreme nile floods and famines in medieval Egypt (AD 930–1500) and their climatic implications. Quat. Inter. 173, 101–112.
Hausmann, N., Colonese, A., de Lima Ponzoni, A., Hancock, Y., Meredith-Williams, M., Leng, M., Bailey, G., 2017. Isotopic composition of conomurex fasciatus shells as an environmental proxy for the red sea. Quat. Inter. 427, 115–127.
Hausmann, N., Prendergast, A.L., Lemonis, A., Zech, J., Roberts, P., Siozos, P., Anglos, D., 2019. Extensive elemental mapping unlocks Mg/Ca ratios as climate proxy in seasonal records of mediterranean limpets. Sci. Rep. 9, 3698.
Haynes, C.V., 1964. Fluted projectile points: their age and dispersion. Science 145, 1408–1413.
Hays, J.D., Imbrie, J., Shackleton, N.J., 1976. Variations in the Earth's Orbit: Pacemaker of the Ice Ages. Science 194, 1121–1132.
He, M., Yang, B., Br“auning, A., Rossi, S., Ljungqvist, F.C., Shishov, V., Grieß inger, J., Wang, J., Liu, J., Qin, C., 2019. Recent Advances in Dendroclimatology in China.
Heinrich, I., Balanzategui, D., Bens, O., Blasch, G., Blume, T., Bottcher, F., Borg, E., Brademann, B., Brauer, A., Conrad, C., Dietze, E., Drager, N., Fiener, P., Gerke, H.H., Guntner, A., Heine, I., Helle, G., Herbrich, M., Harfenmeister, K., Heussner, K.U., Hohmann, C., Itzerott, S., Jurasinski, G., Kaiser, K., Kappler, C., Koebsch, F., Liebner, S., Lischeid, G., Merz, B., Missling, K.D., Morgner, M., Pinkerneil, S., Plessen, B., Raab, T., Ruhtz, T., Sachs, T., Sommer, M., Spengler, D., Stender, V., Stuve, P., Wilken, F., 2018. Interdisciplinary geo-ecological research across time scales in the northeast German Lowland observatory (tereno-ne). Vadose Zone J. 17.
Helle, G., Schleser, G.H., 2004. Beyond CO_2-fixation by rubisco – an interpretation of $^{13}C/^{12}C$ variations in tree rings from novel intra-seasonal studies on broad-leaf trees. Plant Cell Environ. 27, 367–380.
Hellstrom, J., McCulloch, M., 2000. Multi-proxy constraints on the climatic significance of trace element records from a New Zealand speleothem. Earth Planet. Sci. Lett. 179, 287–297.
Hendy, E., Gagan, M., Alibert, C., McCulloch, M., Lough, J., Isdale, P., 2002. High altitude platform multichannel SAR for wide-area and staring imaging. Science 295, 1511–1514.
Higham, T., Horn, P., 2000. Seasonal dating using fish otoliths: results from the shag river mouth site, New Zealand. J. Arch. Sci. 27, 439–448.
Hoggarth, J.A., Restall, M., Wood, J.W., Kennett, D.J., Bricker, V.R., Chuchiak IV, J.F., Lima, M., Masson, M.A., Paine, R.R., Patch, R.W., 2017. Drought and its demographic effects in the Maya lowlands. Curr. Anthropol. 58, 0.
Holland, K.M., Porter, T.J., Froese, D.G., Kokelj, S.V., Buchanan, C.A., 2020. Ice-wedge evidence of holocene winter warming in the Canadian arctic. Geophys. Res. Lett. 47 e2020GL087942.
Holme, C., Gkinis, V., Lanzky, M., Morris, V., Olesen, M., Thayer, A., Vaughn, B.H., Vinther, B.M., 2019. Varying regional δ^{18}o-temperature relationship in high-resolution stable water isotopes from east Greenland. Climate Past 15, 893–912.
Holmgren, K., Karlén, W., Shaw, P.A., 1995. Paleoclimatic significance of the stable isotopic composition and petrology of a late pleistocene stalagmite from Botswana. Quat. Res. 43, 320–328.
Hu, J., Emile-Geay, J., Partin, J., 2017. Correlation-based interpretations of paleoclimate data-where statistics meet past climates. Earth Planet. Sci. Lett. 459, 362–371.
Huang, N.E., Wu, Z., 2008. A review on hilbert-huang transform: method and its applications to geophysical studies. Rev. Geophys. 46.
Hubeny, J.B., King, J.W., Santos, A., 2006. Subdecadal to multidecadal cycles of late Holocene north Atlantic climate variability preserved by estuarine fossil pigments. Geology 34, 569–572.
Hufthammer, A.K., Høie, H., Folkvord, A., Geffen, A.J., Andersson, C., Ninnemann, U.S., 2010. Seasonality of human site occupation based on stable oxygen isotope ratios of cod otoliths. J. Arch. Sci. 37, 78–83.
Hughen, K.A., Overpeck, J.T., Peterson, L.C., Anderson, R.F., 1996. The nature of varved sedimentation in the cariaco basin, venezuela, and its palaeoclimatic significance. Gegeol. Soc. London Spec. Publ. 116, 171–183.
Huijse, P., Estévez, P.A., Zegers, P., Príncipe, J.C., Protopapas, P., 2011. Period estimation in astronomical time series using slotted correntropy. IEEE Sig. Proc. Lett. 18, 371–374.
Iizuka, Y., Miyamoto, C., Matoba, S., Iwahana, G., Horiuchi, K., Takahashi, Y., Kanna, N., Suzuki, K., Ohno, H., 2019. Ion concentrations in ice wedges: an innovative approach to reconstruct past climate variability. Earth Planet. Sci. Lett. 515, 58–66.
Iriarte, J., Elliott, S., Maezumi, S.Y., Alves, D., Gonda, R., Robinson, M., Gregorio de Souza, J., Watling, J., Handley, J., 2020. The origins of amazonian landscapes: plant cultivation, domestication and the spread of food production in tropical south America. Quat. Sci. Rev. 248, 106582.
Isaksson, E., Hermanson, M., Hicks, S., Igarashi, M., Kamiyama, K., Moore, J., Motoyama, H., Muir, D., Pohjola, V., Vaikmäe, R., van de Wal, R.S., Watanabe, O., 2003. Ice cores from svalbard-useful archives of past climate and pollution history. Phys. Chem. Earth 28, 1217–1228.
Jamieson, R.A., Baldini, J.U., Brett, M.J., Taylor, J., Ridley, H.E., Ottley, C.J., Prufer, K. M., Wassenburg, J.A., Scholz, D., Breitenbach, S.F., 2016. Intra- and inter-annual uranium concentration variability in a belizean stalagmite controlled by prior aragonite precipitation: a new tool for reconstructing hydro-climate using aragonitic speleothems. Geochim. Cosmochim. Acta 190, 332–346.
Jansma, E., 2020. Hydrological disasters in the nw-European Lowlands during the first millennium ad: a dendrochronological reconstruction. Netherlands J. Geosci. Geol. En Mijinbouw 99.
Jazwa, C., Jantz, S., 2019. The effects of heating on δ^{18}O and δ^{13}C in mytilus Californianus shell carbonate: implications of paleoenvironmental reconstruction and season of harvest. J. Calf. Great Basin Anthropol. 39, 171–185.
Jazwa, C., Johnson, K., 2018. Erosion of coastal archaeological sites on Santa Rosa Island, California. West. Am. Nat. 78, 302–327.
Jazwa, C., Kennett, D., Hanson, D., 2012. Late Holocene subsistence change and marine productivity on western Santa Rosa Island, Alta California. Calf. Arch. 4, 69–98.
Jazwa, C., Wolfe, C., Chu, E., Stull, K., 2020. The effects of vertical position in the water column on δ^{18}O and δ^{13}C in *Mytilus californianus* shell carbonate. J. Archaeol. Sci.: Rep. 34, 102587.
Jazwa, C.S., Braje, T.J., Erlandson, J.M., Kennett, D.J., 2015. Central place foraging and shellfish processing on California's northern channel Islands. J. Anthropol. Arch. 40, 33–47.
Jerardino, A., 2016. On the origins and significance of Pleistocene coastal resource use in southern Africa with particular reference to shellfish gathering. J. Anthropol. Arch. 41, 213–230.
Jerardino, A., 2017. Water-worn shell and pebbles in shell middens as proxies of palaeoenvironmental reconstruction, shellfish procurement and their transport: a case study from the West Coast of South Africa. Quat. Int. 427, 103–114.
Jew, N., Erlandson, J., Watts, J., White, F., 2013. Shellfish, seasonality, and stable isotope sampling: δ^{18}O analysis of mussel shells form an 8800-year-old shell midden on California's Channel Islands. J. Island Coast. Arch. 8, 170–189.
Jochim, M., 1998. A Hunter-Gatherer Landscape. Southwest Germany in the Late Paleolithic and Mesolithic. Springer.
Johnsen, S., 2007. Stable isotope homogenization of polar firn and ice. Actes Colloq. 210–219.
Johnson, K.R., Hu, C., Belshaw, N.S., Henderson, G.M., 2006. Seasonal trace-element and stable-isotope variations in a Chinese speleothem: the potential for high-resolution paleomonsoon reconstruction. Earth Planet. Sci. Lett. 244, 394–407.
Jones, P., 2008. Historical climatology - a state of the art review. Weather 63, 181–186.
Jones, P.D., Briffa, K.R., Osborn, T.J., Lough, J.M., Van Ommen, T.D., Vinther, B.M., Luterbacher, J., Wahl, E.R., Zwiers, F.W., Mann, M.E., Schmidt, G.A., Ammann, C. M., Buckley, B.M., Cobb, K.M., Esper, J., Goosse, H., Graham, N., Jansen, E., Kiefer, T., Kull, C., K”uttel, M., Mosley-Thompson, E., Overpeck, J.T., Riedwyl, N., Schulz, M., Tudhope, A.W., Villalba, R., Wanner, H., Wolff, E., Xoplaki, E., 2009. High-resolution palaeoclimatology of the last millennium: a review of current status and future prospects. Holocene 19, 3–49.
Jones, T., Brown, G., Raab, L., McVickar, J., Spaulding, W., Kennett, D., York, A., Walker, P., 1999. Environmental imperatives reconsidered: demographic crises in western North America during the medieval climatic anomaly. Curr. Anthropol. 40, 137–170.
Jones, Matthew D., Roberts, C. Neil, Leng, Melanie J., Türkeş, Murat, 2006. A high-resolution late Holocene lake isotope record from Turkey and links to North Atlantic and monsoon climate. Geology 34, 361–364.
Jouzel, J., 2013. A brief history of ice core science over the last 50 yr. Climate Past 9, 2525–2547.
Jouzel, J., Alley, R.B., Cuffey, K.M., Dansgaard, W., Grootes, P., Hoffmann, G., Johnsen, S.J., Koster, R.D., Peel, D., Shuman, C.A., Stievenard, M., Stuiver, M., White, J., 1997. Validity of the temperature reconstruction from water isotopes in ice cores. J. Geophys. Res.: Oceans 102, 26471–26487.
Jouzel, J., Souchez, R.A., 1982. Melting–refreezing at the glacier sole and the isotopic composition of the Ice. J. Glaciol. 28, 35–42.
Žák, K., Onac, B.P., Persoiu, A., 2008. Cryogenic carbonates in cave environments: a review. Quat. Int. 187, 84–96.

Kaufman, A., Bar-Matthews, M., Ayalon, A., Carmi, I., 2003. The vadose flow above Soreq Cave, Israel: a tritium study of the cave waters. J. Hydrol. 273, 155–163.
Kaufman, D., McKay, N., Routson, C., Erb, M., Dätwyler, C., Sommer, P.S., Heiri, O., Davis, B., 2020. Holocene global mean surface temperature: a multi-method reconstruction approach. Sci. Data 7, 201.
Kaufman, D.S., Axford, Y.L., Henderson, A.C.G., McKay, N.P., Oswald, W.W., Saenger, C., Anderson, R.S., Bailey, H.L., Clegg, B., Gajewski, K., Hu, F.S., Jones, M.C., Massa, C., Routson, C.C., Werner, A., Wooller, M.J., Yu, Z.C., 2016. Holocene climate changes in eastern beringia (nw north america) – a systematic review of multi-proxy evidence. Quat. Sci. Rev. 147, 312–339.
Kennett, D., 2005. The Island Chumash: Behavioral Ecology of a Maritime Society. University of California Press, Berkeley.
Kennett, D., Kennett, J., 2000. Competitive and cooperative responses to climatic instability in coastal southern California. Am. Ant. 65, 379–395.
Kennett, D., Winterhalder, B., 2006. Behavioral Ecology and the Transition to Agriculture. University of California Press, Berkeley.
Kennett, D.J., Breitenbach, S.F.M., Aquino, V.V., Asmerom, Y., Awe, J., Baldini, J.U., Bartlein, P., Culleton, B.J., Ebert, C., Jazwa, C., Macri, M.J., Marwan, N., Polyak, V., Prufer, K.M., Ridley, H.E., Sodemann, H., Winterhalder, B., Haug, G.H., 2012. Development and disintegration of maya political systems in response to climate change. Science 338, 788–791.
Kennett, D.J., Prufer, K.M., Culleton, B.J., George, R.J., Robinson, M., Trask, W.R., Buckley, G.M., Moes, E., Kate, E.J., Harper, T.K., O'Donnell, L., Ray, E.E., Hill, E.C., Alsgaard, A., Merriman, C., Meredith, C., Edgar, H.J.H., Awe, J.J., Gutierrez, S.M., 2020. Early isotopic evidence for maize as a staple grain in the Americas. Sci. Adv. 6.
Kennett, D.J., Voorhies, B., 1996. Oxygen isotopic analysis of archaeological shells to detect seasonal use of wetlands on the Southern pacific coast of Mexico. J. Arch. Sci. 23, 689–704.
Kern, Z., Bocic, N., Sipos, G., 2018. Radiocarbon–dated vegetal remains from the cave ice deposits of velebit mountain, Croatia. Radiocarbon 60, 1391–1402.
Kern, Z., Széles, E., Horvatinčić, N., Fórizs, I., Bočić, N., Nagy, B., 2011. Glaciochemical investigations of the ice deposit of Vukušic ice cave, velebit mountain, Croatia. Cryosphere 5, 485–494.
Keylock, C.J., 2007. A wavelet-based method for surrogate data generation. Phys. D: Nonlinear Phenom. 225, 219–228.
Kiss, A., Wilson, R., Bariska, I., 2011. An experimental 392-year documentary-based multi-proxy (vine and grain) reconstruction of May–July temperatures for Kőszeg, West-Hungary. Int. J. Biometeorol. 55, 595–611.
Kistler, L., Maezumi, S.Y., Gregorio de Souza, J., Przelomska, N.A.S., Malaquias Costa, F., Smith, O., Loiselle, H., Ramos-Madrigal, J., Wales, N., Ribeiro, E.R., Morrison, R.R., Grimaldo, C., Prous, A.P., Arriaza, B., Gilbert, M.T.P., de Oliveira Freitas, F., Allaby, R.G., 2018. Multiproxy evidence highlights a complex evolutionary legacy of maize in South America. Science 362, 1309–1313.
Kistler, L., Thakar, H.B., VanDerwarker, A.M., Domic, A., Bergstr”om, A., George, R.J., Harper, T.K., Allaby, R.G., Hirth, K., Kennett, D.J., 2020. Archaeological central american maize genomes suggest ancient gene flow from South America. Proc. Nat. Acad. Sci. 117, 33124–33129.
Klein, R., Lohmann, K., Thayer, C., 1996. SrCa and $^{13}C^{12}C$ ratios in skeletal calcite of mytilus trossulus: covariation with metabolic rate, salinity, and carbon isotopic composition of seawater. Geochim. Cosmochim. Acta 60, 4207–4221.
Klein, R.G., Bird, D.W., 2016. Shellfishing and human evolution. J. Anthropol. Arch. 44, 198–205. Progress in Theoretically Driven Hunter-Gatherer Research.
Knudson, K., Aufderheide, A., Buikstra, J., 2007. Seasonality and paleodiet in the chiribaya polity of southern peru. J. Arch. Sci. 34, 451–462.
Koerner, R.M., 1997. Some comments on climatic reconstructions from ice cores drilled in areas of high melt. J. Glaciol. 43, 90–97.
Kondrashov, D., Ghil, M., 2006. Spatio-temporal filling of missing points in geophysical data sets. Nonlinear Proc. Geophys. 13, 151–159.
Konecky, B.L., Noone, D.C., Cobb, K.M., 2019. The influence of competing hydroclimate processes on stable isotope ratios in tropical rainfall. Geophys. Res. Lett. 46, 1622–1633.
Koppel, B., Szabó, K., Moore, M., Morwood, M., 2016. Untangling time-averaging in shell middens: defining temporal units using amino acid racemisation. J. Arch. Sci.: Rep 7, 741–750.
Köppen, W., 1936. Handbuch der Klimatologie. Gebrüder Borntraeger, Berlin.
Koslowski, G., Glaser, R., 1999. Variations in reconstructed ice winter severity in the Western Baltic from 1501 to 1995, and their implications for the North Atlantic oscillation. Climatic Change 41, 175–191.
Kostrova, S.S., Meyer, H., Fernandoy, F., Werner, M., Tarasov, P.E., 2020. Moisture origin and stable isotope characteristics of precipitation in southeast Siberia. Hydrol. Proc. 34, 51–67.
de Kraker, A.M., 2006. Historical climatology, 1950–2006. An overview of a developing science with a focus on the low countries. Belgeo. Revue belge de géographie 307–338.
Labotka, D., Grissino-Mayer, H., Mora, C., Johnson, E., 2016. Patterns of moisture source and climate variability in the southeastern United States: a four-century seasonally resolved tree-ring oxygen-isotope record. Climate Dyn. 46, 2145–2154.
Lachniet, M.S., 2009. Climatic and environmental controls on speleothem oxygen-isotope values. Quat. Sci. Rev. 28, 412–432.
Lachniet, M.S., Bernal, J.P., Asmerom, Y., Polyak, V., Piperno, D., 2012. A 2400 yr Mesoamerican rainfall reconstruction links climate and cultural change. Geology 40, 259–262.
Ladurie, E.L.R., Baulant, M., 1980. Grape harvests from the fifteenth through the nineteenth centuries. J. Int. Hist. 839–849.
lambert, M., Engroff, A., Dyer, M., Byer, B., 2021. Empirical mode decomposition.
Landon, D., 1988. The potential applications of tooth cement increment analysis in historical archaeology. Northeast Hist. Arch. 17, 5.
Landshuter, N., Molg, T., Griessinger, J., Brauning, A., Peters, T., 2020. 10-year characteristics of moisture source regions and their potential effect on seasonal isotopic signatures of delta o-18 in tropical trees of southern ecuador. Front. Earth Sci. 8.
Langway, C.C., Shoji, H., Mitani, A., Clausen, H.B., 1993. Transformation process observations of polar firn to ice. Annal. Glaciol. 18, 199–202.
Lansing, J.S., 1987. Balinese "Water Temples" and the management of irrigation. Am. Anthropol. 89, 326–341.
Lara, A., Villalba, R., Urrutia-Jalabert, R., Gonzalez-Reyes, A., Aravena, J.C., Luckman, B. H., Cuq, E., Rodriguez, C., Wolodarsky-Franke, A., 2020. A 5680-year tree-ring temperature record for southern South America. Quat. Sci. Rev. 228.
Lau, K.M., Weng, H., 1995. Climate signal detection using wavelet transform: how to make a time series sing. Bull. Am. Metrol. Soc. 76, 2391–2402.
Lauriol, B., Clark, J.C.M.E.I.D., 1991. Localisation, genèse et fonte de quelques naleds du nord du yukon (canada). Permafrost Periglacial Proc. 2, 225–236.
Lauscher, F., 1985. Beitr”age zur Wetterchronik seit dem Mittelalter. Springer.
LaVigne, M., Nurhati, I., Cobb, K., McGregor, H., Sinclair, D., Sherrell, R., 2013. Systematic ENSO-driven nutrient variability recorded by central equatorial pacific corals. Geophys. Res. Lett. 40, 3956–3961.
Lechleitner, F.A., Amirnezhad-Mozhdehi, S., Columbu, A., Comas-Bru, L., Labuhn, I., Pérez-Mejías, C., Rehfeld, K., 2018. The Potential of speleothems from western europe as recorders of regional climate: a critical assessment of the SISAL database. Quaternary 1, 1–31.
Lechleitner, F.A., Baldini, J.U., Breitenbach, S.F., Fohlmeister, J., McIntyre, C., Goswami, B., Jamieson, R.A., van der Voort, T.S., Prufer, K., Marwan, N., Culleton, B.J., Kennett, D.J., Asmerom, Y., Polyak, V., E.T., I., 2016. Hydrological and climatological controls on radiocarbon concentrations in a tropical stalagmite. Geochim. Cosmochim. Acta 194, 233–252.
Lechleitner, F.A., Breitenbach, S.F., Cheng, H., Plessen, B., Rehfeld, K., Goswami, B., Marwan, N., Eroglu, D., Adkins, J., Haug, G., et al., 2017. Climatic and in-cave influences on δ^{18}O and δ^{13}C in a stalagmite from northeastern India through the last deglaciation. Quart. Res. 88, 458–471.
Lee-Thorp, J., Sponheimer, M., 2015. Contribution of stable light isotopes to paleoenvironmental reconstruction. In: Henke, W., Tattersall, I. (Eds.), Handbook of Paleoanthropology. Springer, Berlin, Heidelberg, pp. 441–464.
Legrand, M., Mayewski, P., 1997. Glaciochemistry of polar ice cores: a review. Rev. Geophys. 35, 219–243.
Lekshmy, P., Midhun, M., Ramesh, R., 2018. Influence of stratiform clouds on δD and δ^{18}O of monsoon water vapour and rain at two tropical coastal stations. J. Hydrol. 563, 354–362.
Leng, M., Lewis, J., 2016. Oxygen isotopes in Molluscan shell: applications in environmental archaeology. Environ. Arch. 21, 295–306.
Leng, M.J., Wagner, B., Boehm, A., Panagiotopoulos, K., Vane, C.H., Snelling, A., Haidon, C., Woodley, E., Vogel, H., Zanchetta, G., Baneschi, I., 2013. Understanding past climatic and hydrological variability in the Mediterranean from lake prespa sediment isotope and geochemical record over the last glacial cycle. Quat. Sci. Rev. 66, 123–136.
Lenoir, G., Crucifix, M., 2018a. A general theory on frequency and time-frequency analysis of irregularly sampled time series based on projection methods – Part 2: Extension to Time–Frequency analysis. Nonlinear Proc. Geophys. 25, 175–200.
Lenoir, G., Crucifix, M., 2018b. A general theory on frequency and Time–Frequency analysis of irregularly sampled time series based on projection methods-Part 1: Frequency analysis. Nonlinear Proc. Geophys. 25, 145.
Leslie, P., Fry, P., 1989. Extreme seasonality of births among nomadic Turkana pastoralists. Am. J. Phys. Anthropol. 79, 103–115.
Leunda, M., González-Sampériz, P., Gil-Romera, G., Bartolomé, M., Belmonte-Ribas, Á., Gómez-García, D., Kaltenrieder, P., Rubiales, J.M., Schw”orer, C., Tinner, W., et al., 2019. Ice cave reveals environmental forcing of long-term pyrenean tree line dynamics. J. Ecol. 107, 814–828.
Li, B., Nychka, D.W., Ammann, C.M., 2010. The value of multiproxy reconstruction of past climate. J. Am. Stat. Assoc. 105, 883–895.
Li, Z.H., Labbé, N., Driese, S.G., Grissino-Mayer, H.D., 2011. Micro-scale analysis of tree-ring δ^{18}O and δ^{13}C on α-cellulose spline reveals high-resolution intra-annual climate variability and tropical cyclone activity. Chem. Geol. 284, 138–147.
Lieberman, D.E., Belfer-Cohen, A., Henry, D.O., Kaufman, D., Mackie, Q., Olszewski, D.I., Rocek, T.R., Sheppard, P.J., Trinkaus, E., Valla, F.R., 1993. The Rise and Fall of seasonal mobility among hunter-gatherers: the case of the southern levant [and Comments and Replies]. Curr. Anthropol. 34, 599–631.
Linderholm, H.W., Chen, D.L., 2005. Central scandinavian winter precipitation variability during the past five centuries reconstructed from pinus sylvestris tree rings. Boreas 34, 43–52.
Lionello, P., Gacic, M., Gomis, D., Garcia-Herrera, R., Giorgi, F., Planton, S., Trigo, R., Theocharis, A., Tsimplis, M.N., Ulbrich, U., Xoplaki, E., 2012. Program focuses on climate of the mediterranean region. Eos. Trans. Am. Geophys. Union 93, 105–106.
Liu, Y., Li, C.Y., Sun, C.F., Song, H.M., Li, Q., Cai, Q.F., Liu, R.S., 2020. Temperature variation at the low-latitude regions of east asia recorded by tree rings during the past six centuries. Int. J. Climatol. 40, 1561–1570.
Liu, Z., Zhu, J., Rosenthal, Y., Zhang, X., Otto-Bliesner, B.L., Timmermann, A., Smith, R. S., Lohmann, G., Zheng, W., Timm, O.E., 2014. The holocene temperature conundrum. Proc. Natl. Acad. Sci. U. S. A. 111, E3501–E3505.
Ljungqvist, F.C., Thejll, P., Bjorklund, J., Gunnarson, B.E., Piermattei, A., Rydval, M., Seftigen, K., Stove, B., Buntgen, U., 2020. Assessing non-linearity in european temperature-sensitive tree-ring data. Dendrochronologia 59.

Locosselli, G.M., Brienen, R.J.W., Martins, V.T.D., Gloor, E., Boom, A., de Camargo, E.P., Saldiva, P.H.N., Buckeridge, M.S., 2020. Intra-annual oxygen isotopes in the tree rings record precipitation extremes and water reservoir levels in the metropolitan area of sao paulo, brazil. Sci. Total Environ. 743.

Loftus, E., Lee-Thorp, J., Leng, M., Marean, C., Sealy, J., 2019. Seasonal scheduling of shellfish collection in the Middle and Later Stone Ages of southern Africa. J. Hum. Evol. 128, 1–6.

Ludlow, F., Stine, A.R., Leahy, P., Murphy, E., Mayewski, P.A., Taylor, D., Killen, J., Baillie, M.G.L., Hennessy, M., Kiely, G., 2013. Medieval irish chronicles reveal persistent volcanic forcing of severe winter cold events, 431–1649 CE. Environ. Res. Lett. 8, 024035.

Luterbacher, J., Dietrich, D., Xoplaki, E., Grosjean, M., Wanner, H., 2004. European seasonal and annual temperature variability, trends, and extremes since 1500. Science 303, 1499–1503.

Lutz, R., Rhoads, D., 1980. Growth patterns within the molluscan shell. In: Rhoads, D., Lutz, R. (Eds.), Skeletal Growth of Aquatic Organisms, Topics in Geobiology. Springer, Boston, MA, pp. 203–254.

Glasgow, Michael A., 1997. Middle Holocene cultural developments in the central Santa Barbara Channel Region. In: Erlandson, J., Glassow, M. (Eds.), The Archaeology of the California Coast During the Middle Holocene. Cotsen Institute of Archaeology, University of California, pp. 73–90.

Mahmud, K., Mariethoz, G., Baker, A., Treble, P.C., 2018. Hydrological characterization of cave drip waters in a porous limestone: Golgotha Cave, Western Australia. Hydrol. Earth Sys. Sci. 22, 977–988.

Malik, N., Bookhagen, B., Marwan, N., Kurths, J., 2012. Analysis of spatial and temporal extreme monsoonal rainfall over south asia using complex networks. Climate Dyn. 39, 971–987.

Mangili, C., Plessen, B., Wolff, C., Brauer, A., 2010. Climatic implications of annual to decadal resolution stable isotope data from calcite varves of the Piànico interglacial lake record. South. Alps. Global. Plant. Change 71, 168–174.

Mannino, M.A., Spiro, B.F., Thomas, K.D., 2003. Sampling shells for seasonality: oxygen isotope analysis on shell carbonates of the inter-tidal gastropod monodonta lineata (da costa) from populations across its modern range and from a mesolithic site in southern britain. J. Arch. Sci. 30, 667–679.

Mannshardt, E., Craigmile, P.F., Tingley, M.P., 2013. Statistical modeling of extreme value behavior in North American tree-ring density series. Climatic Change 117, 843–858.

Manzano, S., Carrión, J.S., López-Merino, L., Jiménez-Moreno, G., Toney, J.L., Amstrong, H., Anderson, R.S., García-Alix, A., Pérez, J.L.G., Sánchez-Mata, D., 2019. A palaeoecological approach to understanding the past and present of Sierra Nevada, a Southwestern European biodiversity hotspot. Global Plant. Change 175, 238–250.

Maraun, D., Kurths, J., Holschneider, M., 2007. Nonstationary gaussian processes in wavelet domain: synthesis, estimation, and significance testing. Phys. Rev. E 75, 016707.

Marcott, S.A., Shakun, J.D., Clark, P.U., Mix, A.C., 2013. A reconstruction of regional and global temperature for the past 11,300 years. Science 339, 1198–1201.

Marean, C.W., 2016. The transition to foraging for dense and predictable resources and its impact on the evolution of modern humans. Philos. Trans. Royal Soc. B: Biol. Sci. 371, 20150239.

Marozzi, M., 2013. Nonparametric simultaneous tests for location and scale testing: a comparison of several methods. Commun. Stat. Simul. Comput. 42, 1298–1317.

Martin, P.S., 1973. The discovery of america. Science 179, 969–974.

Martin-Chivelet, J., Belén Muñoz-García, M., Cruz, J.A., Ortega, A.I., Turrero, M.J., 2017. Speleothem Architectural Analysis: Integrated approach for stalagmite-based paleoclimate research. Sedim. Geol. 353, 28–45.

Martin-Puertas, C., Brauer, A., Dulski, P., Brademann, B., 2012. Testing climate-proxy stationarity throughout the Holocene: an example from the varved sediments of Lake Meerfelder Maar (Germany). Quat. Sci. Rev. 58, 56–65.

Marwan, N., Eroglu, D., Ozken, I., Stemler, T., Wyrwoll, K.H., Kurths, J., 2018. Regime change detection in irregularly sampled time series. Advances in Nonlinear Geosciences. Springer, pp. 357–368.

Marwan, N., Kurths, J., 2015. Complex network based techniques to identify extreme events and (sudden) transitions in spatio-temporal systems. Chaos 25, 097609.

Marwan, N., Romano, M.C., Thiel, M., Kurths, J., 2007. Recurrence plots for the analysis of complex systems. Phys. Rep. 438, 237–329.

Marwan, N., Thiel, M., Nowaczyk, N.R., 2002. Cross recurrence plot based synchronization of time series. Nonlinear Proc. Geophys. 9, 325–331.

Mattey, D., Lowry, D., Duffet, J., Fisher, R., Hodge, E., Frisia, S., 2008. A 53-year seasonally resolved oxygen and carbon isotope record from a modern Gibraltar speleothem: reconstructed drip water and relationship to local precipitation. Earth Planet. Sci. Lett. 269, 80–95.

Mattey, D.P., Fairchild, I.J., Atkinson, T.C., Latin, J.P., Ainsworth, M., Durell, R., 2010. Seasonal microclimate control of calcite fabrics, stable isotopes and trace elements in modern speleothem from St Michaels Cave, Gibraltar. Gegeol. Soc. London Spec. Publ. 336, 323–344.

McCarroll, D., Loader, N.J., 2004. Stable isotopes in tree rings. Quat. Sci. Rev. 23, 771–801.

McCormack, J., Kwiecien, O., 2021. Coeval primary and diagenetic carbonates in lacustrine sediments challenge palaeoclimate interpretations. Sci. Rep. 11, 7935.

McCormack, J., Nehrke, G., Jöns, N., Immenhauser, A., Kwiecien, O., 2019. Refining the interpretation of lacustrine carbonate isotope records: Implications of a mineralogy-specific Lake Van case study. Chem. Geol. 513, 167–183.

McCullough, M., Sakellariou, K., Stemler, T., Small, M., 2016. Counting forbidden patterns in irregularly sampled time series. i. the effects of under-sampling, random depletion, and timing jitter. Chaos: Interdisc. J. Nonlinear Sci. 26, 123103.

McDermott, F., 2004. Palaeo-climate reconstruction from stable isotope variations in speleothems: a review. Quat. Sci. Rev. 23, 901–918.

McKay, N.P., Kaufman, D.S., 2014. An extended Arctic proxy temperature database for the past 2,000 years. Sci. Data 1, 140026.

McRobie, F.H., Stemler, T., Wyrwoll, K.H., 2015. Transient coupling relationships of the holocene australian monsoon. Quat. Sci. Rev. 121, 120–131.

Medill, S., Derocher, A.E., Stirling, I., Lunn, N., 2010. Reconstructing the reproductive history of female polar bears using cementum patterns of premolar teeth. Polar Biol. 33, 115–124.

Medina-Elizalde, M., Burns, S.J., Lea, D.W., Asmerom, Y., von Gunten, L., Polyak, V., Vuille, M., Karmalkar, A., 2010. High resolution stalagmite climate record from the Yucatán Peninsula spanning the Maya terminal classic period. Earth Planet. Sci. Lett. 298, 255–262.

Meeker, L.D., Mayewski, P.A., 2002. A 1400-year high-resolution record of atmospheric circulation over the north atlantic and asia. Holocene 12, 257–266.

Melin, A.D., Young, H.C., Mosdossy, K.N., Fedigan, L.M., 2014. Seasonality, extractive foraging and the evolution of primate sensorimotor intelligence. J. Hum. Evol. 71, 77–86.

Merlivat, L., Jouzel, J., 1979. Global climatic interpretation of the deuterium-oxygen 18 relationship for precipitation. J. Geophys. Res. Oceans Atmos. 84, 5029–5033.

Meyer, H., Opel, T., Laepple, T., Dereviagin, A.Y., Hoffmann, K., Werner, M., 2015. Long-term winter warming trend in the siberian arctic during the mid-to late holocene. Nat. Geosci. 8, 122–125.

Meyer, H., Schirrmeister, L., Yoshikawa, K., Opel, T., Wetterich, S., Hubberten, H.W., Brown, J., 2010. Permafrost evidence for severe winter cooling during the younger dryas in northern alaska. Geophys. Res. Lett. 37, L03501.

Meyer, M.C., Faber, R., Spötl, C., 2006. The WinGeol Lamination Tool: new software for rapid, semi-automated analysis of laminated climate archives. Holocene 16, 753–761.

Milano, S., Prendergast, A., Schöne, B., 2016. Effects of cooking on mollusc shell structure and chemistry: implications for archeology and paleoenvironmental reconstruction. J. Arch. Sci.: Rep 7, 14–26.

Milano, S., Schöne, B.R., Witbaard, R., 2017. Changes of shell microstructural characteristics of Cerastoderma edule (Bivalvia) – a novel proxy for water temperature. Palaegeol. Palaeoclimatol. Palaeocol. 465, 395–406.

Milankovitch, M., 1930. Mathematische Klimalehre und astronomische Theorie der Klimaschwankungen. In: Köppen, W., Geiger, R. (Eds.), Handbuch der Klimatologie. Gebrüder Borntraeger, Berlin.

Milner, N., 2005. Can seasonality studies be used to identify sedentism in the past? In: Bailey, D., Cummings, V., Whittle, A. (Eds.), (Un)settling the Neolithic. Oxbow Books, pp. 32–37.

Monks, G., 1977. An examination of relationships between artifact classes and food resource remains at Deep Bay, DiSe7. Ph.D. thesis. Department of Anthropology, Santa Barbara, CA.

Monks, G., 1981. Seasonality Studies. Adv. Arch. Method Theor. 4, 177–240.

Morgan, C., 2009. Climate change, uncertainty and prehistoric hunter-gatherer mobility. J. Anthropol. Arch. 28, 382–396.

Mortimer, R., 1981. William Merle's weather diary and the reliability of historical evidence for medieval climate. Climate Mon. 10, 42–45.

Moss, P., Ulm, S., Mackenzie, L., Wallis, L., Rosendahl, D., Steinberger, L., 2019. Robust local vegetation records from dense archaeological shell matrixes: a palynological analysis of the Thundiy shell deposit, Bentinck Island, Gulf of Carpentaria, Australia. Arch. Anthropol. Sci. 11, 511–520.

Mudelsee, M., 2013. Climate Time Series Analysis. Springer.

Mudelsee, M., Fohlmeister, J., Scholz, D., 2012. Effects of dating errors on nonparametric trend analyses of speleothem time series. Climate Past 8, 1637–1648.

Mudelsee, M., Scholz, D., Röthlisberger, R., Fleitmann, D., Mangini, A., Wolff, E.W., 2009. Climate spectrum estimation in the presence of timescale errors. Nonlinear Process. Geophys. 16, 43–56.

Murton, J.B., 2013. Ground ice and cryostratigraphy. In: Shroder, J., Giardino, R., Harbor, J. (Eds.), Treatise on Geomorphology. Academic Press, San Diego, pp. 173–201 volume 8 Glacial and Periglacial Geomorphology.

Musial, J.P., Verstraete, M.M., Gobron, N., 2011. Comparing the effectiveness of recent algorithms to fill and smooth incomplete and noisy time series. Atmos. Chem. Phys. 11, 7905–7923.

Myers, C.G., Oster, J.L., Sharp, W.D., Bennartz, R., Kelley, N.P., Covey, A.K., Breitenbach, S.F., 2015. Northeast Indian stalagmite records Pacific decadal climate change: Implications for moisture transport and drought in India. Geophys. Res. Lett. 42, 4124–4132.

Nagavciuc, V., Ionita, M., Per?oiu, A., Popa, I., Loader, N.J., McCarroll, D., 2019. Stable oxygen isotopes in Romanian oak tree rings record summer droughts and associated large-scale circulation patterns over Europe. Climate Dyn. 52, 6557–6568.

Nagavciuc, V., Kern, Z., Ionita, M., Hartl, C., Konter, O., Esper, J., Popa, I., 2020. Climate signals in carbon and oxygen isotope ratios of pinus cembra tree-ring cellulose from the calimani mountains, romania. Int. J. Climatol. 40, 2539–2556.

Naji, S., Colard, T., Blondiaux, J., Bertrand, B., d'Incau, E., Bocquet-Appel, J.P., 2016. Cementochronology, to cut or not to cut? Int. J. Paleopathol. 15, 113–119.

Nash, D.J., Adamson, G.C., 2014. Recent advances in the historical climatology of the tropics and subtropics. Bull. Am. Meterol. Soc. 95, 131–146.

Nava-Fernandez, C., Hartland, A., Gázquez, F., Kwiecien, O., Marwan, N., Fox, B., Hellstrom, J., Pearson, A., Ward, B., French, A., Hodell, D.A., Immenhauser, A., Breitenbach, S.F.M., 2020. Pacific climate reflected in Waipuna Cave drip water hydrochemistry. Hydrol. Earth Sys. Sci. 24, 3361–3380.

Naveau, P., Ammann, C., 2005. Statistical distributions of ice core sulfate from climatically relevant volcanic eruptions. Geophys. Res. Lett. 32.

Nehme, C., Verheyden, S., Nader, F.H., Adjizian-Gerard, J., Genty, D., De Bondt, K., Minster, B., Salem, G., Verstaeten, D., Claeys, P., 2019. Cave dripwater isotopic signals related to the altitudinal gradient of Mount-Lebanon: implication for speleothem studies. Int. J. Speleol. 48, 63–74.
Neukom, R., Luterbacher, J., Villalba, R., K”uttel, M., Frank, D., Jones, P.D., Grosjean, M., Wanner, H., Aravena, J.C., Black, D.E., et al., 2011. Multiproxy summer and winter surface air temperature field reconstructions for southern South America covering the past centuries. Climate Dyn. 37, 35–51.
Neukom, R., Nash, D.J., Endfield, G.H., Grab, S.W., Grove, C.A., Kelso, C., Vogel, C.H., Zinke, J., 2014. Multi-proxy summer and winter precipitation reconstruction for southern Africa over the last 200 years. Climate Dyn. 42, 2713–2726.
Nicault, A., Alleaume, S., Brewer, S., Carrer, M., Nola, P., Guiot, J., 2008. Mediterranean drought fluctuation during the last 500 years based on tree-ring data. Climate Dyn. 31, 227–245.
Nitze, I., Grosse, G., Jones, B.M., Romanovsky, V.E., Boike, J., 2018. Remote sensing quantifies widespread abundance of permafrost region disturbances across the arctic and subarctic. Nat. Commun. 9, 5423.
Noone, S., Broderick, C., Duffy, C., Matthews, T., Wilby, R.L., Murphy, C., 2017. A 250-year drought catalogue for the island of Ireland (1765–2015). Int. J. Climatol. 37, 239–254.
Noronha, A.L., Hardt, B.F., Banner, J.L., Jenson, J.W., Partin, J.W., James, E.W., Lander, M.A., Bautista, K.K., 2017. Trade winds drive pronounced seasonality in carbonate chemistry in a tropical Western Pacific island cave-Implications for speleothem paleoclimatology. Geochem. Geophys. Geosyst. 18, 384–399.
Nwogu, E.C., Iwueze, I.S., Nlebedim, V.U., 2016. Some tests for seasonality in time series data. J. Mod. Appl. Stat. Methods 15, 24.
Ogilvie, A., Farmer, G., 1997. Documenting the medieval climate. In: Climates British Isles: Present Past Future, pp. 112–133.
Ojala, A.E., Kosonen, E., Weckström, J., Korkonen, S., Korhola, A., 2013. Seasonal formation of clastic-biogenic varves: the potential for palaeoenvironmental interpretations. GFF 135, 237–247.
Olafsdottir, K.B., Geirsdottir, A., Miller, G.H., Larsen, D.J., 2013. Evolution of nao and amo strength and cyclicity derived from a 3-ka varve-thickness record from iceland. Quat. Sci. Rev. 69, 142–154.
Ólafsdóttir, K.B., Schulz, M., Mudelsee, M., 2016. REDFIT-X: cross-spectral analysis of unevenly spaced paleoclimate time series. Comput. Geosci. 91, 11–18.
Oliveira, D., Goñi, M.F.S., Naughton, F., Polanco-Martínez, J., Jimenez-Espejo, F.J., Grimalt, J.O., Martrat, B., Voelker, A.H., Trigo, R., Hodell, D., et al., 2017. Unexpected weak seasonal climate in the western Mediterranean region during MIS 31, a high-insolation forced interglacial. Quat. Sci. Rev. 161, 1–17.
O'Neil, J.R., Clayton, R.N., Mayeda, T.K., 1969. Oxygen isotope fractionation in divalent metal carbonates. J. Chem. Phys. 51, 5547–5558.
Opel, T., Laepple, T., Meyer, H., Dereviagin, A., Wetterich, S., 2017. Northeast siberian ice wedges confirm arctic winter warming over the past two millennia. Holocene 27, 1789–1796.
Opel, T., Meyer, H., Wetterich, S., Laepple, T., Dereviagin, A., Murton, J., 2018. Ice wedges as archives of winter paleoclimate: a review. Permafrost Periglacial Proc. 29, 199–209.
Opel, T., Murton, J.B., Wetterich, S., Meyer, H., Ashastina, K., Gunther, F., Grotheer, H., Mollenhauer, G., Danilov, P.P., Boeskorov, V., Savvinov, G.N., Schirrmeister, L., 2019. Past climate and continentality inferred from ice wedges at batagay megaslump in the northern hemisphere's most continental region, yana highlands, interior yakutia. Climate Past 15, 1443–1461.
Orland, I.J., Bar-Matthews, M., Ayalon, A., Matthews, A., Kozdon, R., Ushikubo, T., Valley, J.W., 2012. Seasonal resolution of Eastern Mediterranean climate change since 34ka from a Soreq Cave speleothem. Geochim. Cosmochim. Acta 89, 240–255.
Orland, I.J., Bar-Matthews, M., Kita, N.T., Ayalon, A., Matthews, A., Valley, J.W., 2009. Climate deterioration in the Eastern Mediterranean as revealed by ion microprobe analysis of a speleothem that grew from 2.2 to 0.9 ka in Soreq Cave, Israel. Quart. Res. 71, 27–35.
Orland, I.J., Burstyn, Y., Bar-Matthews, M., Kozdon, R., Ayalon, A., Matthews, A., Valley, J.W., 2014. Seasonal climate signals (1990-2008) in a modern Soreq Cave stalagmite as revealed by high-resolution geochemical analysis. Chem. Geol. 363, 322–333.
Orland, I.J., He, F., Bar-Matthews, M., Chen, G., Ayalon, A., Kutzbach, J.E., 2019. Resolving seasonal rainfall changes in the Middle East during the last interglacial period. Proc. Nat. Acad. Sci. 116, 24985–24990.
Oster, J.L., Kelley, N.P., 2016. Tracking regional and global teleconnections recorded by western North American speleothem records. Quat. Sci. Rev. 149, 18–33.
Oster, J.L., Montañez, I.P., Santare, L.R., Sharp, W.D., Wong, C., Cooper, K.M., 2015. Stalagmite records of hydroclimate in central California during termination 1. Quat. Sci. Rev. 127, 199–214.
Oster, J.L., Sharp, W.D., Covey, A.K., Gibson, J., Rogers, B., Mix, H., 2017. Climate response to the 8.2 ka event in coastal California. Sci. Rep. 7, 3886.
Oster, J.L., Warken, S.F., Sekhon, N., Arienzo, M.M., Lachniet, M., 2019. Speleothem Paleoclimatology for the Caribbean, Central America, and North America. Quaternary 2.
Overland, J.E., Wood, K., 2003. Accounts from 19th-century Canadian Arctic explorers' logs reflect present climate conditions. Eos. Trans. Am. Geophys. Union 84, 410–412.
Overton, N.J., Taylor, B., 2018. Humans in the environment: plants, animals and landscapes in mesolithic britain and ireland. J. World Prehist. 31, 385–402.
Owen, R., Day, C.C., Henderson, G.M., 2018. Cavecalc: a new model for speleothem chemistry & isotopes. Comput. Geosci. 119, 115–122.
Ozken, I., Eroglu, D., Breitenbach, S.F., Marwan, N., Tan, L., Tirnakli, U., Kurths, J., 2018. Recurrence plot analysis of irregularly sampled data. Phys. Rev. E 98, 052215.
Paluš, M., 2007. From nonlinearity to causality: statistical testing and inference of physical mechanisms underlying complex dynamics. Contemp. Phys. 48, 307–348.
Pannella, G., 1971. Fish otoliths: daily growth layers and periodical patterns. Science 173, 1124–1127.
Parker, W., Yanes, Y., Surge, D., Mesa-Hernández, E., 2017. Calibration of the oxygen isotope ratios of the gastropods *Patella candei* crenata and *Phorcus atratus* as high-resolution paleothermometers from the subtropical eastern Atlantic Ocean. Palaeogeo. Palaeoclimatol. Palaeoecol. 487, 251–259.
Parnell, A.C., Buck, C.E., Doan, T.K., 2011. A review of statistical chronology models for high-resolution, proxy-based holocene palaeoenvironmental reconstruction. Quat. Sci. Rev. 30, 2948–2960.
Partin, J.W., Cobb, K.M., Adkins, J.F., Clark, B., Fernandez, D.P., 2007. Millennial-scale trends in west Pacific warm pool hydrology since the Last Glacial Maximum. Nature 449, 452–455.
Partin, J.W., Jenson, J.W., Banner, J.L., Quinn, T.M., Taylor, F.W., Sinclair, D., Hardt, B., Lander, M.A., Bell, T., Miklavic, B., Jocson, J.M.U., Taboroši, D., 2012. Relationship between modern rainfall variability, cave dripwater, and stalagmite geochemistry in Guam, USA. Geochem. Geophys. Geosyst. 13.
Pascale, S., Lucarini, V., Feng, X., Porporato, A., et al., 2014. Projected changes of rainfall seasonality and dry spells in a high concentration pathway 21st century scenario. arXiv:1410.3116.
Patterson, W.P., Dietrich, K.A., Holmden, C., Andrews, J.T., 2010. Two millennia of North Atlantic seasonality and implications for Norse colonies. Proc. Nat. Acad. Sci. 107, 5306–5310.
Paun, V.I., Icaza, G., Lavin, P., Marin, C., Tudorache, A., Persoiu, A., Dorador, C., Purcarea, C., 2019. Total and potentially active bacterial communities entrapped in a late glacial through holocene ice core from Scarisoara Ice Cave, Romania. Front. Microb. 10, 1193.
Peavoy, D., Franzke, C., 2010. Bayesian analysis of rapid climate change during the last glacial using Greenland δ^{18}O data. Climate Past 6, 787.
Percival, D.B., Walden, A.T., et al., 1993. Spectral Analysis for Physical Applications. Cambridge University Press.
Perşoiu, A., Ionita, M., Weiss, H., 2019. Atmospheric blocking induced by the strengthened siberian high led to drying in west asia during the 4.2 ka bp event – a hypothesis. Climate Past 15, 781–793.
Perşoiu, A., Onac, B.P., Wynn, J.G., Blaauw, M., Ionita, M., Hansson, M., 2017. Holocene winter climate variability in Central and Eastern Europe. Sci. Rep. 7, 1196.
Persoiu, A., Onac, B.P., Wynn, J.G., Bojar, A.V., Holmgren, K., 2011. Stable isotope behavior during cave ice formation by water freezing in Scarisoara Ice Cave, Romania. J. Geophys. Res.: Atmos. 116.
Petrie, C.A., Bates, J., 2017. 'Multi-cropping', intercropping and adaptation to variable environments in Indus South Asia. J. World Prehist. 30, 81–130.
Petterson, G., Odgaard, B.V., Renberg, I., 1999. Image analysis as a method to quantify sediment components. J. Paleolimnol. 22, 443–455.
Peyron, O., Goring, S., Dormoy, I., Kotthoff, U., Pross, J., De Beaulieu, J.L., Drescher-Schneider, R., Vannière, B., Magny, M., 2011. Holocene seasonality changes in the central Mediterranean region reconstructed from the pollen sequences of Lake Accesa (Italy) and Tenaghi Philippon (Greece). Holocene 21, 131–146.
Pezzulli, S., Stephenson, D.B., Hannachi, A., 2005. The variability of seasonality. Journal of Climate 18, 71–88.
Pfister, C., 1992. Monthly temperature and precipitation in central Europe 1525–1979: quantifying documentary evidence on weather and its effects. Climate Since AD 1500, 118–142.
Pfister, C., 2010. The vulnerability of past societies to climatic variation: a new focus for historical climatology in the twenty-first century. Climate Change 100, 25–31.
Pfister, C., Brázdil, R., 1999. Climatic variability in sixteenth-century Europe and its social dimension: a synthesis. Climatic Change 43, 5–53.
Piperno, D.R., 2001. On maize and the sunflower. Science 292, 2260–2261.
Piperno, D.R., 2011. The origins of plant cultivation and domestication in the new world tropics: patterns, process, and new developments. Curr. Anthropol. 52, S453–S470.
Porter, T.J., Opel, T., 2020. Recent advances in paleoclimatological studies of arctic wedge- and pore-ice stable-water isotope records. Permafr. Periglac. Process. 31, 429–441.
Porter, T.J., Schoenemann, S.W., Davies, L.J., Steig, E.J., Bandara, S., Froese, D.G., 2019. Recent summer warming in northwestern Canada exceeds the holocene thermal maximum. Nat. Commun. 10, 1631.
Potts, R., 1998. Environmental hypotheses of hominin evolution. Am. J. Phys. Anthropol. Suppl 27, 93–136.
Poulain, C., Gillikin, D., Thébault, J., Munaron, J.M., Bohn, M., Robert, R., Paulet, Y.M., Lorrain, A., 2015. An evaluation of Mg/Ca, Sr/Ca, and Ba/Ca ratios as environmental proxies in aragonite bivalve shell. Chem. Geol. 396, 42–50.
Prasad, S., Witt, A., Kienel, U., Dulski, P., Bauer, E., Yancheva, G., 2009. The 8.2 ka event: evidence for seasonal differences and the rate of climate change in western Europe. Global Planet. Change 67, 218–226.
Prendergast, A., Stevens, R., O'connell, T., Fadlalak, A., Touati, M., Al-Mzeine, A., Sch“one, B., Hunt, C., Barker, G., 2016. Changing patterns of eastern Mediterranean shellfish exploitation in the late glacial and early holocene: oxygen isotope evidence from gastropod in Epipaleolithic to Neolithic human occupation layers at the Haua Fteah cave, Libya. Quat. Int. 407, 80–93.
Prendergast, A.L., Pryor, A.J., Reade, H., Stevens, R.E., 2018. Seasonal records of palaeoenvironmental change and resource use from archaeological assemblages. J. Archeol. Sci.: Rep. 21, 1191–1197.
Prendergast, A.L., Schöne, B.R., 2017. Oxygen isotopes from limpet shells: Implications for palaeothermometry and seasonal shellfish foraging studies in the Mediterranean. Palaeogeography, Palaeoclimatology. Paleoecology 484, 33–47.

Prentice, I.C., Guiot, J., Harrison, S.P., 1992. Mediterranean vegetation, lake levels and palaeoclimate at the last glacial maximum. Nature 360, 658–660.
Pritzkow, C., Heinrich, I., Grudd, H., Helle, G., 2014. Relationship between wood anatomy, tree-ring widths and wood density of *Pinus sylvestris* L. and climate at high latitudes in northern Sweden. Dendrochronologia 32, 295–302.
Proctor, C., Baker, A., Barnes, W., 2002. A three thousand year record of North Atlantic climate. Climate Dyn. 19, 449–454.
Pu, T., Kong, Y., Wang, S., Shi, X., Wang, K., Niu, H., Chen, P., 2020. Modification of stable isotopes in snow and related post-depositional processes on a temperate glacier of Mt. Yulong, southeast Tibetan Plateau. J. Hydrol. 584, 124675.
Pumijumnong, N., Brauning, A., Sano, M., Nakatsuka, T., Muangsong, C., Buajan, S., 2020. A 338-year tree-ring oxygen isotope record from thai teak captures the variations in the asian summer monsoon system. Sci. Rep. 10.
Quiers, M., Perrette, Y., Chalmin, E., Fanget, B., Poulenard, J., 2015. Geochemical mapping of organic carbon in stalagmites using liquid-phase and solid-phase fluorescence. Chem. Geol. 411, 240–247.
Railsback, L.B., Brook, G.A., Chen, J., Kalin, R., Fleisher, C.J., 1994. Environmental controls on the petrology of a late holocene speleothem from Botswana with annual layers of aragonite and calcite. J. Sediment. Res. 64, 147–155.
Ramos, A.M., Builes-Jaramillo, A., Poveda, G., Goswami, B., Macau, E.E., Kurths, J., Marwan, N., 2017. Recurrence measure of conditional dependence and applications. Phys. Rev. E 95, 052206.
Rasband, W.S., 1997-2018. ImageJ. U. S. National Institutes of Health, Bethesda, Maryland, USA. https://imagej.nih.gov/ij/.
Reaux, D.J., Smith, G.M., Adams, K.D., Jamaldin, S., George, N.D., Mohr, K., Rosencrance, R.L., 2018. A first look at the terminal pleistocene/early holocene record of guano valley, oregon, usa. PaleoAmerica 4, 162–176.
Rehfeld, K., Marwan, N., Heitzig, J., Kurths, J., 2011. Comparison of correlation analysis techniques for irregularly sampled time series. Nonlin. Process. Geophys. 18, 389–404.
Reitz, E., Saul, B.M., Moak, J.W., Carroll, G.D., Lambert, C.W., 2012. Interpreting seasonality from modern and archaeological fishes on the Georgia coast. In: Reitz, E., Quitmyer, I., Thomas, D. (Eds.), Seasonality and Human Mobility along the Georgia Bight, vol. 97, pp. 51–81.
Rendu, W., 2010. Hunting behavior and Neanderthal adaptability in the Late Pleistocene site of Pech-de-l'Azé I. J. Archeol. Sci. 37, 1798–1810.
Retsö, D., 2002. A contribution to the history of European winters: some climatological proxy data from early-sixteenth century Swedish documentary sources. Clim. Change 52, 137–173.
Ridley, H.E., Asmerom, Y., Baldini, J.U.L., Breitenbach, S.F.M., Aquino, V.V., Prufer, K. M., Culleton, B.J., Polyak, V., Lechleitner, F.A., Kennett, D.J., Zhang, M., Marwan, N., Macpherson, C.G., Baldini, L.M., Xiao, T., Peterkin, J.L., Awe, J., Haug, G.H., 2015. Aerosol forcing of the position of the intertropical convergence zone since AD 1550. Nat. Geosci. 8, 195–200.
Riedwyl, N., Küttel, M., Luterbacher, J., Wanner, H., 2009. Comparison of climate field reconstruction techniques: application to Europe. Climate Dyn. 32, 381–395.
Rivals, F., Uno, K.T., Bibi, F., Pante, M.C., Njau, J., de la Torre, I., 2018. Dietary traits of the ungulates from the HWK EE site at Olduvai Gorge (Tanzania): diachronic changes and seasonality. J. Hum. Evol. 120, 203–214.
Roberts, J., Curran, M., Poynter, S., Moy, A., van Ommen, T., Vance, T., Tozer, C., Graham, F.S., Young, D.A., Plummer, C., et al., 2017. Correlation confidence limits for unevenly sampled data. Comput. Geosci. 104, 120–124.
Rodrigo, F.S., Barriendos, M., 2008. Reconstruction of seasonal and annual rainfall variability in the iberian Peninsula (16th-20th centuries) from documentary data. Global Planet. Change 63, 243–257.
Rodrigo, F.S., Esteban-Parra, M., Pozo-Vázquez, D., Castro-Díez, Y., 1999. A 500-year precipitation record in Southern Spain. Int. J. Climatol.: J. Royal Meteorol. Soc. 19, 1233–1253.
Rodrigo, F.S., Pozo-Vázquez, D., Esteban-Parra, M.J., Castro-Díez, Y., 2001. A reconstruction of the winter North Atlantic Oscillation index back to AD 1501 using documentary data in southern Spain. J. Geophys. Res.: Atmos. 106, 14805–14818.
Roeser, P., Draeger, N., Brykala, D., Ott, F., Pinkerneil, S., Gierszewski, P., Lindemann, C., Plessen, B., Brademann, B., Kaszubski, M., Fojutowski, M., Schwab, M.J., Slowinski, M., Blaszkiewicz, M., Brauer, A., 2021. Advances in understanding calcite varve formation: new insights from a dual lake monitoring approach in the southern Baltic lowlands. Boreas 50, 419–440.
Romero-Viana, L., Julià, R., Camacho, A., Vicente, E., Miracle, M.R., 2008. Climate signal in varve thickness: lake la cruz (Spain), a case study. J. Paleolimnol. 40, 703–714.
Román-González, A., Scourse, J., Butler, P., Reynolds, D., Richardson, C., Peck, L., Brey, T., Hall, I., 2017. Analysis of ontogenetic growth trends in two marine Antarctic bivalves yoldia eightsi and laternula elliptica: implications for sclerochronology. Paleogeogr. Paleoclimatol. Paleoecol. 465, 300–306.
Ronay, E.R., Breitenbach, S.F.M., Oster, J.L., 2019. Sensitivity of speleothem records in the Indian summer monsoon region to dry season infiltration. Scinti. Rep. 9, 5091.
del Rosario Prieto, M., Herrera, R.G., 2009. Documentary sources from South America: potential for climate reconstruction. Paleogeogr. Paleoclimatol. Paleoecol. 281, 196–209.
Rossi, A., Massei, N., Laignel, B., 2011. A synthesis of the time-scale variability of commonly used climate indices using continuous wavelet transform. Global Planet. Change 78, 1–13.
Rother, M.T., Huffman, J.M., Harley, G.L., Platt, W.J., Jones, N., Robertson, K.M., Orzell, S.L., 2018. Cambial phenology informs tree-ring analysis of fire seasonality in coastal plain pine savannas. Fire Ecol. 14, 164–185.
Royer, D., Berner, R., Montanez, I., Tabor, N., Beerling, D., 2004. CO_2 as a primary driver of phanerozoic climate. GSA Today 14, 4–10.
Roys, R.L., 1967. The Book of Chilam Balam of Chumayel. Technical Report. Carnegie Institution.
Rudzka, D., McDermott, F., Baldini, L., Fleitmann, D., Moreno, A., Stoll, H., 2011. The coupled δ^{13}C-radiocarbon systematics of three late glacial/early holocene speleothems; insights into soil and cave processes at climatic transitions. Geochim. Cosmochim. Acta 75, 4321–4339.
Rutherford, S., Mann, M.E., Osborn, T.J., Briffa, K.R., Jones, P.D., Bradley, R.S., Hughes, M.K., 2005. Proxy-based northern hemisphere surface temperature reconstructions: sensitivity to method, predictor network, target season, and target domain. J. Climate 18, 2308–2329.
Rutlidge, H., Baker, A., Marjo, C.E., Andersen, M.S., Graham, P.W., Cuthbert, M.O., Rau, G.C., Roshan, H., Markowska, M., Mariethoz, G., Jex, C.N., 2014. Dripwater organic matter and trace element geochemistry in a semi-arid karst environment: implications for speleothem paleoclimatology. Geochim. Cosmochim. Acta 135, 217–230.
Saarni, S., Muschitiello, F., Weege, S., Brauer, A., Saarinen, T., 2016. A late Holocene record of solar-forced atmospheric blocking variability over Northern Europe inferred from varved lake sediments of lake Kuninkaisenlampi. Quat. Sci. Rev. 154, 100–110.
Saarni, S., Saarinen, T., Lensu, A., 2015. Organic lacustrine sediment varves as indicators of past precipitation changes: a 3,000-year climate record from Central Finland. J. Paleolimnol. 53, 401–413.
Sadler, J., Carré, M., Azzoug, M., 2012. Reconstructing past upwelling intensity and the seasonal dynamics of primary productivity along the Peruvian coastline from mollusk shell stable isotopes. Geochem. Explor. Environ. Anal. 13, 1–17.
Sakellariou, K., McCullough, M., Stemler, T., Small, M., 2016. Counting forbidden patterns in irregularly sampled time series. II. reliability in the presence of highly irregular sampling. Chaos: Interdis. J. Nonlinear Sci. 26, 123104.
Sancho, C., Ánchel Belmonte, Bartolomé, M., Moreno, A., Leunda, M., López-Martínez, J., 2018. Middle-to-late holocene palaeoenvironmental reconstruction from the A294 ice-cave record (Central Pyrenees, northern Spain). Earth Planet. Sci. Lett. 484, 135–144.
Sandweiss, D., 2012. Terminal Pleistocene through mid-holocene archaeological sites as paleoclimatic archives for the Peruvian coast. Paleogeogr. Paleoclimatol. Paleoecol. 194, 23–40.
Sanger, M.C., Quitmyer, I.R., Colaninno, C.E., Cannarozzi, N., Ruhl, D.L., 2020. Multiple-proxy seasonality indicators: an integrative approach to assess shell midden formations from late archaic shell rings in the coastal Southeast North America. J. Island Coast. Archaeol. 15, 333–363.
Santer, B.D., Po-Chedley, S., Zelinka, M.D., Cvijanovic, I., Bonfils, C., Durack, P.J., Fu, Q., Kiehl, J., Mears, C., Painter, J., Pallotta, G., Solomon, S., Wentz, F.J., Zou, C.Z., 2018. Human influence on the seasonal cycle of tropospheric temperature. Science 361.
Saranya, P., Krishan, G., Rao, M., Kumar, S., Kumar, B., 2018. Controls on water vapor isotopes over Roorkee, India: impact of convective activities and depression systems. J. Hydro. 557, 679–687.
Sayani, H., Cobb, K., DeLong, K., Hitt, N., Druffle, E., 2019. Intercolony δ^{18}O and Sr/Ca variability among porites spp. corals at palmyra atoll: toward more robust coral-based estimates of climate. Geochem. Geophys. Geosyst. 20, 5270–5284.
Scargle, J.D., 1982. Studies in astronomical time series analysis. II-Statistical aspects of spectral analysis of unevenly spaced data. Astrophys. J. 263, 835–853.
Scargle, J.D., 1989. Studies in astronomical time series analysis. III-Fourier transforms, autocorrelation functions, and cross-correlation functions of unevenly spaced data. Astrophys. J. 343, 874–887.
van Schaik, C., Brockman, D., 2005. Seasonality in Primates: Studies of Living and Extinct Human and Non-Human Primates. Cambridge Studies in Biological and Evolutionary Anthropology. Cambridge University Press.
Scheidegger, Y., Baur, H., Brennwald, M.S., Fleitmann, D., Wieler, R., Kipfer, R., 2010. Accurate analysis of noble gas concentrations in small water samples and its application to fluid inclusions in stalagmites. Chem. Geol. 272, 31–39.
Schimmelmann, A., Lange, C.B., Schieber, J., Francus, P., Ojala, A.E., Zolitschka, B., 2016. Varves in marine sediments: a review. Earth-Sci. Rev. 159, 215–246.
Schöne, B., 2008. The curse of physiology-challenges and opportunities in the interpretation of geochemical data from mollusk shells. Geo-Mar. Lett. 28, 269–285.
Schöne, B., Radermacher, P., Zhang, Z., Jacob, D., 2013. Crystal fabrics and element impurities (Sr/Ca,Mg/Ca, and Ba/Ca) in shells of Arctica Islandica-implications for paleoclimate reconstructions. Palaeogeogr. Palaeoclimatol. Palaeoecol. 373, 50–59.
Schneider, B., Leduc, G., Park, W., 2010. Disentangling seasonal signals in holocene climate trends by satellite-model-proxy integration. Paleoceanography 25.
Schneider, T., Bischoff, T., Haug, G.H., 2014. Migrations and dynamics of the intertropical convergence zone. Nature 513, 45–53.
Schneuwly, D.M., Stoffel, M., 2008. Tree-ring based reconstruction of the seasonal timing, major events and origin of rockfall on a case-study slope in the Swiss Alps. Nat. Hazards Earth Syst. Sci. 8, 203–211.
Schollaen, K., Heinrich, I., Helle, G., 2014. UV-laser-based microscopic dissection of tree rings - a novel sampling tool for δ^{13}C and δ^{18}O studies. New Phytolog. 201, 1045–1055.
Schollaen, K., Heinrich, I., Neuwirth, B., Krusic, P.J., D'Arrigo, R.D., Karyanto, O., Helle, G., 2013. Multiple tree-ring chronologies (ring width, delta c-13 and delta o-18) reveal dry and rainy season signals of rainfall in Indonesia. Quat. Sci. Rev. 73, 170–181.
Scholz, D., Hoffmann, D.L., 2011. Stalage-an algorithm designed for construction of speleothem age models. Quat. Geochronol. 6, 369–382.
Schöne, B.R., Fiebig, J., 2009. Seasonality in the north sea during the Allerød and late medieval climate optimum using bivalve sclerochronology. Int. J. Earth Sci. 98, 83–98.

Schreiber, T., Schmitz, A., 2000. Surrogate time series. Phys. D: Nonlin. Phenom. 142, 346–382.
Schulz, M., Mudelsee, M., 2002. Redfit: estimating red-noise spectra directly from unevenly spaced paleoclimatic time series. Comput. Geosci. 28, 421–426.
Schulz, M., Stattegger, K., 1997. Spectrum: spectral analysis of unevenly spaced paleoclimatic time series. Comput. Geosci. 23, 929–945.
Schwamborn, G., Meyer, H., Fedorov, G., Schirrmeister, L., Hubberten, H.W., 2006. Ground ice and slope sediments archiving late quaternary paleoenvironment and paleoclimate signals at the margins of el'gygytgyn impact crater, Ne Siberia. Quat. Res. 66, 259–272.
Schwarz-Zanetti, G., Schwarz-Zanetti, W., 1992. Simultaneous weather diaries-a unique body of evidence for reconstructing the climate history of Southern Germany from 1480 to 1530. European climate reconstructed from documentary data: methods and results. Paleoclim. Res. 7, 33–43.
Schweikhardt, P., Ingram, B., Lightfoot, K., Luby, E., 2011. Geochemical methods for inferring seasonal occupation of an estuarine shellmound: a case study from San Francisco Bay. J. Archeol. Sci. 38, 2301–2312.
Schweingruber, F., 1989. Tree rings – basics and applications of dendrochronology. J. Trop. Ecol. 5, 352–352.
Schweingruber, F., 1996. Tree Rings and Environment: Dendroecology. Paul Haupt Publishers, Berne.
Shackleton, N., 1973. Oxygen isotope analysis as a means of determining season of occupation of prehistoric midden sites. Archeometry 15, 133–141.
Shahi, S., Abermann, J., Heinrich, G., Prinz, R., Schöner, W., 2020. Regional variability and trends of temperature inversions in Greenland. J. Climate 33.
Shen, C.C., Lin, K., Duan, W., Jiang, X., Partin, J.W., Edwards, R.L., Cheng, H., Tan, M., 2013. Testing the annual nature of speleothem banding. Sci. Rep. 3, 2633.
Sheppard, P.R., 2010. Dendroclimatology: extracting climate from trees. Wiley Interdis. Rev.: Climate Change 1, 343–352.
Sherwin, C.M., Baldini, J.U., 2011. Cave air and hydrological controls on prior calcite precipitation and stalagmite growth rates: implications for palaeoclimate reconstructions using speleothems. Geochim. Cosmochim. Acta 75, 3915–3929.
Shi, F., Guo, Z., Goosse, H., Yin, Q., et al., 2017a. Multi-proxy reconstructions of precipitation field in China over the past 500 years. Climate Past 13.
Shi, S., Li, J., Shi, J., Zhao, Y., Huang, G., 2017b. Three centuries of winter temperature change on the southeastern Tibetan Plateau and its relationship with the atlantic multidecadal oscillation. Climate Dyn. 49, 1305–1319.
Shi, X., Gallagher, C., 2019. Estimating Unknown Cycles in Geophysical Data. Earth and Space Science.
Shirai, K., Schöne, B., Miyaji, T., Radermacher, P., Krause, R., Tanabe, K., 2014. Assessment of the mechanism of elemental incorporation into bivalve shells (Arctica Islandica) based on elemental distribution at the microstructural scale. Geochim. Cosmochim. Acta 126, 307–320.
Shopov, Y.Y., Ford, D.C., Schwarcz, H.P., 1994. Luminescent microbanding in speleothems: high-resolution chronology and paleoclimate. Geology 22, 407–410.
Singh, J., Yadav, R.R., Wilmking, M., 2009. A 694-year tree-ring based rainfall reconstruction from Himachal Pradesh, India. Climate Dyn. 33, 1149–1158.
Sinha, A., Kathayat, G., Cheng, H., Breitenbach, S.F., Berkelhammer, M., Mudelsee, M., Biswas, J., Edwards, R., 2015. Trends and oscillations in the Indian summer monsoon rainfall over the last two millennia. Nat. Commun. 6, 6309.
Sjolte, J., Adolphi, F., Vinther, B.M., Muscheler, R., Sturm, C., Werner, M., Lohmann, G., 2020. Seasonal reconstructions coupling ice core data and an isotope-enabled climate model - methodological implications of seasonality, climate modes and selection of proxy data. Climate Past 16, 1737–1758.
Slotta, F., Wacker, L., Riedel, F., Heußner, K.U., Hartmann, K., Helle, G., 2021. High-resolution ^{14}c bomb peak dating and climate response analyses of subseasonal stable isotope signals in wood of the African baobab – a case study from Oman. Biogeosciences 18, 3539–3564.
Smirnov, D.A., Marwan, N., Breitenbach, S.F., Lechleitner, F., Kurths, J., 2017. Coping with dating errors in causality estimation. EPL (Europhys. Lett.) 117, 10004.
Souvatzi, S., 2008. A Social Archaeology of Households in Neolithic Greece: An Anthropological Approach. Cambridge University Press, Cambridge.
Spengler, R.N., 2014. Niche dwelling vs. niche construction: landscape modification in the bronze and iron ages of Central Asia. Human Ecol. 42, 813–821.
Speth, J.D., 1987. Early hominid subsistence strategies in seasonal habitats. J. Archeol. Sci. 14, 13–29.
St George, S., Meko, D.M., Cook, E.R., 2010. The seasonality of precipitation signals embedded within the north American drought atlas. Holocene 20, 983–988.
Stambaugh, M.C., Marschall, J.M., Abadir, E.R., Jones, B.C., Brose, P.H., Dey, D.C., Guyette, R.P., 2018. Wave of fire: an anthropogenic signal in historical fire regimes across central Pennsylvania, USA. Ecosphere 9, e02222.
Steen-Larsen, H.C., Masson-Delmotte, V., Hirabayashi, M., Winkler, R., Satow, K., Prié, F., Bayou, N., Brun, E., Cuffey, K.M., Dahl-Jensen, D., Dumont, M., Guillevic, M., Kipfstuhl, S., Landais, A., Popp, T., Risi, C., Steffen, K., Stenni, B., Sveinbj“ornsdottír, A.E., 2014. What controls the isotopic composition of greenland surface snow? Climate Past 10, 377–392.
Steinhardt, J., Butler, P., Carroll, M., Hartley, J., 2016. The application of long-lived bivalve sclerochronology in environmental baseline monitoring. Front. Mar. Sci. 3, 1–26.
Stenni, B., Scarchilli, C., Masson-Delmotte, V., Schlosser, E., Ciardini, V., Dreossi, G., Grigioni, P., Bonazza, M., Cagnati, A., Karlicek, D., Risi, C., Udisti, R., Valt, M., 2016. Three-year monitoring of stable isotopes of precipitation at Concordia station, East Antarctica. Cryosphere 10, 2415–2428.
Stephens, M., Mattey, D., Gilbertson, D., Murray-Wallace, C., 2008. Shell-gathering from mangroves and the seasonality of the Southeast Asian monsoon using high-resolution stable isotopic analysis of the tropical estuarine bivalve (*Geloina erosa*) from the great cave of Niah, Sarawak: methods and reconnaissance of molluscs of early Holocene and modern times. J. Archeol. Sci. 35, 2686–2697.
Stoffel, M., Beniston, M., 2006. On the incidence of debris flows from the early Little Ice Age to a future greenhouse climate: a case study from the Swiss Alps. Geophys. Res. Lett. 33, L16404.
Stoffel, M., Bollschweiler, M., 2008. Tree-ring analysis in natural hazards research – an overview. Nat. Hazards Earth Syst. Sci. 8, 187–202.
Stoica, P., Sandgren, N., 2006. Spectral analysis of irregularly-sampled data: paralleling the regularly-sampled data approaches. Digi. Sig. Process. 16, 712–734.
Stoll, H.M., M”uller, W., Prieto, M., 2012. I-stal, a model for interpretation of Mg/Ca, Sr/Ca and Ba/Ca variations in speleothems and its forward and inverse application on seasonal to millennial scales. Geochem. Geophys. Geosyst. 13.
Støren, E., Dahl, S., 2012. Nonglacial varves recorded in a lake sediment sequence from Southern Norway. Terra Nostra 1, 85–86.
Surge, D., Barrett, J., 2012. Marine climatic seasonality during medieval times (10th to 12th centuries) based on isotopic records in viking age shells from Orkney, Scotland. Paleogeogr. Paleoclimatol. Paleoecol. 350, 236–246.
Swarts, K., Gutaker, R.M., Benz, B., Blake, M., Bukowski, R., Holland, J., Kruse-Peeples, M., Lepak, N., Prim, L., Romay, M.C., Ross-Ibarra, J., Sanchez-Gonzalez, J.d.J., Schmidt, C., Schuenemann, V.J., Krause, J., Matson, R.G., Weigel, D., Buckler, E.S., Burbano, H.A., 2017. Genomic estimation of complex traits reveals ancient maize adaptation to temperate North America. Science 357, 512–515.
Szymczak, S., Barth, J., Bendix, J., Huneau, F., Garel, E., Hausser, M., Juhlke, T., Knerr, I., Santoni, S., Mayr, C., Trachte, K., van Geldern, R., Brauning, A., 2020. First indications of seasonal and spatial variations of water sources in pine trees along an elevation gradient in a mediterranean ecosystem derived from δ18 o. Chem. Geol. 549.
Tadros, C.V., Treble, P.C., Baker, A., Fairchild, I.J., Hankin, S., Roach, R., Markowska, M., McDonald, J., 2016. ENSO - cave dripwater hydrochemical relationship: a 7-year dataset from SE Australia. Hydrol. Earth Syst. Sci. 20, 4625–4640.
Takesue, R., van Geen, A., 2004. Mg/Ca, Sr/Ca, and stable isotopes in modern and Holocene Protothaca staminea shells from a northern California coastal upwelling region. Geochim. Cosmochim. Acta 68, 3845–3861.
Tan, L., Shen, C.C., L“owemark, L., Chawchai, S., Edwards, R.L., Cai, Y., Breitenbach, S.F., Cheng, H., Chou, Y.C., Duerrast, H., et al., 2019. Rainfall variations in central indo-pacific over the past 2,700 y. Proc. Nat. Acad. Sci. 116, 17201–17206.
Tarand, A., Nordli, P.Ø., 2001. The Tallinn temperature series reconstructed back half a millennium by use of proxy data. The Iceberg in the Mist: Northern Research in pursuit of a "Little Ice Age". Springer, pp. 189–199.
Taricco, C., Mancuso, S., Ljungqvist, F., Alessio, S., Ghil, M., 2015. Multispectral analysis of Northern Hemisphere temperature records over the last five millennia. Climate Dyn. 45, 83–104.
Tary, J.B., Herrera, R.H., Han, J., van der Baan, M., 2014. Spectral estimation-what is new?. what is next? Rev. Geophys. 52, 723–749.
Tavabe, K.R., Azarnivand, H., 2013. Biodiversity in Qanats (The case study of Kerman County, Iran). Desert 18, 99–104.
Templado, J., Moreno, D., 1997. La lapa ferrugínea. Biológica 6, 80–81.
Testart, A., Forbis, R., Hayden, B., Ingold, T., Perlman, S., Pokotylo, D., Rowley-Conwy, P., Stuart, D., 1982. The significance of food storage among hunter-gatherers: residence patterns, population densities, and social inequalities [and comments and reply]. Curr. Anthropol. 23, 523–537.
Thackeray, J.F., Fitchett, J.M., 2016. Rainfall seasonality captured in micromammalian fauna in Late Quaternary contexts, South Africa. Paleontol. Africa. 51, 1–9.
Thakar, H., 2014. Food and fertility in prehistoric California: a case-study of risk-reducing foraging behavior and prehistoric population growth from Santa Cruz Island, California. Ph.D. thesis. Dept. Anthropology, Univ. California, Santa Barbara, CA.
Thakur, G., Brevdo, E., Fučkar, N.S., Wu, H.T., 2013. The synchrosqueezing algorithm for time-varying spectral analysis: robustness properties and new paleoclimate applications. Sig. Process. 93, 1079–1094.
Theiler, J., Galdrikian, B., Longtin, A., Eubank, S., Farmer, J.D., 1991. Testing for nonlinearity in time series: the method of surrogate data. technical report. Los Alamos National Lab, NM (United States).
Therrell, M.D., Stahle, D.W., Soto, R.A., 2004. Aztec drought and the "curse of one rabbit". Bull. Am. Meteorol. Soc. 85, 1263–1272.
Thomas, K., 2015. Molluscs emergent, Part I: themes and trends in the scientific investigation of mollusc shells as resources for archaeological research. J. Archeol. Sci. 56, 133–140.
Thompson, L.G., Yao, T., Davis, M.E., Mosley-Thompson, E., Wu, G., Porter, S.E., Xu, B., Lin, P.N., Wang, N., Beaudon, E., Duan, K., Sierra-Hernández, M.R., Kenny, D.V., 2018. Ice core records of climate variability on the third pole with emphasis on the guliya ice cap, western kunlun mountains. Quat. Sci. Rev. 188, 1–14.
Thompson, P., Schwarcz, H.P., Ford, D.C., 1976. Stable isotope geochemistry, geothermometry, and geochronology of speleothems from West Virginia. GSA Bull. 87, 1730–1738.
Tonkin, J.D., Bogan, M.T., Bonada, N., Rios-Touma, B., Lytle, D.A., 2017. Seasonality and predictability shape temporal species diversity. Ecology 98, 1201–1216.
Torrence, C., Compo, G.P., 1998. A practical guide to wavelet analysis. Bull. Am. Meteorol. Soc. 79, 61–78.
Treble, P., Mah, M., Griffiths, A.D., Baker, A., Deininger, M., Kelly, B., Scholz, D., Hankin, S., 2019. Separating Isotopic Impacts of Karst and In-Cave Processes from Climate Variability Using an Integrated Speleothem Isotope-Enabled Forward Model. EarthArXiv.

Treble, P.C., Bradley, C., Wood, A., Baker, A., Jex, C.N., Fairchild, I.J., Gagan, M.K., Cowley, J., Azcurra, C., 2013. An isotopic and modelling study of flow paths and storage in quaternary calcarenite, sw Australia: implications for speleothem paleoclimate records. Quat. Sci. Rev. 64, 90–103.

Tremaine, D.M., Froelich, P.N., 2013. Speleothem trace element signatures: a hydrologic geochemical study of modern cave dripwaters and farmed calcite. Geochim. Cosmochim. Acta 121, 522–545.

Tremaine, D.M., Froelich, P.N., Wang, Y., 2011. Speleothem calcite farmed in situ: modern calibration of δ^{18}O and δ^{13}C paleoclimate proxies in a continuously-monitored natural cave system. Geochim. Cosmochim. Acta 75, 4929–4950.

Tung, T.A., Dillehay, T.D., Feranec, R.S., DeSantis, L.R.G., 2020. Early specialized maritime and maize economies on the north coast of peru. Proc. Nat. Acad. Sci. 117, 32308–32319.

Twaddle, R., Wurster, C., Bird, M., Ulm, S., 2017. Complexities in the palaeoenvironmental and archaeological interpretation of isotopic analyses of the mud shell *Geloina erosa* (Lightfoot, 1786). J. Archeol. Sci.: Rep. 12, 613–624.

Urey, H.C., 1947. The thermodynamic properties of isotopic substances. J. Chem. Soc. Apr. 562–581.

Urey, H.C., 1948. Oxygen isotopes in nature and in the laboratory. Science 108, 489–496.

Vaks, A., Gutareva, O.S., Breitenbach, S.F.M., Avirmed, E., Mason, A.J., Thomas, A.L., Osinzev, A.V., Kononov, A.M., Henderson, G.M., 2013. Speleothems reveal 500,000-year history of Siberian permafrost. Science 340, 183–186.

Vallve, M.B., Martin-Vide, J., 1998. Secular climatic oscillations as indicated by catastrophic floods in the Spanish mediterranean coastal area (14th–19th centuries). Climatic Change 38, 473–491.

van Beynen, P., Bourbonniere, R., Ford, D., Schwarcz, H., 2001. Causes of colour and fluorescence in speleothems. Chem. Geol. 175, 319–341.

van Engelen, A.F.V., Buisman, J., Ijnsen, F., 2001. A millennium of weather, winds and water in the low countries. In: Jones, P.D., Ogilvie, A.E.J., Davies, T.D., Briffa, K.R. (Eds.), History and Climate: Memories of the Future?. Springer, Boston, MA, pp. 101–124.

Van Neer, W., Augustynen, S., Linkowski, T., 1993. Daily growth increments on fish otoliths as seasonality indicators on archaeological sites: the Tilapia from late palaeolithic Makhadma in Egypt. Int. J. Osteoarcheol. 3, 241–248.

VanderPlas, J.T., 2018. Understanding the lomb-scargle periodogram. Astrophys. J. Suppl. Ser. 236, 16.

Vansteenberge, S., de Winter, N.J., Sinnesael, M., Verheyden, S., Goderis, S., Van Malderen, S.J.M., Vanhaecke, F., Claeys, P., 2020. Reconstructing seasonality through stable-isotope and trace-element analyses of the Proserpine stalagmite, Han-Sur-Lesse Cave, Belgium: indications for climate-driven changes during the last 400 years. Climate Past 16, 141–160.

Varpe, Øystein, 2017. Life history adaptations to seasonality. Integrat. Comp. Biol. 57, 943–960.

Vasil'chuk, Y.K., Budantseva, N.A., Farquharson, L.M., Maslakov, A.A., Vasil'chuk, A.C., Chizhova, J.N., 2018. Isotopic evidence for Holocene january air temperature variability on the east chukotka Peninsula. Permafr. Periglac. Process. 29, 283–297.

Vautard, R., Ghil, M., 1989. Singular spectrum analysis in nonlinear dynamics, with applications to paleoclimatic time series. Phys. D: Nonlin. Phenom. 35, 395–424.

Vejmelka, M., Paluš, M., 2009. Detecting nonlinear oscillations in broadband signals. Chaos: Interdis. J. Nonlin. Sci. 19, 015114.

Venema, V., Ament, F., Simmer, C., 2006. A stochastic iterative amplitude adjusted fourier transform algorithm with improved accuracy. Nonlin. Process. Geophys. 13, 321–328.

Verheyden, S., Nader, F.H., Cheng, H.J., Edwards, L.R., Swennen, R., 2008. Paleoclimate reconstruction in the Levant region from the geochemistry of a Holocene stalagmite from the Jeita cave, Lebanon. Quat. Res. 70, 368–381.

Veski, S., Seppä, H., Stancikaite, M., Zernitskaya, V., Reitalu, T., Gryguc, G., Heinsalu, A., Stivrins, N., Amon, L., Vassiljev, J., Heiri, O., 2015. Quantitative summer and winter temperature reconstructions from pollen and chironomid data between 15 and 8 ka BP in the Baltic-Belarus area. Quat. Int. 388, 4–11.

Vinther, B., Jones, P., Briffa, K., Clausen, H., Andersen, K., Dahl-Jensen, D., Johnsen, S., 2010. Climatic signals in multiple highly resolved stable isotope records from Greenland. Quat. Sci. Rev. 29, 522–538.

Wall-Scheffler, C.M., Foley, R.A., 2008. Digital cementum luminance analysis (DCLA): a tool for the analysis of climatic and seasonal signals in dental cementum. Int. J. Osteoarcheol. 18, 11–27.

Walsh, R., Lawler, D., 1981. Rainfall seasonality: description, spatial patterns and change through time. Weather 36, 201–208.

Wang, R.S., Wang, S.W., 1990. Reconstruction of winter temperature in east China during the last 500 years using historical documents. Acta Meterorol. Sini. 48, 108–189.

Wang, T., Surge, D., Mithen, S., 2012. Seasonal temperature variability of the neoglacial (3300–2500 BP) and roman warm period (2500–1600 BP) reconstructed from oxygen isotope ratios of limpet shells (*Patella vulgata*), Northwest Scotland. Paleogeogr. Paleoclimatol. Paleoecol. 317, 104–113.

Wassenburg, J., Scholz, D., Jochum, K., Cheng, H., Oster, J., Immenhauser, A., Richter, D., Häger, T., Jamieson, R., Baldini, J., Hoffmann, D., Breitenbach, S., 2016. Determination of aragonite trace element distribution coefficients from speleothem calcite-aragonite transitions. Geochim. Cosmochim. Acta 190, 347–367.

Wassenburg, J.A., Immenhauser, A., Richter, D.K., Jochum, K.P., Fietzke, J., Deininger, M., Goos, M., Scholz, D., Sabaoui, A., 2012. Climate and cave control on Pleistocene/Holocene calcite-to-aragonite transitions in speleothems from Morocco: elemental and isotopic evidence. Geochim. Cosmochim. Acta 92, 23–47.

Wassenburg, J.A., Riechelmann, S., Schröder-Ritzrau, A., Riechelmann, D.F., Richter, D. K., Immenhauser, A., Terente, M., Constantin, S., Hachenberg, A., Hansen, M., Scholz, D., 2020. Calcite Mg and Sr partition coefficients in cave environments: implications for interpreting prior calcite precipitation in speleothems. Geochim. Cosmochim. Acta 269, 581–596.

Wealker, J., 2000. Raised field abandonment in the upper Amazon. Cul. Agri. 22, 27–31.

Wefer, G., Berger, W., 1981. Isotope paleontology: growth and composition of extant calcareous species. Mar. Geol. 100, 207–248.

Weiss, H., 2017. Megadrought and collapse: from early agriculture to Angkor. Oxford University Press.

Welch, P., 1967. The use of fast fourier transform for the estimation of power spectra: a method based on time averaging over short, modified periodograms. IEEE Trans. Audio Electr. 15, 70–73.

West, C., Burchell, M., Andrus, C., 2018. Molluscs and paleoenvironmental reconstruction in island and coastal settings: variability, seasonality, and sampling. In: Giovas, C., LeFebvre, M. (Eds.), Zooarchaeology in Practice: Case Studies in Methodology and Interpretation in Archaeofaunal Analysis. Springer International, Cham, Switzerland, pp. 191–208.

Westerhold, T., Marwan, N., Drury, A.J., Liebrand, D., Agnini, C., Anagnostou, E., Barnet, J.S., Bohaty, S.M., De Vleeschouwer, D., Florindo, F., et al., 2020. An astronomically dated record of earth's climate and its predictability over the last 66 million years. Science 369, 1383–1387.

Wetter, O., Pfister, C., Weingartner, R., Luterbacher, J., Reist, T., Trösch, J., 2011. The largest floods in the High Rhine basin since 1268 assessed from documentary and instrumental evidence. Hydrol. Sci. J. 56, 733–758.

Whyte, K.P., 2013. On the role of traditional ecological knowledge as a collaborative concept: a philosophical study. Ecol. Process. 2, 7.

de Winter, N.J., Agterhuis, T., Ziegler, M., 2021. Optimizing sampling strategies in high-resolution paleoclimate records. Climate Past 17, 1315–1340.

de Winter, N.J., Goderis, S., Dehairs, F., Jagt, J.W., Fraaije, R., Van Malderen, S., Vanhaecke, F., Claeys, P., 2017. Tropical seasonality in the late Campanian (late Cretaceous): Comparison between multiproxy records from three bivalve taxa from Oman. Palaeogeogr. Palaeoclimatol. Paleoecol. 485, 740–760.

de Winter, N.J., Agterhuis, T., Ziegler, M., 2021a. Optimizing sampling strategies in high-resolution paleoclimate records. Climate of the Past 17, 1315–1340.

de Winter, N.J., Müller, I.A., Kocken, I.J., Thibault, N., Ullmann, C.V., Farnsworth, A., Lunt, D.J., Claeys, P., Ziegler, M., 2021b. Absolute seasonal temperature estimates from clumped isotopes in bivalve shells suggest warm and variable greenhouse climate Communications. Earth & Environment 2, 121.

Winterhalder, B., Puleston, C., Ross, C., 2015. Production risk, inter-annual food storage by households and population-level consequences in seasonal prehistoric agrarian societies. Environ. Archeol. 20, 337–348.

Wirth, S.B., Gilli, A., Simonneau, A., Ariztegui, D., Vannière, B., Glur, L., Chapron, E., Magny, M., Anselmetti, F.S., 2013. A 2000 year long seasonal record of floods in the southern European Alps. Geophys. Res. Lett. 40, 4025–4029.

Wirtz, K.W., Lohmann, G., Bernhardt, K., Lemmen, C., 2010. Mid-Holocene regional reorganization of climate variability: analyses of proxy data in the frequency domain. Paleogeogr. Paleoclimatol. Paleoecol. 298, 189–200.

Witt, A., Schumann, A., 2005. HOLOCENE climate variability on millennial scales recorded in Greenland ice cores. Nonlinear Proc. Geophys. 12, 345–352.

Wittwer-Backofen, U., Gampe, J., Vaupel, J.W., 2004. Tooth cementum annulation for age estimation: results from a large known-age validation study. Am. J. Phys. Anthropol. 123, 119–129.

Wolda, H., 1988. Insect seasonality: why? Ann. Rev. Ecol. Syst. 19, 1–18.

Wolf, A., Roberts, W.H.G., Ersek, V., Johnson, K.R., Griffiths, M.L., 2020. Rainwater isotopes in central vietnam controlled by two oceanic moisture sources and rainout effects. Sci. Rep. 10, 16482.

Wong, C.I., Banner, J.L., Musgrove, M., 2011. Seasonal dripwater Mg/Ca and Sr/Ca variations driven by cave ventilation: implications for and modeling of speleothem paleoclimate records. Geochim. Cosmochim. Acta 75, 3514–3529.

Wong, C.I., Breecker, D.O., 2015. Advancements in the use of speleothems as climate archives. Quat. Sci. Rev. 127, 1–18.

Wu, Z., Huang, N.E., Long, S.R., Peng, C.K., 2007. On the trend, detrending, and variability of nonlinear and nonstationary time series. Proc. Nat. Acad. Sci. 104, 14889–14894.

Xoplaki, E., Luterbacher, J., Paeth, H., Dietrich, D., Steiner, N., Grosjean, M., Wanner, H., 2005. European spring and autumn temperature variability and change of extremes over the last half millennium. Geophys. Res. Lett. 32.

Xu, C., 2019. Detection test for periodic signals revisited against various stochastic models. IEEE Access 7, 92203–92209.

Xu, G.B., Liu, X.H., Sun, W.Z., Szejner, P., Zeng, X.M., Yoshimura, K., Trouet, V., 2020. Seasonal divergence between soil water availability and atmospheric moisture recorded in intra-annual tree-ring delta o-18 extremes. Environ. Res. Lett. 15.

Yang, H., Johnson, K.R., Griffiths, M.L., Yoshimura, K., 2016. Interannual controls on oxygen isotope variability in Asian monsoon precipitation and implications for paleoclimate reconstructions. J. Geophys. Res.: Atmos. 121, 8410–8428.

Yi, L., Yu, H., Ge, J., Lai, Z., Xu, X., Qin, L., Peng, S., 2012. Reconstructions of annual summer precipitation and temperature in north-central China since 1470 AD based on drought/flood index and tree-ring records. Clim. Change 110, 469–498.

Yu, Z., Ito, E., 1999. Possible solar forcing of century-scale drought frequency in the northern Great Plains. Geology 27, 263–266.

Zander, P.D., Zarczyński, M., Tylmann, W., Rainford, S., Grosjean, M., 2021. Seasonal climate signals preserved in biochemical varves: insights from novel high-resolution sediment scanning techniques. Climate Past 17, 2055–2071.

Zbilut, J.P., Marwan, N., 2008. The Wiener–Khinchin theorem and recurrence quantification. Phys. Lett. A 372, 6622–6626.

Zechmeister, M., Kürster, M., 2009. The generalised Lomb-Scargle periodogram-a new formalism for the floating-mean and Keplerian periodograms. Astron. Astrophys. 496, 577–584.

Zender, M.U., 2004. A Study of Classic Maya Priesthood. University of Calgary.

Zeng, X., Liu, X., Evans, M.N., Wang, W., An, W., Xu, G., Wu, G., 2016. Seasonal incursion of Indian Monsoon humidity and precipitation into the southeastern Qinghai-Tibetan Plateau inferred from tree ring δ^{18}O values with intra-seasonal resolution. Earth Planet. Sci. Lett. 443, 9–19.

Zhang, T., Barry, R.G., Gilichinsky, D., Bykhovets, S.S., Sorokovikov, V.A., Ye, J., 2001. An amplified signal of climatic change in soil temperatures during the last century at Irkutsk, Russia. Climatic Change 49, 41–76.

Zhang, Y.G., Pagani, M., Liu, Z., Bohaty, S.M., DeConto, R., 2013. A 40-million-year history of atmospheric CO_2. Philos. Trans. Roy Soc. A 371, 20130096.

Zhou, H., Chen, Y., Hao, X., Zhao, Y., Fang, G., Yang, Y., 2019. Tree rings: a key ecological indicator for reconstruction of groundwater depth in the lower Tarim River. Northwest China Ecohydrol. 12, e2142.

Zolitschka, B., Brauer, A., Negendank, J., Stockhausen, H., Lang, A., 2000. Annually dated late Weichselian continental paleoclimate record from the Eifel, Germany. Geology 28, 783–786.

Zolitschka, B., Francus, P., Ojala, A.E., Schimmelmann, A., 2015. Varves in lake sediments - a review. Quat. Sci. Rev. 117, 1–41.